THE SMC04388 OMEGA AMINO TRANSAMINASE FROM *SINORHIZOBIUM MELILOTI*

THE SMC04388 OMEGA AMINO TRANSAMINASE FROM *SINORHIZOBIUM MELILOTI*

By

Guianeya Perez Hernandez

A Thesis

Submitted to the School of Graduate Studies
In Partial Fulfillment of the Requirements

For the Degree
Master of Science

McMaster University

MASTER OF SCIENCE (Biology) MCMASTER UNIVERSITY

Hamilton, Ontario

TITLE: The Smc04388 omega amino transaminase from *Sinorhizobium meliloti*

AUTHOR: Guianeya Perez Hernandez, M.Sc.

SUPERVISOR: Dr. T.M. Finan

NUMBER OF PAGES: XIII, 93

ABSTRACT

Hydroxyproline (*trans*-4-hydroxy-L-proline (4-L-Hyp)) can be used by certain microorganisms as a source of carbon and nitrogen. The nitrogen fixing bacterium, *Sinorhizobium meliloti* carries a cluster (*hyp* cluster) of 14 genes responsible for the transport and degradation of this amino acid in the cell. The biological functions of several gene products in the *hyp* cluster are still unknown. So far, it is known that the conversion of *trans*-4-hydroxy-proline to α-ketoglutarate, one of the intermediate of the TCA cycle, occurs in four enzymatic reactions.

The whole *hyp* cluster is up regulated in the presence of 4-hydroxy-proline in the media. Previous studies have shown several other 4-hydroxy-proline-inducible genes. One of these genes, *smc04388,* has been annotated as a putative omega amino transaminase. The role of this omega transaminase in the main catabolic pathway of 4-hydroxy-proline has not been investigated. In order to address this, two mutant strains; a single *smc04388* mutant and a double *smc04388 hypD* mutant were created. Growth curves of these mutants in minimal media showed that the Smc04388 protein is not required for the growth of *S. meliloti* in the presence of *trans*-4-hydroxy-L-proline as the sole carbon and nitrogen source.

The Smc04388 protein was overexpressed as a Strep-tagged and purified from *S. meliloti*. The purified enzyme showed amino transaminase activity with pyruvate and α-methylbenzylamine. In addition, an enzymatic reaction using the product of the second enzyme of the 4-hydroxy-proline pathway, Δ^1-pyrroline-4-hydroxy-2-carboxylate, was carried out to test the activity of Smc04388 with this compound. Mass spectrometry analysis of this reaction mixture revealed the formation of L-alanine from pyruvate and Δ^1-pyrroline-4-hydroxy-2-

carboxylate, suggesting the utilization of this compound as an amino donor by the Smc04388 transaminase. It was also shown that transamination activity in cell extracts increase in the absence of Δ^1-pyrroline-4-hydroxy-2-carboxylate deaminase, the enzyme that catalyzes the conversion of this compound in the 4-hydroxy-proline pathway. These results confirmed the hypothesis that the Smc04388 omega amino transaminase is involved in a secondary pathway related to the known catabolic pathway of 4-hydroxy-proline in bacteria. Further understanding of this secondary pathway will contribute to the study of the metabolism of 4-hydroxy-proline in bacteria. In addition to this, the complete characterization of the Smc04388 omega amino transaminase could have practical application in the pharmaceutical industry.

AKNOWLEDGEMENTS

I would like to thank my committee members for reviewing and accepting this document as part of my examination for the Master of Science Degree. I am especially grateful to my supervisor, Dr. Turlough M. Finan, for his understanding and patience during these three years. I have an enormous gratitude to Dr. Richard Morton for his help, support and guidance on my professional career.

I would like to thank Dr. Philip Britz-McKibbin and Mai Yamamoto from Chemical Biology Department for making possible the determination of alanine by CE-MS. Thank you to all my past and present fellows lab for an unforgettable experience; specially my friend Mary Fernandez, for her smile and help with my second language.

I want to specially thank my family and friends back in Cuba for always believing in me and encourage me from the distance. Thank you to my Canadian family for making easier and pleasant my life in Canada; and my partner Trev for giving me the best of my life.

TABLE OF CONTENTS

	Page
Descriptive note	III
Abstract	IV
Acknowledgements	VI
Table of contents	VII
List of Figures	IX
List of Tables	XI
Abbreviations	XII
Chapter 1. Introduction	1
Biological Nitrogen fixation	1
Rhizobia-legume symbiosis	2
Characteristic of the rhizobia bacteria	4
Sinorhizobium meliloti	5
Catabolic pathway of hydroxyproline in bacteria	6
Hydroxyproline gene cluster in *S. meliloti*	6
Possible role of Smc04388 in 4-hydroxy-proline pathway	10
Amino transaminase enzymes	11
Omega amino transaminases	13
Characterization of omega amino transaminases	15
Chapter 2. Materials and Methods	16
Bacterial strains and growth conditions	16
Growth curve	21
Expression of reporter gene *gusA*	21
PCR amplifications	22
Cloning and DNA manipulation	23
Cloning of the *smc04388* gene into pTH1227 vector	24
Transformation of DNA into bacteria	25
Conjugal transference of DNA	25
Construction of a single *smc04388* mutant	26
Construction of a double *smc04388 hypD* mutant	27
SDS-PAGE	28
Bradford assay for quantification of protein	29
Expression and purification of the Smc04388 omega amino transaminase	29
French Press	29
Ultracentrifugation	30
Purification	30
Dialysis	31
Amino transaminase enzymatic assay	32
Preparation of cell extracts	32
Malate dehydrogenase assay	33
Purification of *cis*-4-hydroxy-D-proline dehydrogenase from *P. putida*	33

Enzymatic Assay for *cis*-4-hydroxy-D-proline dehydrogenase 35
Analysis of L-alanine formation 35

Chapter 3. Results 36
Omega amino transaminases in *S. meliloti* 36
Expression of the *smc04388* gene 40
Construction of a single and double mutant of the *smc04388* gene 42
Growth of the two omega transaminase mutants in the presence of *trans*-4-hydroxy-L-proline 44
Amino transamination enzymatic activity in cell extracts 50
Cloning, purification and activity of the Smc04388 omega amino transaminase 53
Characterization of the Smc04388 omega amino transaminase 57
Substrate specificity 57
Effect of the pH on the activity of the Smc04388 transaminase 59
Activity towards the open form of Δ^1-pyrroline-4-hydroxy-2-carboxylate 60

Chapter 4. Discussion 66
Induction and phenotype of the Smc04388 omega amino transaminase in the presence of 4-hydroxy-L-proline 66
Characterization of the Smc04388 omega amino transaminase 68

Chapter 5. Conclusions 72

Bibliography 73
Appendix 80

LIST OF FIGURES

Page

Figure 1. The *hyp* cluster located in the pSymB megaplasmid of *Sinorhizobium meliloti.* 7
Figure 2. Schematic representation of the 4-hydroxy-proline catabolic pathway in *Sinorhizobium meliloti*. 9
Figure 3. Transamination reaction between α-methylbenzylamine (α-MBA) as an amino donor and pyruvate as an amino acceptor. 13
Figure 4. Multiple alignment of protein sequences from known omega amino transaminases and the putative Smc04388 transaminase from *S. meliloti*. 38
Figure 5. Representation of the phylogenetic tree of known omega amino transaminases and the putative Smc04388 transaminase from *S. meliloti*. 39
Figure 6. Schematic representation of the SmFL1068 fusion library strain. 40
Figure 7. Expression of the *smc04388* gene from *S. meliloti*. 42
Figure 8: Disruption of the *smc04388* gene by insertion of an omega cassette Sm^rSp^r. 43
Figure 9. Growth curve of Rm5000 wild type strain in different minimal media at 30 ^oC. 45
Figure 10. Growth curve of a single *smc04388* mutant, RmP3081, in different minimal media at 30 ^oC. 46
Figure 11. Growth curve of RmP110 wild type strain in different minimal media at 30 ^oC. 47
Figure 12. Growth curve of a *hypD* mutant, RmP2510, in different minimal media at 30 ^oC. 48
Figure 13. Growth curve of a *smc04388 hypD* double mutant, RmP3272, in different minimal media at 30 ^oC. 49
Figure 14. Schematic representation of the transaminase reaction between α-methylbenzylamine (α-MBA) as an amino donor and pyruvate as an amino acceptor, L-alanine forming and acetophenone. 51
Figure 15. Enzymatic activity in cell extracts. 52
Figure 16. Cloning and purification of the recombinant Smc04388 omega amino transaminase from RmP3016. 54
Figure 17. Transaminase reaction of the Smc04388 purified protein. 56
Figure 18. Transamination reaction of the Smc04388 purified protein using α-ketoglutarate or pyruvate as amino acceptors and α-MBA as the amino donor. 57
Figure 19. Pyruvate as an amino acceptor in the transamination reaction. 58
Figure 20. Effect of the pH on the specific activity of the purified Smc04388 omega aminotransferase. 60
Figure 21. Diagram of the coupled enzymatic reaction with the D-HypDH from *P. putida* and the purified Smc04388 omega amino transaminase from *S. meliloti*. 62
Figure 22: CE-MS of the coupled enzymatic reaction with the D-HypDH and the purified Smc04388 omega amino transaminase. 64
Figure 23. Second and third reactions of the hydroxyproline catabolic pathway in mammals. 80
Figure 24. pTH1522 vector used to create the fusion library strains. 81

Figure 25. pUCP30T vector used for the construction of the pTH2816 recombinant plasmid. 82
Figure 26. Vector pHP45 that carries the Sm/Sp resistant cassette. 83
Figure 27. Restriction digests from different recombinant plasmids pTH2816 after the Sm/Sp resistant cassette was inserted. 84
Figure 28. Protein Standard curve of BSA. 85
Figure 29. Purification of *cis*-4-hydroxy-D-proline dehydrogenase from *P. putida* strain. 86
Figure 30. Principle of an enzymatic assay to detect the activity of *cis*-4-hydroxy-D-proline dehydrogenase enzyme (D-HypDH). 87
Figure 31. L-alanine standard curve. 88
Figure 32. β-glucuronidase activity in recombinant plasmids harbouring the *smc04388* gene. 89
Figure 33. Spectra of each reactant of the reaction mixture and acetophenone. 90
Figure 34. Spectra of 0.1 mM acetophenone at different pHs. 91
Figure 35. CE-MS of the control 2 (without pyruvate) in the coupled reaction with the D-HypDH from *P. putida* and the purified Smc04388 omega amino transaminase. 92
Figure 36. CE-MS of the enzymatic reaction with the D-HypDH from *P. putida*. 93

LIST OF TABLES

Page

Table 1. Plasmids used in this study. 17
Table 2. Bacterial strains used in this study. 18
Table 3. Primers used in this study. 19
Table 4. Omega amino transaminases in *S. meliloti*. 36
Table 5. Doubling time (hours) in different minimal media. 50
Table 6. Purification summary of the omega amino transaminase Smc04388 from *S. meliloti*. 55
Table 7. Purification summary of *cis*-4-hydroxy-D-proline dehydrogenase (D-HypDH) from *P. putida* strain (M2116). 86

ABBREVIATIONS

LB- Luria Bertani broth

4-L-Hyp- *trans*-4-hydroxy-L-proline

4-D-Hyp- *cis*-4-hydroxy-D-proline

P4OH2C- Δ^1-pyrroline-4-hydroxy-2-carboxylate

Amp- Ampicillin

Cm- Chloramphenicol

Gm- Gentamycin

Km- Kanamycin

Nm- Neomycin

Rif- Rifampicin

Sm- Streptomycin

Sp- Spectinomycin

Tc- Tetracycline

r- resistant

s- sensitive

PCR- Polymerase chain reaction

bp- base pair

SDS-PAGE- sodium dodecyl sulphate polyacrylamide gel electrophoresis

α-MBA- α-methylbenzylamine

PLP- pyridoxal 5'phosphate

PMP- pyridoxamine 5'-phosphate

EDTA- ethylenediaminetetraacetic acid

INT- iodonitrotetrazolium chloride

PMS- phenazine methosulfate

CE-MS- capillarity electrophoresis-mass spectrometry

CHAPTER 1

INTRODUCTION

Biological Nitrogen Fixation

Nitrogen is one of the most important elements required by life in our planet. It occurs in DNA, RNA and proteins, which are present in all living cells. It is the fifth most abundant element on our planet and its largest reservoir in the atmosphere, as di nitrogen gas (N_2) (Canfield, 2010). Despite its abundance in our atmosphere, N_2 gas is inert and cannot be assimilated by the majority of living organisms; therefore nitrogen is one of the limiting nutrients in terrestrial and marine ecosystems (Schröder, 2001). Only a few prokaryote organisms have the ability to convert nitrogen gas to its inorganic form ammonium, through a complex and specialized process known as "Biological Nitrogen Fixation" (Dixon & Kahn, 2004).

Organisms able to reduce N_2 gas to ammonia are named diazotrophs. This ability was first ascribed to few microorganisms, however now diazotrophic organisms have been described along the majority of bacterial groups and archaea. New findings indicate that the presence of these organisms in nature is wider and more diverse than originally thought. New nitrogen fixing microorganisms have been identified by using genetic and molecular techniques (Dixon & Kahn, 2004). One of the newly discovered nitrogen fixers is the bacterium *Burkholderia*, which can fix nitrogen efficiently on legumes, as can its close relative, rhizobia (Vitousek, 2013).

Biological Nitrogen Fixation is the most important biological process in nature after photosynthesis. It plays an important role in maintaining the nitrogen cycle on our planet and it is crucial for agriculture (Canfield, 2010). N_2-fixation is catalyzed by the nitrogenase enzymatic complex present in all diazotrophic organisms. This enzyme is a complex of metalloenzymes, comprising of two components: an iron dimeric protein and a molybdenum-iron protein. The

former is an ATP-dependent electron donor and the second component has been identified to contain the catalytic site. The molybdenum-iron nitrogenase enzyme is highly sensitive to oxygen, therefore N_2 fixation must occur at very low levels of oxygen (Dixon & Kahn, 2004). In aerobic organisms, such as rhizobia, there are physiological mechanisms that allow to reduce N_2. In the case of rhizobia, the presence of the enzyme leghemoglobina allows these bacteria to reduce N_2 in microaerobic conditions inside the plant's root nodule (Ott et al., 2005).

N_2-fixation requires high levels of energy. For instance, *Azotobacter*, a free living bacterium, requires up to 100 units of glucose per each unit of nitrogen converted to ammonia. However, rhizobia in symbiotic association with legumes require 6 to 8 units of glucose (Osorio, 2007). The energy necessary for N_2-fixation can be obtained from different sources, depending primarily on the habitat of the organism. Free living plant-associated nitrogen fixers obtain energy from the metabolism of organic compounds present in the rhizosphere and organisms that carry out nitrogen fixation in symbiosis obtain energy from their host. The energetic cost of the N_2-fixation is likely responsible for the high level of gene regulation observed (Caetano-Anolles & Gresshoff, 1991).

Rhizobia-legume symbiosis

Symbiotic N_2-fixation has been described for three groups of bacteria. The first are cyanobacteria that interact with plants like ferns, cycads and dicotyledons. The second group are *Frankia* actinomycetes that form nodules on a large group of angiosperms that include *Alnus* and *Prusia*. The third symbiotic group establish are bacteria that form nodules on leguminous. With one exception, this interaction has been exclusively described among legume: *Parasponia* is the only non-legume plant that interacts with rhizobia (Lloret & Martínez-Romero, 2005).

Rhizobia bacteria are of special interest because of their association with important crops and forage legumes. More than 88% of these plants have been described as having one or more symbiont rhizobia species. The symbiotic relationship with rhizobia is present among the three subfamilies of legumes *Papilionoideae*, *Mimosoideae* and *Caesalpinioideae*, and only members of the subfamily *Caesalpinoideae* are non-nodulating (Bais, 2006).

Rhizobia-legume associations are generally specific. This means that usually there is a specific rhizobia species that interacts with a specific host legume plant. This specificity has different levels from narrow to broad. For example, *Azorhizobium caulinodans* the only species of described to date that forms N_2-fixing nodules on the marine legume *Sesbania rostrata* (Canpoen et al., 2010). An example of a broad host range is *Rhizobium* strain NGR234, which is able to form nodules on 232 different species of legume (Bais, 2006).

The rhizobia-legume symbiosis has been extensively characterized. The ammonium produced by rhizobia is assimilated by the legume plants and also serves as an organic source of nitrogen for other plants, soil and animals in the ecosystem (Canfield, 2010). According to a recent study in the period of 1860-1995 the contribution of nitrogen per year by legume in association with rhizobia was about 20Tg (Vitousek et al., 2013). For this reason legume plants are one of the primary choices when considering the development of sustainable agricultural systems.

The rhizobia-legume is a complex process and for its successful completion requires a molecular dialogue between both rhizobia and legume. The first signals are plant isoflavones excreted to the rhizosphere. Rhizobia perceive these molecules and in response produce and secret lipo-oligosaccharide molecules known as “Nod factors” (Long, 1996). These molecules induce a variety of responses in the plant, leading to deformation of the root hair that allows the

invasion of rhizobia into cortical cells, and finally the formation of the nodule (Relic et al., 1994; Pacios-Bras, 2005; Long, 1996 & Gage, 2004).

The nodules are specialized plant organelles (Capoen, 2010) and within these structures rhizobia differentiate into a new physiological and morphological cellular form, called bacteroids. These specialized rhizobial cells have an adjusted metabolism enabling them to live inside the nodule and to carry out the N_2-fixation efficiently (Gage, 2004; Luyten & Vanderleyden, 2000).

Characteristic of the rhizobia bacteria

Rhizobia are rod shaped Gram negative bacteria, with dimension between 0.5 to 0.9 microns wide and 1.2 to 3.0 microns long. Their cells are motile due to the presence of flagella, however they do not present endospores. These bacteria are also known to produce and accumulate granules of polyhydroxybutyrate (PHB). They are aerobic microorganisms, however they metabolize at very low levels of oxygen inside the nodule (Frioni, 1990).

The taxonomy of rhizobia is still in flux, however a recent study by Berrada & Fikri (2014) has reported 98 species in total grouped in 14 genera. The majority of rhizobial species described to date belong to either α- or β-proteobacteria subdivisions. The rhizobial species that belong to α-proteobacteria class have been divided in nine genera: *Azorhizobium, Bradyrhizobium, Mesorhizobium, Rhizobium, Sinorhizobium* (*Ensifer*), *Methylobacteriu, Devosia*, *Microvirga* and *Ochorobactrum*. The β-proteobacteria class grouped species in two genera: *Burkholderia* and *Cupriavidus*. Most recently some species have been identified to belong to *Pseudomonas* sp in γ-proteobacteria class. This classification is based on the comparison of their 16SrRNA molecule and new techniques such as Multilocus sequence analysis (MLSA) and Multilocus sequence typing (MLST) (Berrada & Fikri, 2014).

Despite the genetic differences among rhizobia genera, there are certain physiological and morphological characteristics specific for each genus that allow classification of these bacteria using basic microbiology techniques. For instance, slow growing bacteria which share similar colony morphology and excretion of basic compound to the media are grouped in *Bradyrhizobium*. On the other hand, *Rhizobium* and *Sinorhizobium* comprise fast growing species of rhizobia, which are characterized by the secretion of acid and mucus into the media and very similar colony appearance (Lloret & Martinez-Romero, 2005).

Regarding nutritional requirements, rhizobia are heterotrophic bacteria that are able to metabolize a variety of carbon sources. Fast growing rhizobia such as *Rhizobium* and *Sinorhizobium* can metabolize carbon compounds such as saccharose and mannitol, whereas low growing genera such as *Bradyrhizobium* prefer glycerol and pentose in general (L-arabinose, xylose, ribose) (Graham, 1975). Lastly, *Mezorhizobium* species share intermediate characteristics between the two groups above.

Sinorhizobium meliloti

Sinorhizobium meliloti has been one of the most studied species of its genus since it is the known symbiont of the alfalfa forage legume *Medicago sativa*. *S. meliloti* can also produce nodules on species of *Melilotis* and *Trigonella* legumes (Bais, 2006). The genome of *S. meliloti* strain 1021 includes a chromosome of 3.65 Mb and two megaplasmids, pSymA and pSymB, 1.35 Mb and 1.68 Mb respectively (Galibert et al., 2001).

The soil, the natural environment for rhizobia, is one of the most complex and diverse ecosystems in nature. Organisms living in the rhizosphere, the region of soil surrounding plant roots, are exposed to a diverse composition of nutrients (Bais, 2006). This is the reason for these bacteria to develop a specialized and diverse metabolism.

Catabolic pathway of Hydroxyproline in bacteria

Hydroxyproline is a cyclic secondary amino acid which forms part of both plant and animal proteins. There are three kinds of stable hydroxyproline in nature: 4-hydroxy-proline, 3-hydroxy-proline and 3, 4-hydroxy-proline. In animals 4-hydroxy-proline is present in collagen and in smaller proportion in other small proteins. On the other hand, in plants 4-hydroxy-proline is forms part of cell wall proteins named extensin. These proteins play an important role promoting rigidity of the cell wall. Interestingly, it has been suggested that both collagen and extension proteins share analogous function in animals and plants respectively (Adams & Frank, 1980).

Hydroxyproline is also present in some antibiotics produced by bacteria, indicating that there is a metabolic pathway for this amino acid in this group of microorganisms. Further, more research indicated that certain bacteria can utilize this amino acid as a carbon and nitrogen source (Adams & Frank, 1980). The first catabolic pathway for 4-hydroxy-proline was identified by Adams (1973) in *Pseudomonas*, a soil free living bacteria. However, analogous pathways have been found in other bacteria such as another *Pseudomonas* species (Jayaraman & Radhakrishnan, 1965 & Thacker, 1969) and *Achromobacter* (Jayaraman & Radhakrishnan, 1965).

Hydroxyproline gene cluster in S. meliloti

In *S. meliloti* a cluster of fourteen genes present in the pSymB megaplasmid, the *hyp* cluster (Figure 1), is responsible for the transport and catabolism of hydroxyproline. These genes produce five different transcripts. Three of these transcripts- *hypR, hypD* and *hypH* encode for single genes, whereas *hypST* comprises two genes and the largest transcript

hypMNPQO(RE)XYZ) is formed by nine genes expressed under the same promoter (White et al., 2012).

Transcription of the *hyp* genes is repressed by HypR, a helix-turn-helix GntR-like negative regulator (MacLean et al., 2009). In the absence of 4-hydroxy-proline, HypR represses the expression of the genes in the cluster. However, in the presence of 4-hydoxy-proline the regulator releases this repression leading to expression of the enzymes required for the transport and degradation of 4-hydroxy-proline (MacLean et al., 2009 & White et al., 2012).

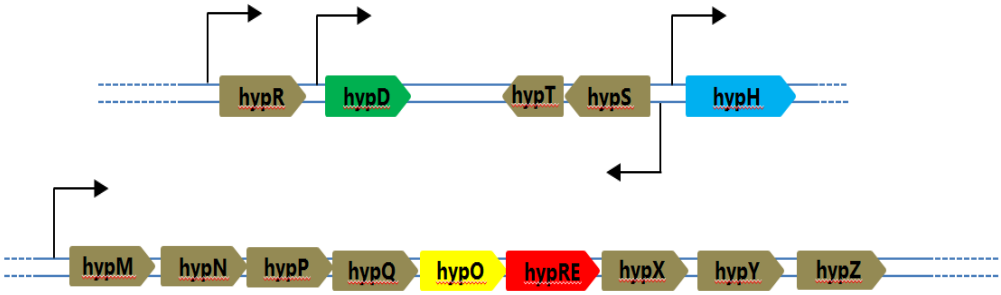

Figure 1. **The *hyp* cluster located in the pSymB megaplasmid of *Sinorhizobium meliloti.*** The *hypR* gene encodes for the negative regulator. The *hypD* gene encodes for the Δ^1-pyrroline-4-hydroxy-2-carboxylate deaminase, *hypT* encodes for a protein of unknown function whereas *hypS* encodes for a putative dehydrogenase. The *hypH* gene encodes for the α-ketoglutarate dehydrogenase. The four genes *hypMNPQ* encode for an ABC-like transport system. The *hypO* gene encodes for the *cis*-4-hydroxy-D-proline dehydrogenase (oxidase) and the *hypRE* encodes for the 4-hydroxy-proline epimerase. Products of the *hypX*, *hypY* and *hypZ* have not been identified. Genes are transcribed in the direction of the boxes. Promoters are represented by black arrows.

The largest transcript in the *hyp* cluster comprises genes responsible for the transport of 4-hydroxy-proline. A high affinity transport system encoded by four genes *hypMNPQ* was described by MacLean et al. (2009). Apart *from* these genes, five more are in the same operon, which are up regulated in the presence of *trans*-4-hydroxy-L-proline (4-L-Hyp) and *cis*-4-hydroxy-D-proline (4-D-Hyp). The *hypM* gene encodes for a periplasmic solute binding protein,

whereas both *hypN* and *hypP* encode for transporter permease proteins. Lastly an ATP-binding protein is the product of *hypQ*. In addition, a mutant lacking the *hypMNPQ* genes had a significant growth defect with 4-L-Hyp as the sole carbon source, suggesting that these proteins play a crucial role for 4-L-Hyp metabolism in *S. meliloti* (MacLean et al., 2009).

More recently White et al. (2012) identified the genes from the *hyp* cluster that correspond to the four enzymatic reactions in the catabolic pathway of 4-hydroxy-proline described by Adams (1973). The catabolism of 4-hydroxy-proline in bacteria involves four main reactions (Figure 2). In the first reaction *trans*-4-hydroxy-L-proline (4-L-Hyp) is converted to *cis*-4-hydroxy-D-proline (4-D-Hyp) by an epimerase. In the second step, 4-D-Hyp is oxidized to Δ^1-pyrroline-4-hydroxy-2-carboxylate (P4OH2C) by an oxidase (dehydrogenase) with concomitant reduction of an acceptor, potentially oxygen. The next reaction is the deamination of P4OH2C to α-ketoglutarate semialdehyde (α -KGSA) which is catalyzed by a deaminase. Finally, α-KGSA is oxidized to α-ketoglutarate by a dehydrogenase with the simultaneously reduction of NAD^+ to NADPH (Adams & Frank, 1980; Watanabe et al., 2012).

In *S. meliloti*, the 4-hydroxy-proline epimerase (HypRE) is encoded by the *hypRE* gene (Gavina et al., 2010 & White et al., 2012), and the D-amino acid oxidase (HypO) is the product of the *hypO* gene. Both genes are located in the same transcript and expressed under the same promoter. The former is the most studied enzyme of the pathway and has been characterized in different soil bacteria such as *Pseudomonas, Burkholderia, Brucella* (Adams & Frank, 1980; Goytia et al., 2007) and *Sinorhizobium* (White et al., 2012). On the other hand, the identification of the second enzyme, the *cis*-4-hydroxy-D-proline dehydrogenase has been more difficult due to its association with the membrane. However, a new study carried out by Watanabe et al. (2012) has identified and characterized the *cis*-4-hydroxy-D-proline dehydrogenase (oxidase) (D-

HypDH) from *P. putida* and *P. aeruginosa*. Interestingly, these authors suggest that both enzymes are not close phylogenetically based on its structural differences. However, both enzymes contain one or more FAD molecules as a prosthetic group.

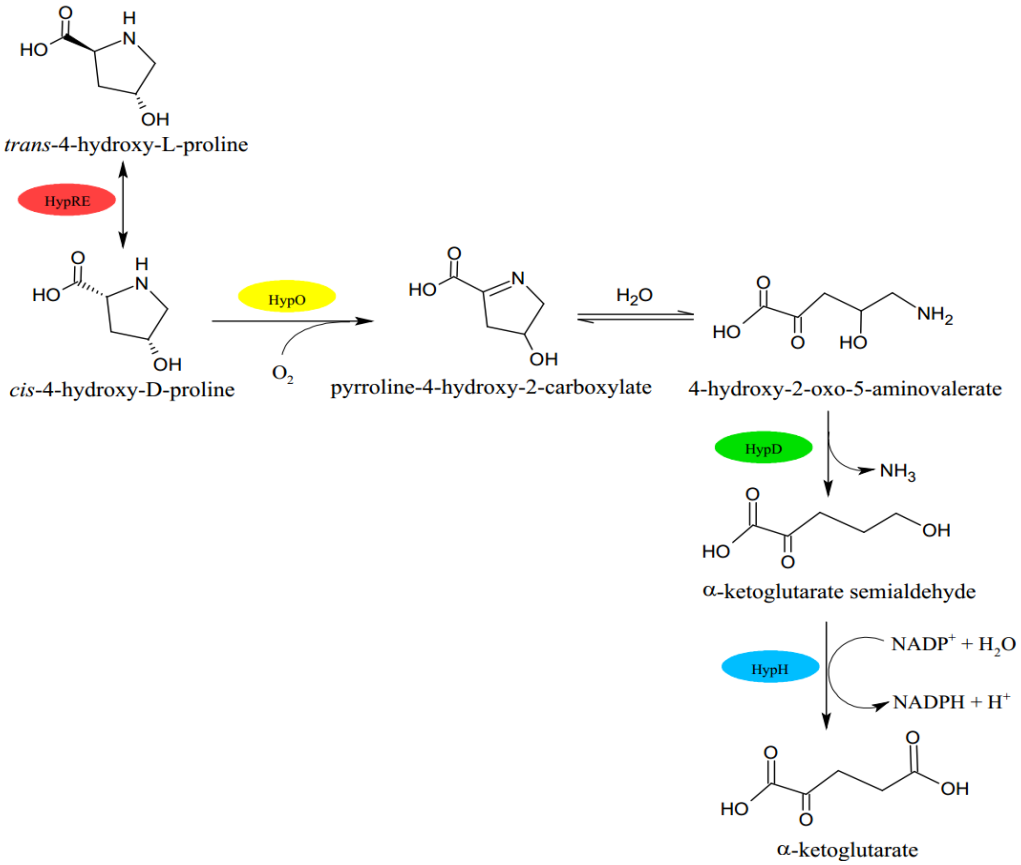

Figure 2. **Schematic representation of the 4-hydroxy-proline catabolic pathway in *Sinorhizobium meliloti*.** The enzymes involved are HypRE: 4-hydroxy-proline epimerase (EC 5.1.18), HypO: *cis*-4-hydroxy-D-proline dehydrogenase (oxidase), HypD: 1-pyrrole-4-hydroxy-2-carboxylate deaminase and HypH: ketoglutarate semialdehyde dehydrogenase (EC 1.2.26).

Furthermore, the Δ^1-pyrroline-4-hydroxy-2-carboxylate deaminase (HypD) and the α-KGSA dehydrogenase (HypH) are encoded by two separated genes, *hypD* and *hypH* respectively (White et al., 2012). The Δ^1-pyrroline-4-hydroxy-2-carboxylate deaminase from *P. putida* and *P. aeruginosa* has also been recently characterized by Watanabe et al. (2012). According to new observations this enzyme belongs to the dihydrodipicolinate synthase/N-acetylneuraminate lyase

protein family (Watanabe et al., 2012). Finally, the α-KGSA dehydrogenase was first characterized by Koo & Adams (1974), who reported the induction of this enzyme by 4-L-Hyp.

A recent microarray study conducted by White et al. (2012) in *S. meliloti* showed that the fourteen genes within the *hyp* cluster are induced in the presence of 4-L-Hyp. The expression of these genes in the presence of 4-L-Hyp as the sole carbon and nitrogen source was higher compared to the expression in media with glycerol as carbon source (White et al., 2012).

Interestingly, the same study reported the induction of other genes by 4-L-Hyp. The comparison between the expression levels in the presence of 4-L-Hyp and the expression in glycerol showed that several genes were induced in addition to those present in the *hyp* cluster. Some of these genes were identified to encode for several enzymes involved in the TCA cycle such as α-ketoglutarate dehydrogenase, succinyl-CoA synthetase, phospoenolpyruvate carboxykinase and fructose phosphate aldolase. A second group of 4-hydroxy-proline inducible genes encode for enzymes involve in the Calvin-Benson cycle of CO_2 fixation. Additionally, the upregulation of genes involved in thiamine biosynthesis was also detected (White et al., 2012).

Furthermore, a number of genes involved in amino acid metabolism were over expressed in the presence of 4-L-Hyp as a sole carbon and nitrogen source. One of these genes, *smc04388*, was induced at similar level as many genes present in the *hyp* cluster, suggesting a possible role of the Smc04388 protein in the metabolism of 4-hydroxy-proline (White et al., 2012). The product of the *smc04388* gene has been annotated as an omega amine:pyruvate transaminase enzyme (CAC47872.1). Here we refer the Smc04388 protein as omega amino transaminase.

Possible role of the Smc04388 transaminase in 4-hydroxy-proline pathway

In the major mammalian catabolic pathway for 4-hydroxy-proline first described by Adams & Frank (1980), the third reaction is a transamination. In this reaction, 4-hydroxyglumate

transaminase transfers the amino group from 4-hydroxyglutamate to α-ketoglutarate resulting in the formation of L-aspartate and 4-hydroxy-2-oxoglutarate (Figure 23 in Appendix). Unlike the mammalian hydroxyproline catabolic pathway, the bacterial pathway (Figure 2) does not involve any transamination reaction. However, it is known that the P4OH2C intermediate formed in the second reaction of the pathway is spontaneously hydrolyzed in the presence of water to an open form, 4-hydroxy-2-oxo-5-aminovalerate (Adams & Frank, 1980 & Watanabe et al., 2012). The amino group of 4-hydroxy-2-oxo-5-aminovalerate is non-alpha position relative to the alpha carbon. Thus 4-hydroxy-2-oxo-5-aminovalerate could be an amino donor in a transamination reaction.

Amino transaminase enzymes

Amino transaminases are pyridoxal-5'-phosphate (PLP) dependent enzymes that play an important role in amino acid and nitrogen metabolism (Hwang et al., 2005). These enzymes were divided by Mehta et al. (1993) into four different subgroups (I, II, III and IV) according to their sequence similarities and their substrate specificities. Amino transaminases in subgroups I, III and IV are more closely related than enzymes in subgroup II. Subgroups I, III and VI are characterized by the transfer of an amino group in the α-position. The members of these subgroups are aspartate, alanine, tyrosine, histidinol-phosphate and phenylalanine amino transaminase in subgroup I; D-alanine and branched-chain amino acid amino transaminases from subgroup III and serine and phosphoserine amino transaminase in subgroup IV.

Unlike the other subgroups, amino transaminases in subgroup II share a very high sequence similarity and the presence of a distal amino group in the majority of their substrates (Hwang et al., 2005; Mehta et al., 1993 & Park et al., 2010). Observations indicated that these enzymes can only transfer an amino group in the non α-position of amino acids as well as chiral

amines (Shin et al., 2003). Five different enzymes belong to this group of enzymes: acetylornithine, ornithine, omega-amino acid, 4-aminobutyrate and diamino-pelargonate amino transaminases.

Among the amino transaminase of the subgroup II enzymes, the omega amino transaminases are of special interest, since they catalyze the formation of non-natural amino acids and chiral amines. These compounds are very desirable for pharmaceutical industries because they are the active component of many drugs. The wide substrate specificity of these enzymes combined with high reaction rate and stability make them a potential target for industrial processes (Hwang et al., 2005). However, these enzymes usually undergo product and substrate inhibition, which sometimes limit their effective industrial use. New researches are taking special interest in these matters and finding interesting solutions (Park et al., 2012).

In general, the transaminase reaction involves the transfer of an amino (NH_2) group from an amino acid or amine to a keto (=O) group of an oxo acid (keto acid). The reaction is reversible and has been described as occurring in two steps or half reactions with the requirement of pyridoxal 5'-phosphate (PLP) as cofactor (Metha et al., 1993; Shin and Kim, 2002 & Hwang et al., 2005). The following mechanism was described by Park et al. (2012), using the amino transaminase reaction between pyruvate and α-methylbenzylamine (α-MBA) as a model (Figure 3). According to these authors the first half reaction involves the oxidative deamination of the amino donor, in this case α-MBA. The amino group from α-MBA is transferred to the complex formed between the enzyme and PLP (E-PLP), and as a result the enzymatic complex is converted to E-PMP (pyridoxamine 5'-phosphate), and acetophenone is formed from α-MBA as one of the final products of the reaction. The second half reaction is the reductive amination of the amino acceptor pyruvate. In this reaction, the amino group of the E-PMP complex replaces

the carbonyl group of pyruvate molecule. As a result, the E-PLP complex is regenerated and the second product (L-alanine) is formed from pyruvate (Park et al., 2012).

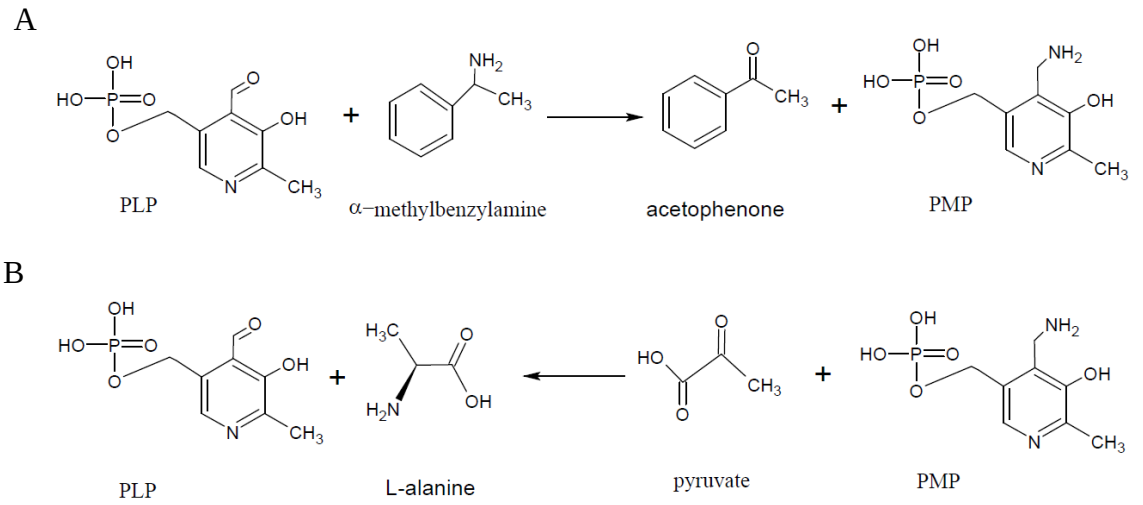

Figure 3. Transamination reaction between α-methylbenzylamine (α-MBA) as an amino donor and pyruvate as an amino acceptor. (A) Oxidative deamination of α-MBA forming acetophenone and the pyridoxamine 5'phosphate (PMP). (B) Reductive amination of pyruvate forming L-alanine and generation of pyridoxal 5'phosphate (PLP).

Omega amino transaminases

Omega amino transaminases are enzymes ubiquitously found in microorganisms. The first omega amino transaminase described to have activity against pyruvate was the taurine-pyruvate aminotransferase identified by Yonaha et al., 1976. Most recently, the omega amino transaminase characterized from *V. fluvialis* JS17, showed activity only toward L-alanine among 20 amino acids tested. Unlike the other enzymes of subgroup II it did not show reactivity with β-alanine and pyruvate was the most reactive keto acid acceptor (Shin et al., 2003). In addition, the novel amino transaminase showed reactivity towards chiral amines such as (S)- α-methylbenzylamine, (S) L-aminoindan, and (S)-1-methyl-3-phenylpropylamine, whereas no reactivity was detected towards β-alanine. The unusual substrate specificity of this enzyme along

its high sequence similarity to the amino transaminases in subgroup II allowed its classification in this subgroup as a novel omega amino transaminase (Malik, 2012).

Omega amino transaminases characterized to date have showed reactivity toward arylic and aliphatic amines, although (S)-α-methylbenzylamine (α-MBA) has been shown to be the most reactive amino donor for these enzymes (Hwang et al., 2005; Hanson et al., 2008; Shin et al., 2001; Shin and Kim, 2002; Kaulmann et al., 2007 & Koszelewski et al., 2010). As amino acceptors, these enzymes showed activity with pyruvate as well as aldehydes such as propanal, benzaldehyde and butyraldehyde (Shin et al., 2001). Regarding to the enantio-selectivity, these enzymes have preferably reactivity toward the (*S*) enantiomers. Indeed, omega amino transaminases with (*R*) selectivity are not very common in bacteria (Malik, 2012). Only one enzyme that shows reactivity toward the (*R*) enantiomer has been identified so far (Iwasaki et al., 2003; Iwasaki et al., 2006).

Despite the broad substrate specificity of the omega amino transaminases the mechanism of substrate recognition is the same among these enzymes. A model of the substrate recognition was described by Shin & Kim (2002) using the structure of the omega amino transaminase from *V. fluvialis* JS17. According to these authors the active site of these enzymes is formed by two recognition sites, one small site named the S pocket and a large site or L pocket. The small size of the S pocket is a steric exclusion for carboxylate groups and other groups larger than an ethyl group. This restriction on size imposes a steric selectivity for acidic and aromatic amino acids. In contrast, the characteristic of the L pocket, allows for the dual recognition of both a carboxylate group and a hydrophobic substituent (Shin and Kim, 2002). On the basis of these differences between both recognition sites, the S pocket has been suggested to be responsible for the

substrate specificity among omega amino transaminases (Hwang et al., 2005 & Hirotsu et al., 2005).

Recent research has found that six key residues inside the L and S pockets that are conserved among 20 different omega transaminases (Park et al., 2012). The identification of the amino acid residues involved in substrate recognition was carried out by docking simulation using the X-ray structure of the omega amino transaminase from *Pseudomonas putida*. The results showed that four of the six residues are present in the L pocket; Tyr23, Phe88, Tyr152 and Arg414. The three former are involved in hydrophobic interactions within the L pocket, whereas the Arg residue was proposed to be involved in the recognition of the carboxylate group. The other two key residues determined by this study were Trp60 and Ile262, which are both present in the S pocket and presumably involved in the steric exclusion of this site (Park et al., 2012).

Characterization of omega amino transaminases

Several omega amino transaminase enzymes have been described and characterized. Kim and colleagues have reported these enzymes in *Alcaligenes denitrificans* Y2k-2 (Yun et al., 2004), *Vibrio fluvialis* JS17 (Shin et al., 2003) and *Caulobacter crescentus* (Hwang et al., 2005). Recently, two novel omega amino transaminases from *Paracoccus denitrificans* PD1222 (Park et al., 2010) and *Ochrobactrum anthropi* have been characterized (Park & Shin, 2013).

In *S. meliloti* two putative omega amino transaminases enzymes have been annotated to be encoded by the *smc01534* and *smc04388* genes, present in the chromosome of this bacterium. The protein encoded by the *smc04388* gene contains several amino acid residues conserved among other omega amino transaminases described in previous works (White et al., 2012). However, none of these putative amino transaminases in *S. meliloti* has been characterized.

CHAPTER 2

MATERIALS AND METHODS

Bacterial strains and growth conditions

The plasmids and bacterial strains used in this study and their antibiotics sensitivities are summarized in Table 1 and 2, respectively. Luria-Bertani (LB) media contained 10 g/L of tryptone, 5 g/L of yeast extract and 5 g/L of NaCl. Minimal media (M9) was prepared with: 33.9 g/L of Na_2HPO_4, 15 g/L of KH_2PO_4 and 2.5 g/L NaCl and further supplemented with 5g/L of NH_4Cl, 1 mM of $MgSO_4$, 0.250 mM of $CaCl_2$, 1 µg/mL of biotin, 10 ng/mL of $CoCl_2$, and a carbon and/or nitrogen source as required. For solid media, 15 g of agar was added for 1 L of liquid media. All media and solutions were autoclaved before use. Carbon sources and other heat sensitive solutions were sterilized by filtration using a 25 mm syringe filter with 0.22 µm membrane (Millex-GP).

Escherichia coli strains were incubated at 37 ^{o}C, whereas *S. meliloti* and *Pseudomonas* strains were incubated at 30 ^{o}C. For *S. meliloti* LB media was supplemented with 2.5 mM $MgSO_4$ and 2.5 mM $CaCl_2$ (LBmc). Five mL liquid cultures were grown in 150 mm x 18 mm test tubes. When necessary, bigger volumes were grown in Erlenmeyer flasks using 1 media volume: 5 flask volume.

Table 1. Plasmids used in this study.

Plasmid	General characteristics	Reference
pRK600	Plasmid pRK2013 *npt*::Tn9; Cm^r	Finan et al., 1986
pUCP/PaLhpBFE	pUCP26 expression vector containing the *PaLhpB, PaLhpF* and *PaLhpE* genes; Km^r	Wanatabe et al., 2012
pUCP30T	ColE1, *oriT* from RK2 cloning vector, RK2; Gm^r	Schweiser et al., 1996
pHP45ΩaadA	derivative of pBR322 containing the Sm^r/Sp^r cassette from the R100.1 plasmid; $Sm^rSp^rAmp^r$	Prentki & Krisch, 1984
pTH2815	*smc04388* flanked with 300 nt homology regions in pUCP30T via primers 377(F) and 302(R)	This work
pTH2816	pTH2815 where *smc04388* has been disrupted by inserting a Sm^r/Sp^r resistant cassette via *NcoI*	This work
smc04388 cloning		
pTH1227	derivative of pFUS1 plasmid containing the *lacI*^{q}*-ptac* promoter for expression of native protein in *S. meliloti*; Tc^r	Finan collection
pTH2814	*smc04388* in pTH1227 via primers 4(F) and 22(R)	This work

Table 2. Bacterial strains used in this study.

Bacterial strains	Relevant characteristics	Reference
E. coli strains		
DH5α	F^-, *enA1*, *hsdR17* (r_k^-, m_k^-), *supE44*, *thi-1*, *recA1*, *gyrA96*, *relA1*, Δ(*argF-lacZYA*), U169, Φ80d*lacZ*, ΔM15	Invitrogen
MT616	MT607 (pRK600), Cm^r	Finan et al., 1986
M1993	DH5α (pTH2815); Gm^r	This work
M1996	DH5α (pTH2816); $Sp^rSm^rGm^r$	This work
Pseudomonas strains		
KT2442-oxyR1	*oxyR1*derivative of KT2442 *P. putida*; Rif^r	Hishinuma et al., 2006
M2116	KT2442-oxyR1 (pUCP/PalhpBFE), *P. putida*; Rif^r Km^r	This work
S. meliloti strains		
RmP110	Rm1021 *ptsC*$^+$; Sm^r	Yuan et al., 2006
Rm5000	derivative of SU47; Rif^r	Finan et al., 1984
RmFL1068	RmP110 *smc04388*::*gusA*/*rfp*; Gm^rSm^r	Cowie et al., 2006
RmP2510	RmP110 Δ*hypD*; Sm^r	Finan collection
RmP3081	Rm5000 *smc04388*::Ω; $Rif^rSp^rSm^r$	This work
RmP3272	RmP110 *smc04388*::Ω Δ*hypD*; Sp^rSm^r	This work

RmP3016	RmP110 (pTH2814); Tc^r	This work
RmP3020	RmP110 (pTH1227); Tc^r	This work

Table 3. Primers used in this study.

Amplified region	Forward primer	Reverse primer	Features
smc04388	F-12-6430 5' GAA GAT CTC AGG AGG ATG CCA TGA ACG CC 3'	R-Stp-12-6431 5' AAC TGC AGT CA**T TTT TCG AAC TGC GGG TGG CTC CAA GCG CT**C TTC ACC CGC TTC AAC GCA TCG 3'	Amplifies *smc04388* via restriction enzymes *Bgl*II and *Pst*I. *Strep*II tag (bolded) and stop codon (underlined) are included in reverse primer
smc04388 check out	F90 5' GTG GAA TTG TGA GCG GAT AA 3'	ML4876-seq3-gusA 5'ATA AGG GAC TCC TCA TTA AGA TAA C 3'	Primers for sequencing into the cloning site of pTH1227 vector
RmP3081 Construction	F377-12-7549 5' GCT CTA GAA TCT CCA CCA GTT CCT CCG 3'	R302-12-7550 5'AAC TGC AGG ACG GTA TCG GTG GTA TCG 3'	Amplifies *smc04388* together with 300 nucleotides flaking regions
	M13F 5' GTA AAA CGA CGG CCA GT 3'	M13R-48 5'AGC GGA TAA CAA TTT CAC ACA GGA 3'	Primers for sequencing into the cloning site of pUCP30T vector

RmP3081 and RmP3272 check out	F1-131 5' TTC CTC GCC CTC ATG CAC C 3'	R1-cassette 5' TTA CCC GAG AGC TTG GCA C 3'	Amplifies a region outside the borders of the 377 nt homology and inside the Sm^r/Sp^r resistant cassette

Antibiotic stock solutions, sterilized by filtration, were prepared in double deionized water (ddH_2O) for streptomycin (Sm), gentamycin (Gm), kanamycin (Km), neomycin (Nm), spectinomycin (Sp) and ampicillin (Amp); in 70% ethanol (high grade) for tetracycline (Tc) and Chloramphenicol (Cm); and in methanol (HPLC grade) for rifampicin (Rif). Stock solutions were kept at -20 ^oC. The concentrations of antibiotics used in media varied depending on the strain and the kind of media used. For *E. coli*, the following concentrations for liquid media were used: streptomycin at 50 µg/mL, gentamycin 5 µg/mL, kanamycin 10 µg/mL, spectinomycin 50 µg/mL, ampicillin 50 µg/mL; tetracycline 5 µg/mL and chloramphenicol 10 µg/mL. For *S. meliloti* the following concentrations were used: streptomycin at 100 µg/mL, gentamycin 30 µg/mL, neomycin at 100 µg/mL, spectinomycin 100 µg/mL, tetracycline 5 µg/mL and rifampicin 20 µg/mL. For *Pseudomonas* strains the concentrations used were: rifampicin 50 µg/mL and kanamycin 50 µg/mL. Except for *Pseudomonas* strains, double these concentrations were used when solid media was prepared.

Other reagents, such as isopropyl-β-D-1-thiogalactopyranoside (IPTG) and 5-bromo-4-chloro-3-indolyl-β-D-galactopyranoside (X-gal), were used for protein induction and positive screening of transformants. Stock solutions of IPTG and X-gal were prepared in ddH_2O and dimethylformamide respectively and filter sterilized as described previously. IPTG was added to

growing cultures at different concentrations as specified. X-gal was present in the media at the final concentration of 80 µg/mL.

Growth curve

Growth curves were performed in M9 minimal media supplemented with various carbon and nitrogen sources depending on the purpose of the experiment. Cultures were pre-inoculated in LB with the required antibiotics and incubated overnight at 30 °C. Next day cultures were reinoculated in M9 minimal media supplemented with 15 mM glucose but without any nitrogen source in order to eliminate the nitrogen stored in the cells. Cultures were incubated overnight at 30 °C and then 1 mL of these cultures was spun down and the cells washed with 0.85% NaCl twice and suspended in the same solution. Media were inoculated with the cell suspension to OD_{600} 0.05 in a total volume of 150 µL into 96 well plates. Three independent cultures were prepared for each condition. Plates were incubated at 30 °C for 48 hours and absorbance readings were taken every 15 minutes using a TECAN plate reader. At the termination of each growth curve, one of the triplicates for each sample was tested for contamination by streaking onto LB agar plates.

Expression of reporter gene GusA

The fusion library strain used in this work was previously constructed by Cowie et al. (2006). Fusion library strains were created using the *S. meliloti* suicide vector pTH1522, which contains the genes encoding for green fluorescent protein (*gfp*) and β-galactosidase (*lacZ*) in one direction and red fluorescent protein (tdimer2) and β-glucuronidase in the opposite direction (Figure 24 in Appendix).

In this work, β-glucuronidase (GusA) activity from the fusion strain RmFL1068 (RmP110 *smc04388*::*gusA*/*rfp*) was measured as a means to quantify transcription from the

smc04388 promoter. Cultures were grown overnight in LB with antibiotics at 30 °C. The next day appropriate media were inoculated at OD_{600} of 0.05 and incubated at 30°C to OD_{600} of 0.4-0.6. At this time cultures were spun down and the pellet was washed twice with 0.85% NaCl and resuspended in 1 mL of the same solution. Three independent cultures of the same strain were prepared each time.

The reaction mixture for expression measurements was prepared in 96 well plates with 15 µL of suspended cells and 85 µL of GusA buffer. GusA buffer was prepared fresh each time with 50 mM of dithiothreitol (DTT), 1 mM of ethylenediaminetetraacetic acid (EDTA), 0.0125% of sodium dodecyl sulfate (SDS) and 0.5 mg/mL of p-Nitrophenyl-D-glucopyranoside in 50 mM sodium phosphate pH 7. Each sample was prepared in triplicate. The plate was incubated at room temperature until a yellow color was visible. At this point the reaction was stopped by adding 100 µL of 1 M solution of Na_2CO_3. Absorbance readings were taking at 405nm wavelength in a TECAN plate reader (Safire) with XFlour4 Software. The Miller units of specific activity were calculated using the follow equation: OD_{405}*1000/OD_{600}*time(min)*volume(mL). The time in the equation refers to the reaction incubation time and the volume is the volume of the cell suspension added to the reaction.

PCR amplification

PCR master mixtures were performed with either commercial HIFI Taq or purified Taq enzyme in our lab by Dr. Zhang. Primers used in this study were obtained from Mobix Lab and are listed in Table 3. Final concentration of reagents in the master mixture were: 1x buffer, 1.5 mM $MgSO_4$, 0.2 mM dNTPs (Invitrogen), 0.3 µM of forward and reverse primers (Mobix), 10 ng of genomic DNA or 1 colony as equivalent (in case of performing colony PCR) and 1-2.5 units of polymerase. When performing colony PCR the colony was picked directly from an agar

plate with a sterilized pipette tip and resuspended in the PCR mixture. Both PCR reactions, colony PCR and genomic DNA PCR were set up in 25 µL final volume using sterilized ddH_2O.

The conditions of the PCR amplification reactions varied each time depending on the melting temperature (Tm) of the primers and the length of the product to be amplified. The general program used was one cycle at 94 ^oC for 5 minutes, followed by 25 cycles at 94 ^oC for 30 seconds, annealing temperature for 30 seconds, 72 ^oC for extension time: and a final cycle at 72 ^oC for 7 minutes. The annealing temperature (Ta) chosen was usually 3 ^oC less than the average Tm for both primers. The extension time was usually 1 minute per Kb of product.

Cloning and DNA manipulation

Plasmids used in this work were isolated from *E. coli* strains using the alkaline lysis SDS-Minipreparation protocol described in Molecular Cloning: A laboratory Manual (Sambrook and Russel, 2001). QIAprep spin Miniprep from Quiagen or Wizard Plus SV Miniprep Kit from Promega were used for small amounts of plasmid. QIAquick PCR Purification Kit from Qiagen was used for purification of restriction digestions and PCR products. Extraction and purification of DNA from agarose gel was carried out using Qiagen QIAquick Gel Extraction Kit. DNA samples were diluted in sterilized ddH_2O for quantification. Absorbance readings were taking using an Eppendorf BioPhotometer 6131. Agarose gel at 0.8 or 1% of agarose (BioShop, biotechnology grade) depending on the sizes of the DNA fragments to be loaded, were prepared for DNA electrophoresis. Gel pictures were taking under UV light using a MultiImage II-AlphaImager HPsystem.

Restriction digestions were prepared using 0.5 to 1 units of restrictions enzymes per reaction depending on the amount of the DNA to be digested. The reactions were incubated at 37

^{o}C for 4 hours for plasmid DNA digestions and from 6 to 8 hours for PCR products. In all cases the DNA product was stored at -20 ^{o}C.

Ligation reactions were performance with 2 units per reaction of T4 DNA ligase (New England Biolabs) in buffer provided by the same manufacturer. The ratio of free end (picomoles ends per microgram of DNA) of insert and plasmid used were 3:1 to 5:1. The final volume was adjusted to 20 µL with sterilized ddH_2O. The reactions were incubated overnight at 16 ^{o}C. When it was necessary reactions were kept at -20 ^{o}C for storage.

Cloning of the smc04388 gene into pTH1227 vector

The *smc04388* gene (1338 bp) was PCR amplified. The forward primer (F-12-6430) was located 4 nucleotides upstream the start codon of the *smc04388* and did not include the putative promoter of this gene. The reverse primer (R-Stp-12-6431) included 22 nucleotides upstream from the stop codon of the gene and also a *Strep*II-tag to allow purification of the protein. The stop codon in the sequence of the gene was not included in the primer in order to obtain translation of the *Strep*II-tag. Instead, an alternative stop codon was included in the primer after the tag sequence.

The PCR amplified fragment was digested and ligated into the pTH1227 Tc^{r} vector *Bgl*II and *Pst*I sites. Digestion and ligation reactions were carried out as described previously in this section. The pTH1227 vector of 10.5 Kb of length was constructed previously by (Cheng J, Finan lab). It carries the *lacI*^{q}*-ptac* (pMAL-c2x) promoter, which allows expression of native proteins in *S. meliloti*. In addition the *gusA* gene located downstream of the cloning site allows for quantification of the expression of the protein. The integrity of the *smc04388* gene in the pTH2814 recombinant plasmids was verified by sequencing using the primers F90 and ML4876-seq3-*gusA*.

Transformation of DNA into bacteria

Plasmid DNA was transformed into *E. coli* DH5α following the protocol described in Molecular Cloning Laboratory Manual (Sambrook & Russel, 2001). *E. coli* DH5α was grown in LB until culture reached OD_{600} 0.35-0.4. Fifty mL cultures were transferred to a falcon tube and kept on ice for 10 minutes. Next, cultures were centrifuged at 4000 g for 10 minutes at 4 ^{o}C. Pellet was recovered and resuspended in 30 mL of ice cold Mg-$CaCl_2$ solution, made of 80 mM $MgCl_2$ and 20 mM $CaCl_2$. Cells pellets were recovered by centrifugation at the same speed and resuspended in 1 mL of ice cold $CaCl_2$ (0.1M). The cells were kept in this solution on ice at 4 ^{o}C overnight. Next day, aliquots of 200 µL were placed in sterilized Eppendorf tubes and frozen at -80 ^{o}C. Competent cells were defrosted on ice when they were needed. Ten to fifteen µL of ligation mixture was added per tube containing 200 µL of competent cells.

Conjugal transference of DNA

Plasmids-carrying cloned DNA sequences were transferred to *S. meliloti* via conjugation using *E. coli* MT616 (Cm^r) as the helper strain. This strain carries the pRK600 plasmid containing the *tra* genes required for the transfer of DNA (Finan, 1986). The *E. coli* donor strain, the *S. meliloti* recipient and the helper strains were grown in LB with necessary antibiotics to OD_{600} 0.8 to 0.9. At this time 1 mL of each culture was spun down at 9000 g. The resultant pellet was washed twice with 0.85% NaCl, resuspended in 100 µL of the same solution and 25 µL was spotted onto LB agar in a plate. Suspension of recipient strain as well as mixtures of the helper and the recipient strains, and the donor and helper strains; were spotted separately as controls. Plates were incubated at 30 ^{o}C overnight.

The next day, the mating spots were collected with a sterilized inoculation loop and resuspended in 1 mL of 0.85% NaCl. A dilution series between 10^0 to 10^{-7} was prepared from

this solution, plating 0.1 mL according to the number of cells expected to grow. In each case specific antibiotics were used in order to select for each of the donor, recipient or transconjugant strains. The frequency of conjugation was calculated by dividing the number of transconjugant obtained by the number of recipients. Desired transconjugant strains were streak purified three times on selective media and frozen at -80 ^{o}C.

Construction of a single smc04388 mutant

The *smc04388* omega amino transaminase mutant was created by disruption of the *smc04388* gene in *S. meliloti*-RmP110 wild type (Sm^r). The DNA fragment encoding for the *smc04388* gene and about 300 bp upstream and downstream was amplified by PCR using F377-12-7549 and R302-12-7550 primers. The forward was located at the -377 upstream position from the start codon of the gene, whereas the reverse primer was located at 302 bp downstream from the stop codon of the *sm04388* gene. The amplified PCR segment comprising 300 nt downstream and upstream of the gene was cloned into *Xba*I and *Pst*I sites of the pUCP30T (Gm^r) vector (Figure 25 in Appendix). The resulting recombinant plasmid (pTH2815) was verified by sequencing using M13F and M13R-48 primers. After verification, the pTH2815 plasmid was digested with *Nco*I and blunt ends were produced with Klenow DNA polymerase to allow further insertion of the omega cassette. Blunt end reactions were prepared with *Nco*I digested end on pTH2815, 1 unit of enzyme and 0.1 mM of dNTPs in Buffer No.2 (New England Biolabs). Reactions were incubated for 15 minutes at 12 ^{o}C.

The omega cassette (Sm^r/Sp^r) was obtained from the pHP45ΩaadA ($Sm^r/Sp^r/Amp^r$) vector. The J299 *E. coli* strain harbouring the pHP45ΩaadA vector (Figure 26 in Appendix) was grown in 50 mL of LB with Amp. The DNA plasmid was obtained by alkaline lysis with SDS-Midipreparation following the protocol described in Molecular Cloning: A laboratory Manual

(Sambrook and Russel, 2001). The purified plasmid was digested with *Sma*I to obtain the Sm^r/Sp^r resistant cassette. *Sma*I sites are located in both sides of the cassette and *Sma*I produced blunt ends allowing insertion of the omega cassette in the both possible directions. The omega cassette was ligated into the *Nco*I restriction site, previously blunt end. This site is localized 230 nt from the start codon of *smc04388*. The resultant recombinant plasmid pUCP30T::*smc04388*Ω $Sm^r/Sp^r/Amp^r$ was transformed into *E. coli* DH5α strain competent cells. The plasmid harbouring just the *smc04388* without any disruption was also transforms as a control. Positives clones were selected by screening onto LB with Sm, Sp and Gm antibiotics. The correct insertion of the resistant cassette into the sequence of *smc04388* was verified by restriction digest. Restriction sites for *Sph*I allow determine the direction in which the omega cassette was inserted in the recombinant plasmid, since there is only one cut site for this enzyme inside the omega cassette, the *smc04388* gene and the parental plasmid respectively. The restriction fragments obtained by digestion are shown in Figure 27 in Appendix. Moreover, the genotype of the mutant strain was confirmed by colony PCR using F1-131 and R1-cassette primers.

Construction of a double smc04388 hypD mutant

The *smc04388 hypD* double mutant was created by transducing the Δ*smc04388*::Ω Sp^r/Sm^r resistant cassette into the RmP2510 (RmP110- Δ*hypD*) mutant strain (Sm^r). RmP2510 was grown in LBmc with Sm overnight at 30 ^oC. Next day fresh media was reinoculated with overnight cultures to OD_{600} 0.05 and incubated until OD_{600} 0.4. At this point 0.1 mL of undiluted RmP110 ΦM12 phage lysate (Finan *et al*., 1984) was added and left overnight in incubation at 30 ^oC. Next day 0.2 mL of chloroform was added to the RmP2510 phage lysate. The final solution was briefly mixed by vortex and diluted 1:25 in fresh LBmc media.

The recipient strain RmP3081 was incubated overnight to an OD_{600} higher than 1.5. Fifty hundred µL of the culture were taken and mixed with 500 µL of the phage lysate dilution follow by incubation for 20 minutes at 30 ^{o}C. After incubation the cells were spun down and washed twice with 0.85% NaCl. The pellet was resuspended in 0.5 mL of 0.85% NaCl. From this suspension 0.2 mL were plated onto LB supplemented with Sp to select transductants. Desired transductants strains were streak purified three times on selected media and frozen at -80 ^{o}C.

SDS-PAGE

SDS-PAGE gel for electrophoresis of protein was prepared following the protocol described in Molecular Cloning: A Laboratory Manual (Sambrook and Russel, 2001). The concentration of acrylamide in gel varied from 8 to 12% depending on the nature of the samples to be loaded. Samples from whole cells were prepared from fresh bacterial cultures. Volumes of culture for preparation of proteins were taken depending on the cell density of each culture. The equation $V*OD_{600}=3.5$ was used to calculate the volume of cells used in each case in order to keep similar the amount of cells in each sample.

All cell samples were spun down at 9000 g for 1 minute and washed with ddH_2O. The final pellet was resuspended in 60 µL of ddH_2O. For liquid samples no preparation was needed. Samples were then mixed with SDS sample buffer (50 mM Tris-HCl buffer pH 6.8, 2% SDS, 1% β-mercaptoethanol, 12.5 mM EDTA, 10% glycerol, 0.01% bromophenol blue and boiled for 10 minutes. Next, samples were spun down at 9000 g for 3 minutes and 5 or 10 µL of the supernatant of each sample was loaded onto the gel. The electrophoresis was performed using a running buffer containing 25 mM Tris, 200 mM Glycine and 1% SDS, for 50-70 minutes at 150 mV. When the dye front close to the bottom of the gel, the gel was removed and stained with 30% methanol, 20% acetic acid and Comassie blue (0.25%) for at least 4 hours. Follow the

staining step the gel was destained with a solution containing 40% methanol, 10% acetic acid in ddH_2O until the bands were clearly visible.

Bradford Assay for protein quantification

The reaction was prepared with Bradford assay reagent (Bradford, 1976) purchased from BioRad, using 5 to 10 µl of samples in 1 mL reaction. After vortexing the absorbance at 595 nm was measured for each reaction. Two dilutions from the same unknown sample were tested. The reaction for each dilution was prepared in triplicate. A control with ddH_2O instead of sample was included every time the assay was performed. Unknown concentrations of protein were calculated using the protein standard curve (Figure 28 in Appendix) and divide by the amount of sample added to each reaction to get the final concentration of protein.

Expression and purification of the Smc04388 omega amino transaminase

The RmP3016 strain harbouring the recombinant plasmid pTH1227*::smc04388* was grown in 1.5 liters of LBmc with Tc. Cultures were incubated at 30 ^oC to an OD_{600} of 0.4-0.5. At this time 0.4 mM of IPTG was added to the media to induce the Smc04388 omega amino transaminase enzyme. Cultures were re-incubated at 30 ^oC for about 16 hours more (overnight). After this time the cultures were spun down for 10 minutes at 9000 g in a Beckman centrifuge using a JLA-16.250 Beckman rotor. The resultant pellet was washed twice with 0.85% NaCl and the dry weight was determined. The pellet of about 8.6 g was resuspended in 20 mL resuspension buffer (Buffer W: 50 mM Tris-HCl pH 8, containing 150 mM NaCl, 1 mM of EDTA, 20 µM of PLP). When necessary the cell suspension was frozen at -20 ^oC.

French press

Cells were lysed in a French press using the equivalent of 350 OD_{600} units in a volume of 35 mL. The maximum volume that can be used in the medium French press cell is about 20 mL.

For this reason the cell suspension was divided in two equal fractions and the French press was carried out separately for each fraction. The cell suspension fractions and the French press cell were kept at 4 ^{o}C during the entire process. The French press was operated at 1000 psi of pressure. Samples were processed four times until they had a clear, brown color. The final recovered lysate has the equivalent of 50 OD_{600} units out of 350 OD_{600} units after the French press, indicating that more than 85% of lysis occurred.

Ultracentrifugation

Cell lysates from the French press was immediately spun down at low speed (4000 g) for 15 minutes at 4 ^{o}C in order to remove whole cells. The clear lysate was further centrifuged in a Beckman Ultracentrifuge at 245,000 g for 60 minutes at 4 ^{o}C. Due to the large volume of sample a SW41 Ti Beckman rotor of 30 mL total capacity was used. Each of the 6 buckets of the rotor was pre-chilled on ice and 5 mL of clear lysate was dispensed to each one. Because the weight of each bucket is crucial for the ultracentrifugation process, the weight of each bucket containing the lysate was adjusted to be the same (to 2 decimal points within 0.01 g), using an analytical balance. After ultracentrifugation the clear lysate was recovered from each bucket and pooled together in a Falcon tube previously pre-chilled on ice. The pellet from ultracentrifugation was resuspended in the same original volume of 5 mL and samples were frozen at -20 ^{o}C for further analysis.

Purification

The Smc04388 protein was purified from the clear lysate using *Strep*-Tactin® Superflow® high capacity column (500 nmole/mL). The purification process was carried out following the protocol included in the Superflow® manual available at the web site, (Twin-) Strep-tag Purification Short protocol (http://www.iba-lifesciences.com). A 30 mL glass

purification column was packed with 8 mL of resin. The column was washed with the same resuspension buffer (Buffer W) described above. All the clear lysate (28 mL in total) containing about 44.7 mg of protein/mL (determined by Bradford assay) was passed through the column. Eight mL of column was the smallest volume required to bind most of the strep recombinant protein to the resin. Next the column was wash several times with Buffer W to remove the non-specific binding proteins. The last wash fraction eluted from the column was examined using Bradford assay to verify there was no more protein coming through the column. After the wash the recombinant Smc04388 protein was eluted from the column with elution Buffer (Buffer E), containing 50 mM Tris HCl pH 8, containing 150 mM NaCl, 1 mM of EDTA, 20 µM of PLP and 2.5 mM desthiobiotin. Elution fractions were collected in 0.5 or 1 mL depending on the amount of protein expected to be eluted. The amount of protein was quantified during the whole process by Bradford assay.

Dialysis

Fractions eluted from the column were pooled into two portions according to the amount of protein in those fractions, each containing about 8 and 7.5 mL. Both portions were dialyzed against 50 mM Tris-HCl buffer pH 8, 1 mM $MgSO_4$, 10% glycerol and 50 µM PLP. The pooled portions were accommodated into standard cellulose dialysis tubing (25 mm) previously pre-washed and boiled with a solution of 2% $NaHCO_3$ and 1 mM EDTA. The tubing containing the protein solution was tied and placed in a beaker containing with a large volume (300 times) of dialysis buffer. Dialysis was carried out at 4 ^{o}C overnight and the dialysis buffer was changed three times during this time. The resultant protein solution was aliquoted in small volumes of 20 or 200 µL into 1.5 mL Eppendorf tubes pre-chilled on ice. Protein was frozen at -80 ^{o}C.

Amino transaminase enzymatic assay

Enzymatic reactions to detect amino transamination were performed using an UV spectrophotometric assay described by Schatzle et al., (2009). Unless specified otherwise, the reaction mixture was prepared with 2.5 mM α-methylbenzylamine (α-MBA) as amino donor, 2.5 mM Na-pyruvate as amino acceptor, 0.02 mM of pyridoxal 5'- phosphate (PLP) in 100 mM Tris-HCl buffer pH 9. The reaction was started by adding 10-20 μL of crude extract or 5 μL of purified protein in a final volume of 1 mL. Where necessary, samples were diluted in order to get the initial rate of the reaction. Every time the assay was carried out a control reaction was prepared adding everything but the enzyme. The formation of acetophenone was detected at 245 nm. Each reaction was repeated three times and the amount of acetophenone produced was calculated using the molar extinction coefficient of 12 $mM^{-1}cm^{-1}$ reported by Schatzle et al., (2009).

Preparation of cells extracts

Cell extracts were prepared by sonication. Strains were grown in 100 mL of LBmc with the required antibiotics. The *hyp* cluster genes and other genes including *smc04388* were induced by adding 5mM of 4-L-Hyp to the media. The cells were spun down and the pellet was washed twice with 0.85% NaCl. Cell pellets were resuspended in buffer containing 100 mM Tris pH 8, 150 mM NaCl, 1 mM EDTA and 20 μM PLP. Samples for sonication were placed in 1.5 mL Eppendorf tubes with an OD_{600} about 10. Sonication conditions were: cycle continuous, Duty cycle 40, Timer: Hold, output 4. The samples were exposed about 10 times for 10 seconds and 3 minutes on ice in between until OD_{600} values were around 85% less than the initial OD. The lysate was spun down at 9000 g for 20 minutes to remove the unlysed cells. Clear lysates were frozen at -80 ^{o}C after the addition of 10% glycerol.

Malate dehydrogenase assay

Malate dehydrogenase activity was used as a control for the quality of cell extracts. The reaction assay used in this work was described previously by Driscoll & Finan (1993). Reaction mixtures prepared in 1 mL total volume containing 100 mM Glycine-NaOH pH 10, 90 mM sodium –L-Malate and 2.5 mM NAD^+. Reactions were started by adding 2-5 µL of cell extracts. When necessary dilutions of cell extracts were used. Each sample was measured in triplicate and a control reaction without cell extract was carried out each time the assay was performed. Absorbance readings were taken at 340 nm using a Cary 1E UV-visible spectrophotometer. Malate dehydrogenase specific activity (MLDH) was expressed as nmole of NADH produced per minute per mg of protein using the follow equation: OD_{340}*1000/time(min)*6.22*mg of protein.

Purification of cis-4-hydroxy-D-proline dehydrogenase from P. putida

Two recombinant plasmids (pUCP/PaLhpBFE and pUCP/PpLhpB) containing the cloned coding sequence for the *cis*-4-hydroxy-D-proline dehydrogenase (D-HypDH) enzyme from *P. putida* and *P. aeruginosa* were kindly donated by Dr. Wanatabe from the Faculty of Agriculture of Ehime University, Japan. The *PaLhpBFE* genes encode for the D-HypDH enzyme from *P. aeruginosa* whereas the *PpLhpB* encodes for the *P. putida* enzyme (Wanatabe et al., 2012). The plasmid pUCP/PaLhpBFE was transformed into *E. coli* DH5α and further conjugated into *P. putida* strains, KT2442 and KT2442-OxyR1. Transformation and conjugation were carried out following procedures described above. Transconjugants were selected in LB with Rif (50 µg/mL) and Km (50 µg/mL). Desired transforms strains were streak purified three times and frozen at -80 ^oC.

To purify the D-HypDH enzyme the KT2442-OxyR1 *P. putida* strain (M2116) harbouring the plasmid pUCP/PaLhpBFE was grown in 2 liters of LB with 50 µg/mL of Km and Rif. Cultures were incubated at 30 ^{o}C overnight. Next day cells were spun down and washed twice with 0.85% NaCl. The resultant pellet (about 10g) was resuspended in lysis buffer containing 50 mM sodium phosphate buffer pH 8, 2 mM $MgCl_2$, 300 mM NaCl, 1% Tween 20 and 10 mM imidazole. Approximately 4 mL of Lysis buffer were added for 1 g of pellet. The cells were lysed using French Press and following the protocol described before in this section. After French Press the cell lysate was centrifuged at low speed of 4000 g for 10 min at 4 ^{o}C to remove unlysed cells. The resultant supernatant was centrifuged at 245,000 g for 60 minutes at 4^{o}C using a Beckman ultracentrifuge and following the procedure described previously.

The recombinant His-tag protein was purified using a Metal Affinity Resin of Co^{2+}, TALON®Metal Affinity Resin. The purification process was carried out according to the manual available online for this kind of resin (http://www.clontech.com). Any change made to this protocol is specified in this section. A 10 mL portion of the clear lysate was passed through 6 mL of resin previously equilibrated. The total amount of protein passed through the resin was about 445 mg. After the binding step the resin was washed two times with the wash buffer (Buffer W: 50mM sodium phosphate buffer pH 8, 2 mM $MgCl_2$, 300 mM NaCl, 0.1% Tween 20, 20 mM Imidazole) to remove the un-specific binding proteins from the column. Finally, the protein was eluted with 50mM sodium phosphate buffer pH 8, 2 mM $MgCl_2$, 300 mM NaCl, 0.1% Tween 20 and 250 mM Imidazole. Elution fractions were collected in volumes of 0.5 or 1 mL depending on the mount of protein expected to be eluted. Fractions were separated in two separated tubes and both protein solutions were dialyzed against 50 mM Tris-HCl buffer pH 9, 2 mM $MgCl_2$, 20% glycerol. Dialysis was carried out during 18 hours in total and following the same protocol

described above. The protein was kept at -80 ^{o}C in small volumes. The Table 7 and Figure 29 in Appendix summarize the process of purification.

Enzymatic Assay for cis-4-hydroxy-D-proline dehydrogenase

The activity of the purified *cis*-4-hydroxy-D-proline dehydrogenase (D-HypDH) protein was determined using the enzymatic assay described by Watanabe et al., (2012) (Figure 30 in Appendix). The reaction mixture contained 4-D-Hyp as a substrate, 0.06 mM phenazine methosulfate (PMS) as electron transfer and 0.25 mM iodonitrotetrazolium chloride (INT) as electron acceptor in 50 mM Tris-HCl buffer pH 9. 5. Purified enzyme (10-20 µg) was added to the reaction mixture and the reaction was started by adding 100 mM or 50 mM of 4-D-Hyp. A control reaction was carried out containing buffer instead of 4-D-Hyp. The absorbance at 490nm was measured for 2 or 4 minutes depending on the rate of the reaction using a Cary 1E UV-visible spectrophotometer. Reactions were carried out in triplicate and the specific activity was calculated by the equation bellow:

$SA = OD_{490}$/ time (min)*ϵ (INT)*mg of protein

Where ϵ is the absorption coefficient for INT at 490 nm = 15 mM^{-1} cm^{-1}

Analysis of L-alanine formation

L-alanine was detected by single quadruple mass spectrometry (MS) and coupled to capillarity electrophoresis (Hewlett Packard 3D CE) with electron spray ionization (ESI) coaxial sheath-liquid sprayer interface (Agilent Technologies, Waldbronn, Germany). HPLC pump (Agilent Technologies 1260 Infinity) was used to supply sheath-liquid (60:40 MeOH/H_2O with 0.1% formic acid) at the rate of 10 µL /min. All MS analysis was performed using 10 L/min drying gas flow and 10 psi nebulizer pressure at 300 ^{o}C for ESI. Prior to MS analysis, analyte was separated by CE using 110 cm uncoated fused-silica capillary (Polymicro Technologies, AZ,

USA) with 50 µm internal diameter at 25 °C under 30 kV voltage application. All samples were filtered using a 30 KDa molecular filter to remove protein that could interfere with the analysis. Ornithine was added to each sample to a final concentration of 50 µM as internal standard. 1 M formic acid with 15% acetonitrile (pH 1.80) was used as back ground electrolyte (BGE) for all analysis. Samples were injected hydrodynamically with 50 mbar pressure for 10 seconds. The peaks were identified by their relative migration times to that of ornithine and their mass to charge ratios. The masses estimated for 4-hydroxy-proline, P4OH2C and L-alanine were 132, 130 and 90 respectively. The concentration of L-alanine was estimated using external calibration curves (Figure 31 in Appendix) generated by calculating the relative peak area (RPA) of L-alanine to that of ornithine.

CHAPTER 3

RESULTS

Omega Amino transaminases in S. meliloti

In the genome of *S. meliloti* there are two genes, *smc04388* and *smc01534* (Capela et al., 2001), annotated as omega amino transaminases (Table 4). The annotation of these enzymes was based on their sequence similarities with other characterized omega transaminases.

Table 4. Omega amino transaminases from *S. meliloti*.

Gene	Location	No. amino acids	Classification	Annotation
smc04388	Chromosome	445	Amino transaminase subgroup II	Omega amino acid pyruvate aminotransferase
smc01534		442		

The annotation suggests that these enzymes might catalyze the reversible transamination reaction between L-alanine and 3-oxopropanoate, producing pyruvate and β-alanine. No characterization of Smc04388 or Smc01534 has been performed and the natural substrates or

reactions in which these two enzymes are involved in the cells have not been reported. White et al., 2012 reported that *smc04388* gene was induced in cells growing on *trans*-4-hydroxy-L-proline suggesting that smc04388 may play a role in 4-hydroxy-proline catabolism.

A multiple protein alignment using ClustalOmega of the Smc04388 protein sequence with of seven other characterized omega transaminases from *Rhodobacter sphaeroides, Pseudomonas putida, Pseudomonas fluorescens, Ralstonia solanasearum, Paracoccus denitrificans, Acinetobacter baumannii* and *Chromobacterium violaceum* revealed Smc04388 is most similar to the transaminases from *C. violaceum*, *P. putida*, *P. fluorescens* and *A. baumannii* (53%, 50%, 49% and 46% of identity, respectively) (Figure 4). It was interesting to find that the omega amino transaminases from the other two α-proteobacteria *P. denitrificans* and *R. sphaeroides* (36%, 31% of similarity, respectively) are less similar to the Smc04388 protein from *S. meliloti* which belong to the same subfamily. Lastly, the transaminase from the β-proteobacteria *R. solanasearum* shared 34% of similarity with the omega transaminase from *S. meliloti*.

It was found 43 identical residues that are conserved among the seven omega amino transaminases and the Smc04388 transaminase (Figure 4). Three of these highly conserved residues (152, 258 and 287 in Figure 4) are present in the active site of the omega amino transaminase from *P. putida*. Aspartic acid (258) is a key residue found in these proteins. It has been reported that this amino acid plays a role in the hydrogen bond formed between the enzyme and PLP (Yun et al, 2004). The Tyr152 is involved in the hydrophobic interactions present in the L-pocket of the active site of the transaminase from *P. putida* (Park et al., 2012). The Arg411 residue is conserved in Smc04388 and five other omega amino transaminases and this residue is

identified to be involved in hydrophobic interactions located in the L-pocket of the *P. putida* enzyme (Park et al., 2012).

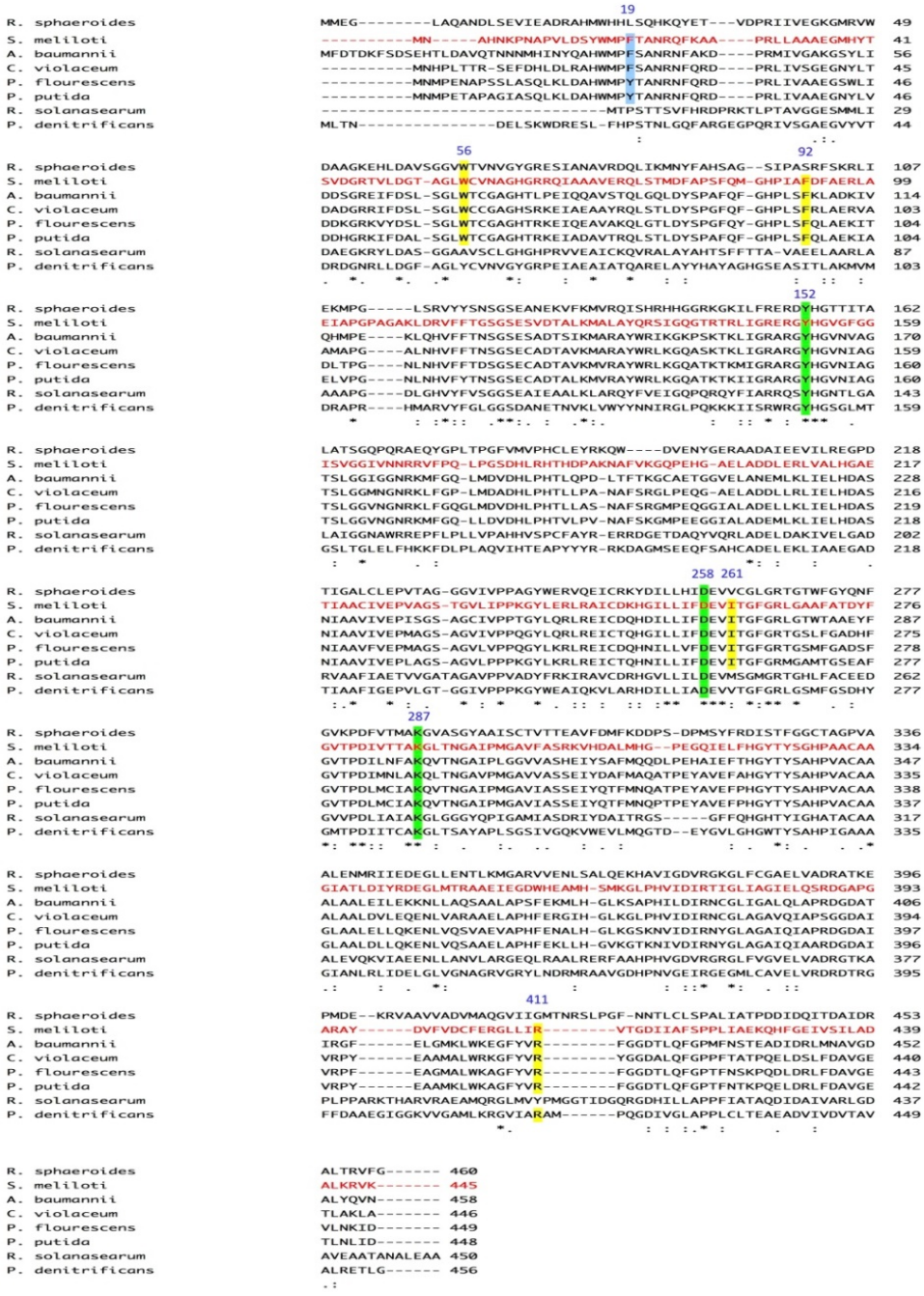

Figure 4. Multiple alignment of protein sequences from known omega amino transaminases and the putative Smc04388 transaminase from *S. meliloti*. Proteins were from: *Rhodobacter sphaeroides* (ACM02193),

Sinorhizobium meliloti (NC_003047), *Acinetobacter baumannii* (ACJ42702),*Chromobacterium violaceum* (AAQ59111), *Pseudomonas fluorescens* (NC_012660), *Pseudomonas putida* (ADR58336), *Ralstonia solanasearum* (CAD13610) and *Paracoccus denitrificans* (ABL68404). The amino acids residues highlighted in the sequences are the conserved residues that have been reported to play an important role in the substrate recognition (Park et al., 2012 & Yun et al., 2014). The numbers in blue correspond to the number of these residues in the sequence of the enzyme from *S. meliloti*. The alignment was made using the ClustalOmega program from EMBL web site (http://www.ebi.ac.uk/Tools/msa/clustalo/).

A phylogenetic tree of the eight omega amino transaminases showed the *S. meliloti* Smc04388 in a separate group, phylogenetically close to the enzymes from *C. violaceum* and *A. baumannii* and the two *Pseudomonas* species (Figure 6). In contrast, the enzymes from *P. denitrificans*, *R. solanasearum* and *R. sphaeroides* appear more distant from the *S. meliloti* transaminase.

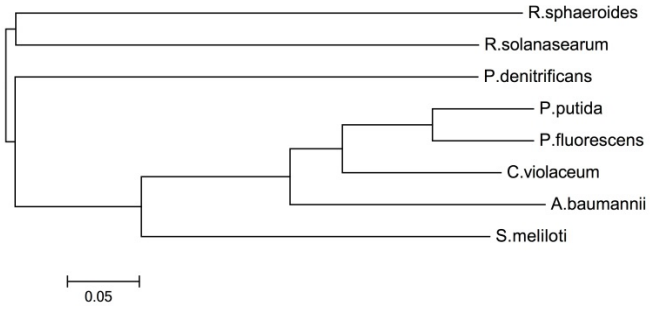

Figure 5. Representation of the phylogenetic tree of known omega amino transaminases and the putative Smc04388 transaminase from *S. meliloti* (NC_003047)**.** The tree was constructed based on the full-length sequences of proteins of (from the top to the bottom): *Rhodobacter sphaeroides* (ACM02193), *Ralstonia solanasearum* (CAD13610), *Paracoccus denitrificans* (ABL68404), *Pseudomonas putida* (ADR58336), *Pseudomonas fluorescens* (NC_012660), *Chromobacterium violaceum* (AAQ59111), *Acinetobacter baumannii* (ACJ42702) and *Sinorhizobium meliloti* putative. The scale bar indicates an evolutionary distance of 0.05 amino acid substitutions per position. The tree was made using the Clustal Omega program from EMBL web site (http://www.ebi.ac.uk/Tools/msa/clustalo/).

Expression of the smc04388 gene

A previous transcriptome study of *S. meliloti* found that the *smc04388* gene was up regulated (20 fold) in the presence of 4-L-Hyp as the sole carbon source versus its expression in media containing glycerol and ammonium (White et al., 2012). To confirm and extend those results we used the GusA promoter fusion strain RmFL1068 (RmP110 *smc04388*::*gusA*/*rfp*) from a previously constructed fusion library (Cowie et al., 2006). The genotype of the fusion strain RmFL1068 and wild type RmP100 are represented in Figure 6.

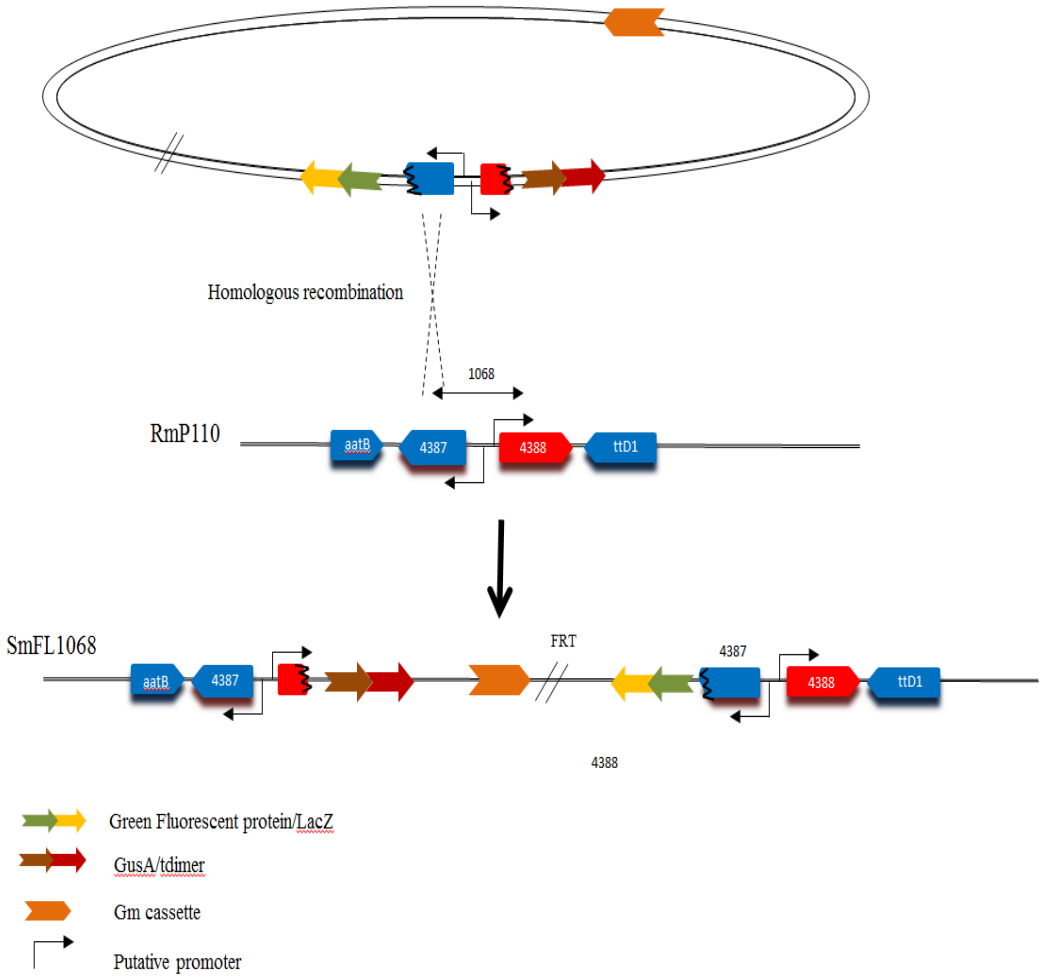

Figure 6. Schematic representation of the SmFL1068 fusion library strain. Genes are transcribed in the direction that has been indicated with arrows. The interruption of some genes by black zigzag lines indicates the

fusion resultant due to recombination. The location of the fusion in wild type strain RmP110 has been indicated with the black arrow above the gene.

The *smc04388*::*gusA* fusion strain RmFL1068 was assayed for β-glucuronidase (GusA) activity in minimal media containing: 15 mM glucose and 20 mM ammonium chloride, 15 mM glucose and 10 mM 4-L-Hyp as nitrogen source, and 10 mM 4-L-Hyp, or 10 mM L-proline or 10 mM D-proline as the sole carbon and nitrogen source. Wild type strain RmP110 without any reporter gene fusion was cultured in the same media and assayed as a negative control.

It was found that the specific activity of GusA in Miller units (Figure 7) was greatest for cells grown with 4-L-Hyp in the media as the carbon or nitrogen source. The highest expression of the omega transaminase gene was observed when 4-L-Hyp was added to the media as the sole carbon and nitrogen source. The expression was 7 fold higher than the background expression in minimal media with glucose and ammonium chloride. It was also observed that the *smc04388* gene was overexpressed 4 fold with 4-L-Hyp as the nitrogen source and glucose as the alternative carbon source (red bar of gluc+Hyp in Figure 7). No expression of *smc04388* was observed in cells grown with D-proline or L-proline as in both cases, the activity of GusA was similar to background levels found in the media containing glucose and ammonia as carbon and nitrogen source, respectively (Figure 7). These results are consistent with previous reports of White et al. (2012).

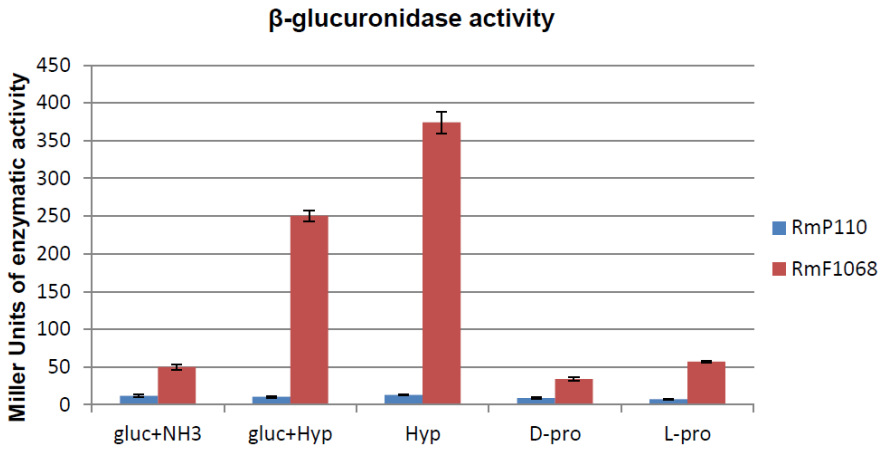

Figure 7. Expression of the *smc04388* gene from *S. meliloti*. Blue bars corresponds to RmP110 wild type strain without any gene fusion, whereas red bars corresponds to RmFL1068 fusion library strain with the GusA reporter gene and the red fluorescent protein (RFP) fused to the promoter of the *smc04388* gene (RmP110 *smc04388*::*rfp*$^{+}$/*gusA*). Cells were cultured in M9 minimal medium containing: 15 mM glucose and 20 mM Ammonium chloride (gluc+NH3); 15 mM glucose and 10 mM 4-L-Hyp (gluc+Hyp); 10 mM 4-L-Hyp (Hyp); 10 mM D-proline (D-pro) and 10 mM L-proline (L-pro). With the exception of D-proline, cultures were grown overnight. Cultures with D-proline were grown for 24 hours. The assay was performed in triplicate; the bars correspond to the average from three independent cultures and the error bars represent standard errors.

Construction of a single and double mutant of the smc04388 gene

The induced expression of *smc04388*in the presence of 4-L-Hyp suggested a possible involvement of this omega transaminase in the metabolism of 4-hydroxy-proline. To address this hypothesis, two mutant strains lacking the Smc04388 transaminase were generated.

A single mutant of the *smc04388*gene was made by inserting a Sm^{r}/Sp^{r} cassette into the *smc04388* gene in a rifampicin resistant (Rif^{r}) wild type strain, Rm5000 (Figure 8A). For this construction, the sequence of *smc04388* including regions 377 bp downstream and 302bp upstream of *smc04388* was amplified by PCR and cloned into *Xba*I and *Pst*I restriction sites present in the pUCP30T (Gm^{r}) vector. Next, the omega cassette Sm^{r}/Sp^{r} was ligated into a

restriction site for *Nco*I located 230bp after the start codon of the *smc04388* gene. The resultant clone was transferred into *S. meliloti* Rm5000 and Gm^s double recombinants were selected on LB with Rif and Sp.

The genotype of this mutant was confirmed by PCR amplification (Figure 8B). One of the primers was designed to be outside the DNA fragment cloned into pUCP30Tand the second one inside the Sm^r/Sp^r cassette. The forward primer was located at 130bp downstream the forward primer used for amplification of the DNA fragment, whereas the reverse primer was located inside the Sm^r/Sp^r cassette at nucleotide 154. The expected PCR product was about 800bp and it was found only in the two mutants strains and not in the wild type strains (Figure 8B), indicating that these mutant strains have inserted the Sm^r/Sp^r cassette in the *smc04388* gene. The final genotype of the single mutant RmP3081 in *S. meliloti* 1021 is represented in Figure 8C.

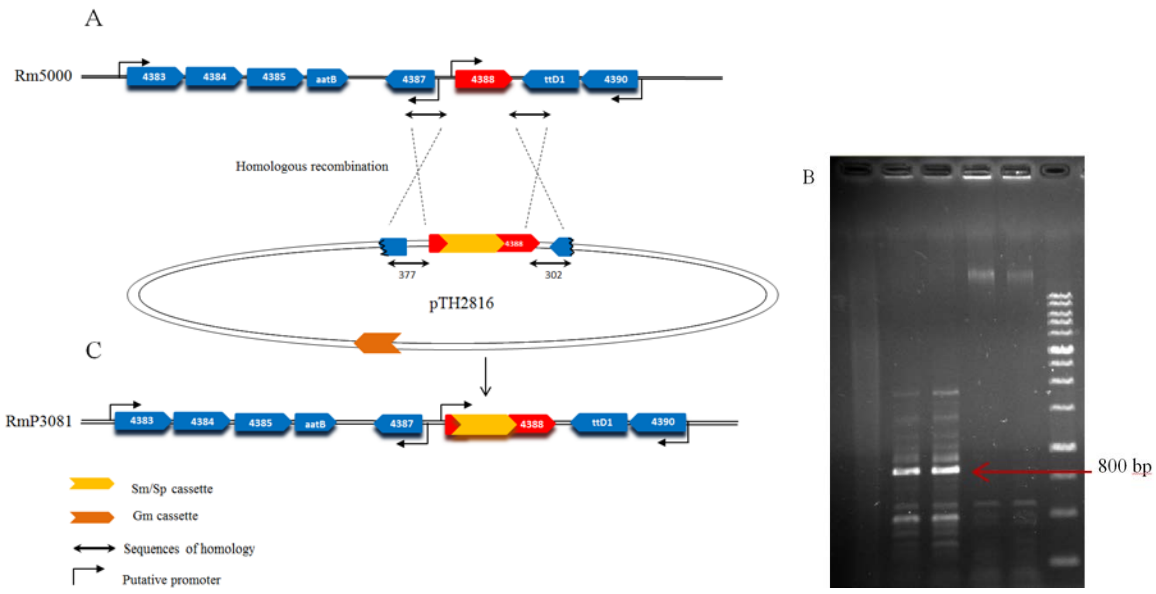

Figure 8: Disruption of the *smc04388* gene by insertion of an omega cassette Sm^rSp^r. (A) Double recombination between the *S. meliloti* Rm5000 wild type and about 300 nucleotides upstream and downstream of the *smc04388* gene cloned into pUCP30T Gm resistant vector creating the recombinant plasmid pTH2816. The omega cassette was inserted in a *Nco*I site located at 230 bp after the start codon *smc04388*. (B) Gel photo of colony

PCR with F1-131 and R1-cassette primers. From left to the right: Lane 1: control PCR with water instead of DNA; Lane 2: single *smc04388* mutant RmP3081; Lane 3: double *smc04388 hypD* mutant RmP3272; Lane 4: Rm5000 wild type; Lane 5: RmP110 wild type and Lane 6: 1 Kb DNA ladder. Red arrow denotes 800 bp.

Furthermore, a double *hypD smc03488* mutant (RmP3272) was constructed by transducing the *smc04388::*Ω Sm^rSp^r from RmP3081 into a *hypD* deletion mutant strain (RmP2510). The parental strain RmP2510 has deleted the *hypD* gene and it was constructed previously by Catharine White (White and Finan, unpublished). According to these authors, RmP2510 has a growth defect in minimal media in the presence of *trans*-4-hydroxy-L-proline, since it is lacking the HypD deaminase.

Growth of the two omega transaminase mutants in the presence of trans-4-hydroxy-L-proline

To investigate a possible role for *smc04388* gene in 4-hydroxy-proline metabolism, the growth of the mutant strain RmP3081 (Rm5000 *smc04388::*Ω Sm^rSp^r) was evaluated in minimal media containing 15mM glucose and 20mM ammonium chloride; 15mM glucose and 10mM 4-L-Hyp as a nitrogen source; 10mM 4-L-Hyp; 10mM D-proline or 10mM L-proline as the sole carbon and nitrogen source (Figure 9 &10).

The wild type strain grew better in a media with glucose as carbon source and 4-L-Hyp as nitrogen source compared to ammonium (Figure 9). On the other hand, the cultures in L-proline and D-proline as the sole carbon and nitrogen source have the lowest cell density. Finally, the growth with 4-L-Hyp as carbon source was intermediate between these last two groups. According to these results wild type strain Rm5000 is able to metabolize 4-L-Hyp better than L-proline or D-proline when used as a source of carbon and nitrogen.

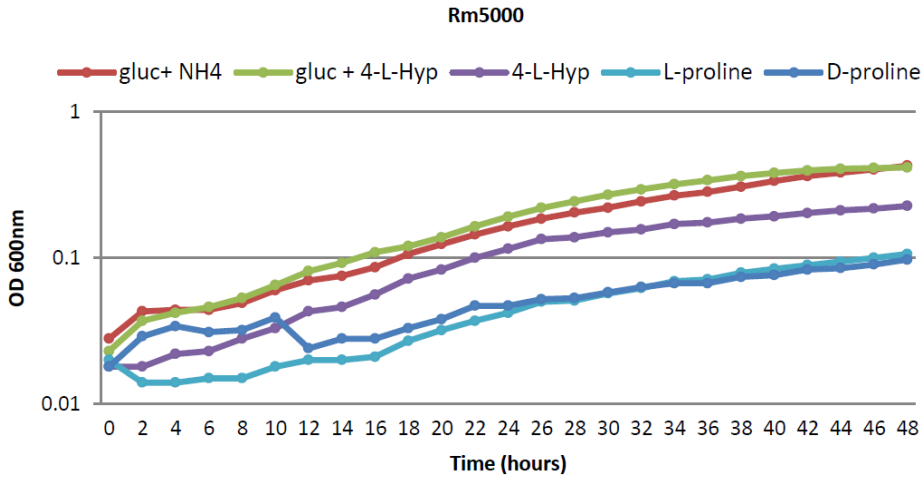

Figure 9.Growth curves for the *S. meliloti* wild type strain Rm5000 with different sources of carbon and nitrogen. Media were inoculated with cells pre-grown in M9 minimal media with 15mM glucose and no nitrogen source. Absorbance readings at 600nm were taken every 15 minutes over 48 hours. Absorbance values are represented with log scale in "y" axis.

The mutant strain RmP3081, which has the *smc04388* gene interrupted by the omega cassette Sm^r/Sp^r, showed similar growth to that of Rm5000 (wild type) in the different minimal media (Figure 10). The greatest cell density was obtained with glucose as carbon source and ammonium or 4-L-Hyp as nitrogen source. In contrast, D-proline and L-proline produced the lowest cell density. Despite induction of *smc04388* upon growth with 4-L-Hyp, *smc04388* was not required for the catabolism of 4-hydroxy-proline in *S. meliloti*.

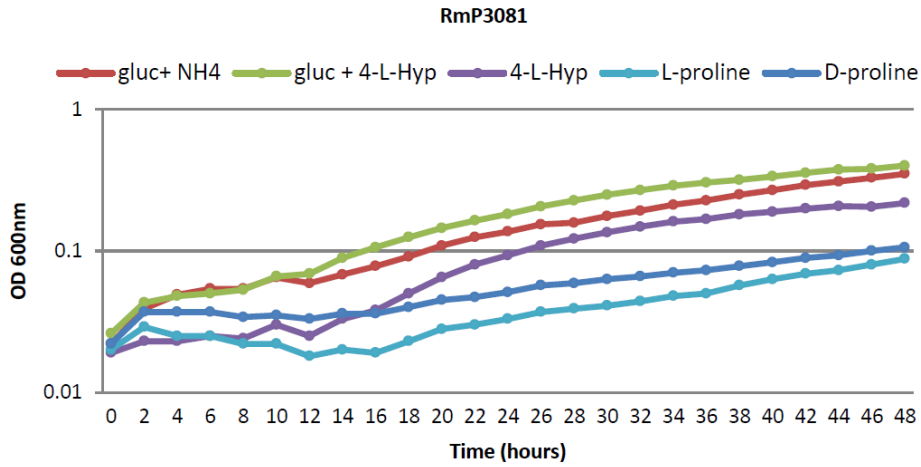

Figure 10. Growth curve of a single *smc04388* mutant, RmP3081, in different minimal media at 30 °C. Media were inoculated with cells pre-grown in M9 minimal media with 15 mM glucose and no nitrogen source. Absorbance readings at 600 nm were taken every 15 minutes during 48 hours. Absorbance values are represented with log scale in "y" axis.

It was suggested that the second intermediate of the 4-hydroxy-proline pathway, P4OH2C, or its open form may serve as an amino donor for the Smc04388 amino transaminase. The P4OH2C is the substrate for the Δ^1-pyrroline-4- hydroxy-2-carboxylate deaminase that catalyzes the second reaction of the 4-hydroxy-proline pathway (Singh & Adams, 1965). A double *smc04388 hypD* mutant (RmP3272) was created in this study, and its growth in minimal media was compared to a single *hypD* mutant (RmP2510) and wild type strain (RmP110).

The growth of the RmP110 wild type strain as shown in the Figure 11 was similar to that of the wild type Rm5000 strain (Figure 9). However, this strain grows better than Rm5000 in media with L-proline. This strain reaches the highest cell density with glucose as the carbon source and either ammonium or 4-L-Hyp as the nitrogen source.

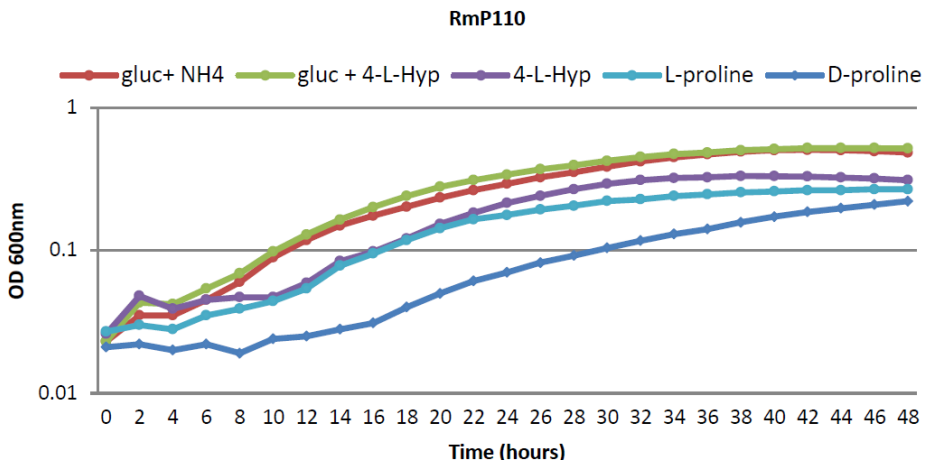

Figure 11. Growth curve of RmP110 wild type strain in different minimal media at 30 °C. Media were inoculated with cells pre-grown in M9 minimal media with 15 mM glucose and no nitrogen source. Absorbance readings at 600 nm were taken every 15 minutes during 48 hours. Absorbance values are represented with log scale in "y" axis.

Unlike for the wild type RmP110 strain, RmP2510 carrying only the *hypD* deletion mutation, failed to grow with 4-L-Hyp as the sole carbon and nitrogen source (Figure 12). This strain grew to a very low density with 4-L-Hyp as the nitrogen source in the presence of glucose as the carbon source. This result suggests the existence of a secondary pathway which might allow the bacteria to utilize 4-L-Hyp as a nitrogen source. The highest cell density is reached in the media with glucose as carbon source and ammonium as nitrogen source. As in the case of the wild type RmP110, D-proline only supported slow growth presumably as it is metabolized at very low rate. However, as for the wild type, the final cell density achieved with D-proline was similar to that with L-proline as a source of carbon and nitrogen.

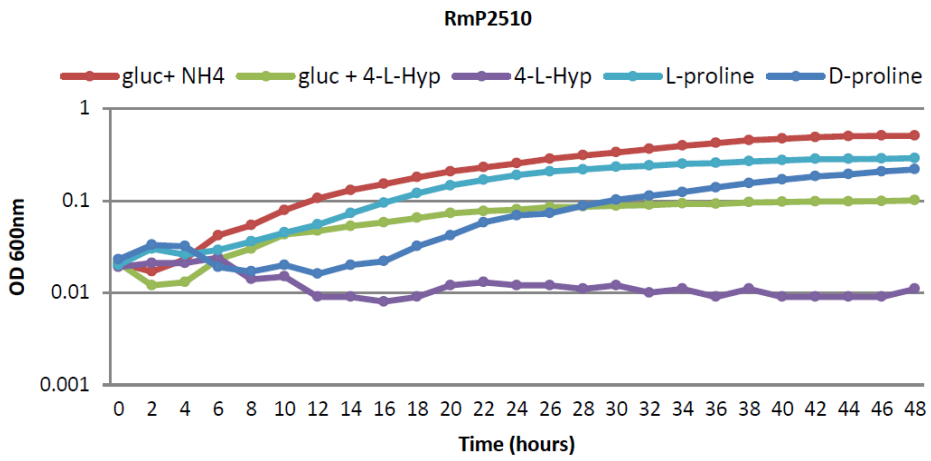

Figure 12. Growth curve of a *hypD* mutant, RmP2510, in different minimal media at 30 °C. Media were inoculated with cells pre-grown in M9 minimal media with 15 mM glucose and no nitrogen source. Absorbance readings at 600 nm were taken every 15 minutes during 48 hours. Absorbance values are represented with log scale in "y" axis.

The *hypD smc04388* double mutant, RmP3272, was unable to grow in media with 4-L-Hyp as the sole carbon and nitrogen source (Figure 13). While RmP3272 (*hypD smc04388*) grew poorly with 4-L-Hyp as a nitrogen source and glucose as carbon source, the growth was comparable to that of the RmP2510 (*hypD*) mutant. The growth RmP3272 (*hypD smc04388*) in media supplemented with glucose, L-proline or D-proline is similar to the wild type and RmP2510 (*hypD*) parental strain. The highest cell density is reached in medium with glucose and ammonia, whereas the lowest cell density was observed in medium supplemented with D-proline.

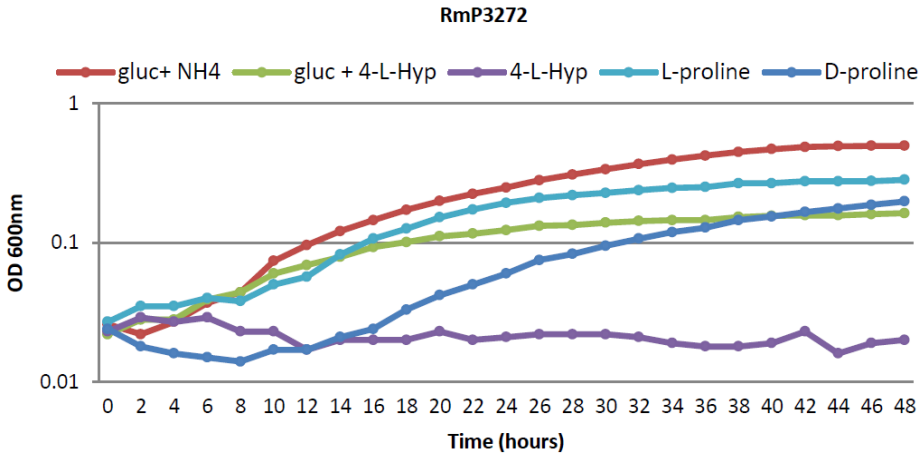

Figure 13. Growth curve of a *smc04388 hypD* double mutant, RmP3272, in different minimal media at 30 °C. Media were inoculated with cells pre-grown in M9 minimal media with 15 mM glucose and no nitrogen source. Absorbance readings at 600 nm were taken every 15 minutes during 48 hours. Absorbance values are represented with log scale in "y" axis.

The doubling times for each strain in the different media evaluated were calculated between absorbance values of 0.1 and 0.3 (Table 5). For minimal media supplemented with 10mM D-proline the doubling times were not calculated since the cultures did not reach the exponential phase within 48 hours or an absorbance higher than 0.3. The same procedure was applied for the *hypD* single mutant (RmP2510) and the *smc04388 hypD* double mutant (RmP3272) in both of the two media containing 4-L-Hyp.

In the medium with glucose and ammonia each of the two wild type strains and its respective mutant had similar doubling times. However, in the presence of 4-L-Hyp as the carbon or nitrogen source the strains carrying the mutation in the *hypD* gene (RmP2510 and RmP3272) have very long doubling times (compare to RmP110 wild type). In contrast, the doubling times for the single *smc04388* mutant (RmP3081) and its parental strain (Rm5000) are very similar in the two media with 4-L-Hyp. Finally, with L-proline medium the doubling times

of the mutants RmP2510 and RmP3272 and RmP110 wild type strain are very close; whereas RmP3081 and Rm5000 wild type strain showed very little growth in this medium.

Table 5. Doubling time (hours) in different minimal media. Cells were grown in M9 minimal medium containing: 15 mM glucose and 20 mM ammonium chloride (gluc+NH3); 15 mM glucose and 10 mM 4-L-Hyp (gluc+Hyp); 10 mM 4-L-Hyp (Hyp) and 10 mM L-proline (L-pro). Standard deviation is included in parentheses. N/A means that doubling time was not calculated since the culture did not reach 0.3 units of absorbance.

	RmP110	RmP2510	RmP3272	Rm5000	RmP3081
gluc + NH3	8.6 (0.2)	10.1 (0.8)	9.5 (0.3)	13.1 (0.5)	15.1 (0.9)
gluc + Hyp	6.9 (0.2)	N/A	N/A	10.9 (2.1)	12.8 (0.4)
Hyp	12.8 (4.8)	N/A	N/A	21.2 (0.2)	19.0 (0.9)
L-pro	21.9 (1.2)	19.2 (1.6)	20.8 (1.9)	N/A	N/A

In summary, it was found that strains carrying a mutation in the *hypD* gene, which encodes for the P4OH2C deaminase, have a growth defect in minimal media supplemented with 4-L-Hyp as the carbon or nitrogen source. A mutation in the *smc04388* gene which encodes for a putative omega amino transaminase did not have an appreciable growth defect in the presence of 4-L-Hyp, despite the induction of this gene in such conditions. Finally, *S. meliloti* grows more rapidly with L-proline than D-proline as the carbon and nitrogen source.

Amino transamination enzymatic activity in cell extracts

The lack of phenotype of a single *smc04388* mutant (RmP3081) and a double *smc04388 hypD* mutant (RmP3272) in the presence of 4-L-Hyp was described above. Here, we evaluated the amino transaminase activity in cell extracts from these mutant strains and compared them with its respective parental strains.

All the strains were grown in the presence of 4-L-Hyp as the sole carbon and nitrogen source. Cell extracts were prepared by sonication and the enzymatic activity of the malate

dehydrogenase (MLDH) enzyme was evaluated as a control of the quality of each cell extract preparation.

The amino transaminase activity in cell extracts was measure using the acetophenone UV spectrometric method (Schätzle et al., 2009). This method is based on the detection of acetophenone produced by the transamination between α-methylbenzylamine (α-MBA) and pyruvate as shown in Figure 14. Acetophenone is detected by spectroscopy since it has a maximum absorbance at 245 nm and a molar extinction coefficient of 12 $mM^{-1}cm^{-1}$.

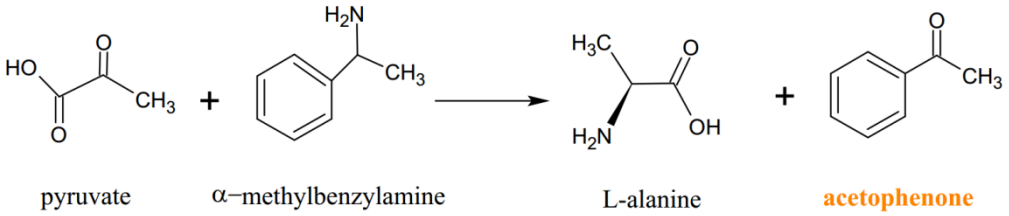

Figure 14. Schematic representation of the transaminase reaction between α-methylbenzylamine (α-MBA) as an amino donor and pyruvate as an amino acceptor, forming L-alanine and acetophenone. α-methylbenzylamine (α-MBA) is used as an omega amino transaminase substrate analogue as the product, acetophenone, has a maximum absorbance at 245 nm. An absorbance spectra of each of the reactants in the reaction is showed in Figure 32 in Appendix.

The results from the specific activity of the MLDH enzyme suggest that in general cell extracts from the single mutant and its parental strain have similar activity (Figure 15, red bars). Extracts from the single *smc04388* mutant (RmP3081) and the Rm5000 wild type strain were very similar. Similarity, cell extracts from the single *hypD* mutant (RmP2510) and the *smc04388 hypD* double mutant (RmP3273) had similar MLDH activity; however, slightly higher than the RmP110 wild type strain.

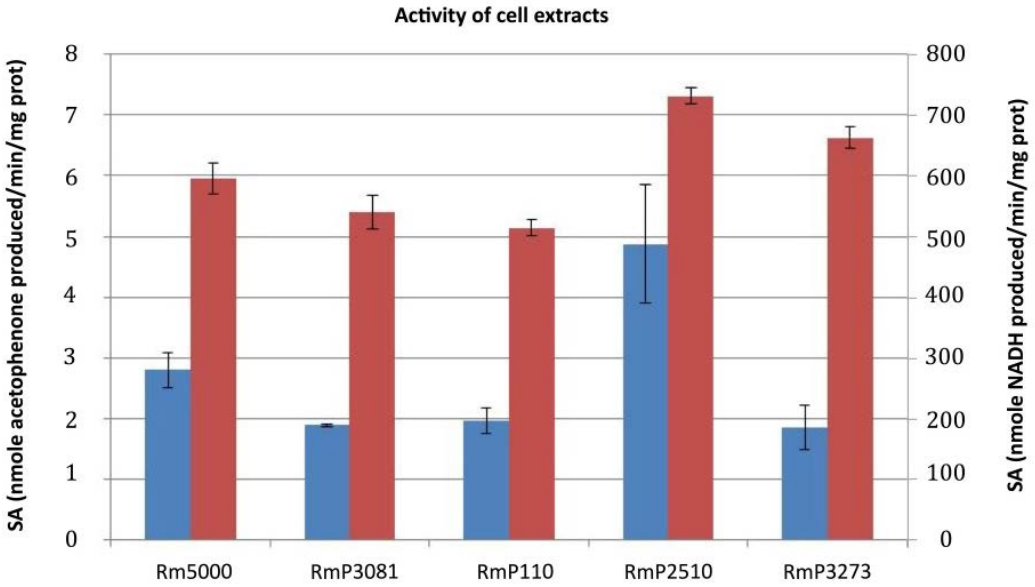

Figure 15. Enzymatic activity in cell extracts. Cultures were grown in minimal media in the presence of 4-L-Hyp as the sole carbon and nitrogen source. Blue bars correspond to the amino transaminase activity and red bars to the MLDH activity. Reaction mixture for amino transaminase reaction contains 2.5 mM of pyruvate and α-MBA, 0.02 mM PLP and 15 µL of cell extracts. Reaction mixture for MLDH contains 0.1 mM Glycine-NAOH pH 10, 0.9 mM L-Na Malate and 3 mM NAD^+. Reactions were carried out in 1mL volume. Data represents the average of three independent reactions and error bars represent standard errors.

The enzyme activity from cells extracts of cultures grown with 4-L-Hyp as the sole carbon and nitrogen source is represented by blue bars (Figure 15). Despite the similarity in the MLDH activity of the single mutant, RmP3081, and Rm5000 wild type strain, there was a slight decrease in the amino transaminase activity of the mutant. These results suggest that a mutation in the *smc04388* gene had an effect on the transamination activity of the cells and this supports the idea that this gene encodes for an omega transaminase enzyme. However, the existence of a second omega transaminase enzyme in *S. meliloti*, possibly encoded by the *smc01534* gene, might be responsible for the activity remaining in this mutant. This slight decrease was not

observed between the double mutant (RmP3273) and wild type RmP110, which may be due to the difference in the cell extract quality observed between these two strains.

Interestingly, the results show an increase in the amino transaminase activity of cell extracts of the *hypD* mutant (RmP2510) compared to the double *hypD smc03488* mutant (RmP3273). The increase observed can be attributed to stimulation of the amino transaminase activity, since the two extracts have similar MLDH activity. According to these results, in the absence of the HypD deaminase the transaminase activity is increased when cells are grown in LB media supplemented with 4-L-Hyp.

Cloning, purification and activity of the Smc04388 omega amino transaminase

To characterize the putative omega amino transaminase encode by *smc04388*, the *smc04388* gene was cloned into the Tc^r broad-host-range expression vector, pTH1227 (Figure 16 A). A *Strep*II-tag was inserted at the N terminal of the gene for further purification of the protein by affinity chromatography. The plasmid was transferred to *S. meliloti* and the resultant clone (RmP3016) was grown in LBmc and the expression of the Smc04388 protein was induced by IPTG. In a previous experiment, the *smc04388* gene was cloned into the Amp^r vector, pET21a; and the Smc04388 was overexpressed as a His-tagged protein in *E. coli* BL21 (DE3). The recombinant protein was insoluble in *E. coli* cells and purification in this condition was unsuccessful.

The approximately molecular weight of the Smc04388 omega amino transaminase was calculated from the amino acid sequence to be 54 kDa; and a protein having this molecular weight was observed after addition of IPTG to the media (red arrow in Figure 16 B). However, no difference was observed in the intensity of the ~54 kDa band when the concentration of IPTG was increased from 0.05 to 1.5 mM (lanes 3-5 in Figure 16 B). A second protein was also

induced by IPTG (blue arrow), corresponding in molecular weight to the product of the *gusA* gene (β-glucuronidase), located downstream of the cloning site of the pTH1227 vector. The intensity of this band was not increased when increasing IPTG. The presence of the *gusA* reporter gene in the vector allows quantification of the expression of any gene cloned downstream. In our case, we evaluated the optimum conditions for the induction of the Smc04388 protein by assaying β-glucuronidase activity (Figure 33 in Appendix).

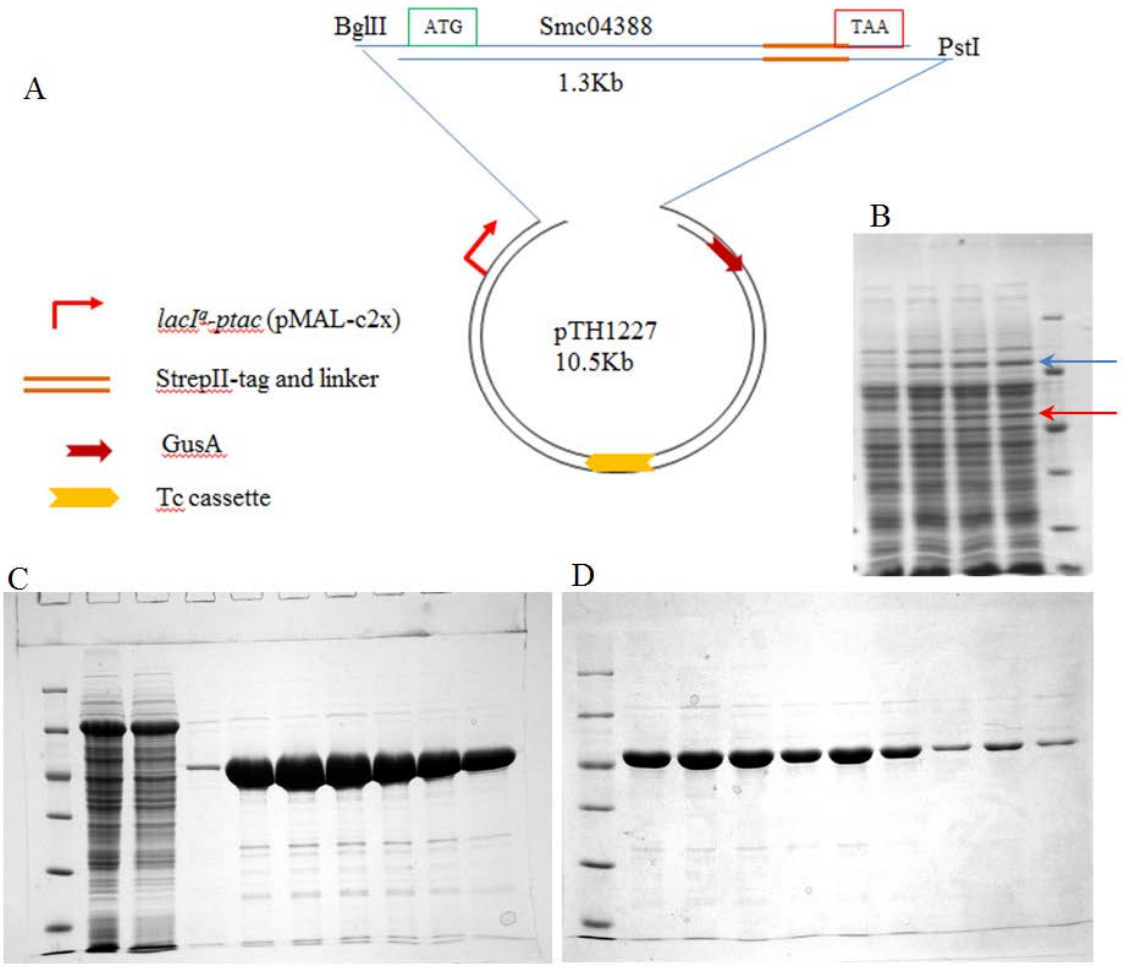

Figure 16. Cloning and purification of the recombinant Smc04388 omega amino transaminase from RmP3016. (A) The *smc04388* gene from *S. meliloti* was cloned into the vector pTH1227. The *Strep*II-tag is part of the reverse primer. The DNA fragment was inserted into the *Bgl*II and *Pst*I sites in the cloning site of pTH1227. (B) Whole cells SDS-PAGE gel with 10% acrylamide. Cells were grown overnight in LBmc with different

concentrations of IPTG. From the left to the right: Lane 1: Protein molecular weight marker; Lane2: culture not induced; Lane 3: culture induced with 0.05mM IPTG; Lane 4: culture induced with 1mM IPTG; Lane 5: cultured induced with 1.5 mM IPTG. (C) Protein purification SDS-PAGE gel with 10% acrylamide. From the left to right: Lane 1: Protein molecular weight marker; Lane 2 1/10 dilution of the flow through; Lane 3 wash fraction; Lane 4-10 Elution fractions. (D) Protein purification SDS-PAGE gel with 10% acrylamide. Lane 1: Protein molecular weight marker; Lane 2-10; Elution fractions.

The recombinant *Strep*II-tag protein was purified using *Strep*-Tactin® Superflow® resin. The gels in Figure 16 C and D shows the fractions obtained after elution from the column and Table 6 summarizes the purification process.

Table 6. Purification summary of the omega amino transaminase Smc04388 from *S. meliloti*.

Numbers in parenthesis refers to standard deviation from three independent measurements.

	Volume (mL)	Protein (mg/mL)	Total protein (mg)	SA (nmole/min/mg prot)	TA (nmole/min)
Cell extract	22	44.7 (3.6)	983.2	4.5 (0.2)	99
Prot Elution 1	6	2.9 (0.1)	17.6	59.3 (6.5)	355.8
Prot Elution 2	5.2	0.82 (0.09)	4.3	56.7 (1.5)	294.8
Total protein	11.2		21.9		650.6

Legend: SA stands for Specific activity, TA stands for Total activity

The fractions eluted from the column were separated into two different samples; fractions with higher concentrations of protein were combined together and referred to as Protein Elution 1, whereas fractions containing lesser amount of protein were combined and labeled as Protein Elution 2. Both fractions were dialyzed against 50 mM Tris-HCl pH 8 buffer containing 1mM $MgSO_4$, 10% glycerol and 0.05 mM PLP. After dialysis the protein was stored at -80^{o}C until utilization. The enzyme retained activity for at least seven months.

The specific activity of the purified Smc04388 omega amino transaminase was measured using the UV spectrophotometric described above (Schätzle *et al*., 2009). The amino transamination reaction was carried out with different amounts of Smc04388 purified protein and 2.5 mM of the amino donor, α-MBA and 2.5 mM of the amino acceptor, pyruvate. The reaction was carried out at room temperature for 20 minutes and the reaction rates for 0.01, 0.02 and 0.03 mg of protein are showed in Figure 17.

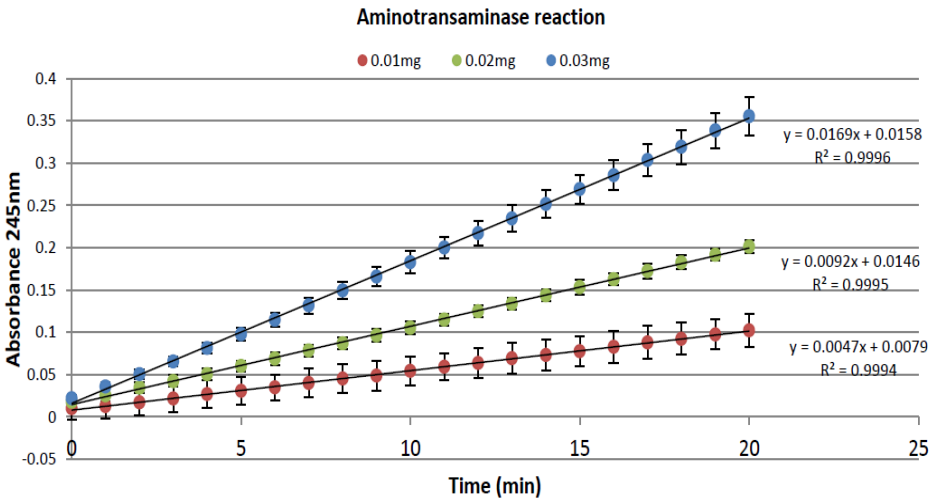

Figure 17. Transaminase reaction of the Smc04388 purified protein. The reaction was carried out with 2.5 mM of pyruvate and α-MBA, 0.02 mM PLP and different amounts of purified protein 0.01, 0.02 and 0.03 mg. The acetophenone formation was monitored at 245 nm every 1 minute. Each point in the curve represents the average of three independent reactions and the errors bars represent standard deviation.

The linearity of the amino transaminase reaction was observed with the three different amounts of protein. The rate of the reaction also increased with the amount of protein added, which indicates that the formation of acetophenone is due to the enzymatic activity of the Smc04388 omega transaminase. This assay showed that the Smc04388 purified enzyme is active and has amino transaminase activity towards pyruvate and α-MBA. In addition, it was

determined that the specific activity of the enzyme at pH 9 and 25 ^{o}C is about 50 nmole of acetophenone formed per minute per mg of protein.

Characterization of the Smc04388 omega amino transaminase

Substrate Specificity

Previous studies have shown that omega transaminase use pyruvate as a common amino acceptor, although other keto acids can be used as amino acceptors. These results showed that the Smc04388 omega amino transaminase has activity toward pyruvate. In addition to pyruvate, we evaluated α-ketoglutarate as an amino acceptor and α-MBA as an amino donor. We found that the enzyme has no activity towards α-ketoglutarate (Figure 18). Similar results have been reported for the transaminase, AptA protein from *A. denitrificans* (Yun et al., 2004) and the transaminase from *V. fluvialis* (Shin et al., 2003). These amino transaminases, like the Smc04388 omega transaminase are not reactive against α-ketoglutarate.

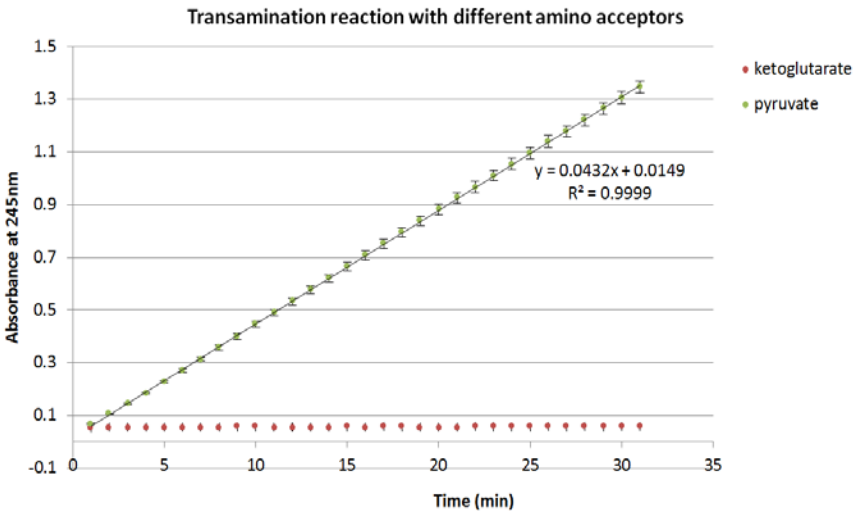

Figure 18. Transamination reaction of the Smc04388 purified protein using α-ketoglutarate or pyruvate as amino acceptors and α-MBA as the amino donor. Both amino acceptors and the amino donor were added at the same concentration (2.5 mM) in the reaction mixture. The reactions were carried out at room

temperature and absorbance readings were taken every 1 minute. Points in the graph are the average of three independent reactions and the error bars correspond to standard errors.

A second experiment was carried out to show the reactivity of the Smc04388 toward pyruvate as an amino acceptor. The transamination reaction was prepared as described previously, but pyruvate was not added in the reaction mixture. This reaction was started by adding 1.53 mg of purified Smc04388 transaminase and absorbance readings were taken at 245nm every 30 minutes (Reaction 1 in Figure 19). No change in absorbance was observed during this time. This result showed that the reaction mixture did not contain any endogenous amino acceptor.

After this reaction was incubated for 120 minutes, pyruvate was added to the reaction mix (Reaction 1 in Figure 19) and incubated for another 120 minutes. Acetophenone formation was detected at 245nm. An increase in absorbance was observed suggesting that pyruvate is necessary for the amino transamination reaction. As a control, a second reaction (Reaction 2 in Figure 19) in which pyruvate continually present was carried out. In this case, linear formation of acetophenone was detected.

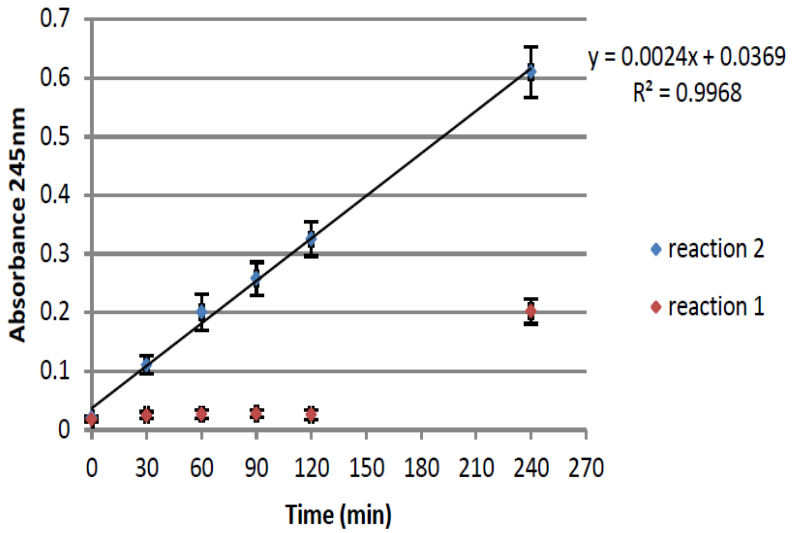

Figure 19. Pyruvate as an amino acceptor in the transamination reaction. Two reactions were carried out in parallel: Reaction 1 contained 2.5 mM α-Methylbenzylamine (α-MBA) as the amino donor and 0.1 mM PLP. After this reaction was incubated for 120 minutes, 2.5 mM pyruvate was added to the reaction mix (Reaction 1). Reaction 2 contained 2.5 mM α-methylbenzylamine (α-MBA) and pyruvate, 0.1 mM PLP. Both reactions were carried out at in 50 mM phosphate buffer (pH 8) with 1.53 mg of purified aminotransferase. Reactions were incubated at 30 ^{o}C. Each point in the graph represents the average of three separate reactions. Errors bars correspond to the standard deviation.

Our result suggests that the purified Smc04388 transaminase uses pyruvate as amino acceptor to produce acetophenone and L-alanine. Previous reports have described the selectivity of other omega amino transaminase enzymes toward pyruvate as the most common amino acceptor (Hwang et al., 2005; Shin et al., 2001 & Park et al., 2012).

Effect of the pH on the activity of Smc04388 transaminase

The specific activity of the putative Smc04388 amino transaminase was evaluated at different pHs. For this purpose, reactions with α-MBA as the amino donor and pyruvate as the amino acceptor were carried out at pHs: 7.2; 7.6; 8.0; 8.4; 8.6; 8.8 and 9.0. The specific activity was calculated using the change in absorbance at 245nm over time. An OD spectra of acetophenone at different pHs was carried (Figure 34 in Appendix)

It was found that the enzymatic activity of the Smc04388 omega transaminase increased as the pH increased (Figure 20). For example, the specific activity of this enzyme at pH 7.2 (1.8nmole/min/mg of protein) was 40-fold lower than the specific activity at pH 9 (70nmole/min/mg of protein).

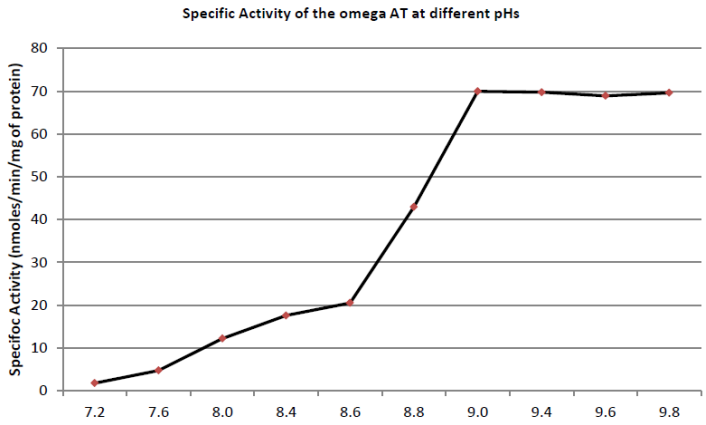

Figure 2.. Effect of the pH on the specific activity of the purified Smc04388 omega aminotransferase. The transamination reactions contain α-methylbenzylamine (α-MBA) as an amino donor and pyruvate as an amino acceptor in different buffers. Reactions at pH 7.2; 7.6 and 8.0 were carried out in 50 mM phosphate buffer whereas reactions at pH higher than 8 were performed in 100 mM Tris-HCl buffer. Each reaction was carried out with 0.054 mg of purified aminotransferase enzyme.

The activity of the Smc04388 transaminase increased with the pH, having its optimum at pH values higher than 9. Almost no activity was observed at pH lower than 8. Similar results have been previously reported for other omega amino transaminases. The optimum pH for the two characterized omega amino transaminases, from *V. fluvialis* and *A. denitrificans* were reported to be 9.2 (Shin et al., 2003) and 9.0 (Yun et al., 2004) respectively. In addition, these authors showed that the relative activity was dramatically reduced below pH 8. Unlike these characterized omega transaminases, the Smc04388 protein had a maximum activity over a wide range of pH (pH 9-pH 9.8).

Activity towards the open form of P4OH2C

These results showed that the Smc04388 protein has amino transaminase activity and is also induced in the presence of 4-L-Hyp. Therefore, it is possible that this enzyme has amino transaminase activity toward one of the intermediates of the catabolic pathway of 4-hydroxy-

proline. A possible candidate amino donor of this enzyme is the P4OH2C intermediate or its open form 4-hydroxy-2-oxo-5-aminovalerate, which is formed spontaneously in water (Adams & Frank, 1980).

It is known that P4OH2C is unstable (Adams, 19673; Watanabe et al., 2012). As well, it is not available commercially. Therefore, in order to test the reactivity of the Smc04388 amino transaminase toward this pyrroline compound, P4OH2C was synthesized enzymatically. The P4OH2C was produced enzymatically in an oxidative reaction catalyzed by the *cis*-4-hydroxy-D-proline dehydrogenase (oxidase) (D-HypDH) from *P. putida* using 4-D-Hyp as substrate. D-HypDH was purified in our lab using a previously constructed clone and kindly donated by Dr. Watanabe (Ehime University, Japan). The purification was carried out using affinity chromatography. For more details view Materials and Methods section and Table7, Figure 29 in Appendix.

The formation of L-alanine by the Smc04388 omega transaminase was evaluated using a coupled reaction with the D-HypDH (Figure 21). The first half reaction to produce P4OH2C was prepared with 50 mM 4-D-Hyp, 0.05 mM PMS, 2 mM $MgCl_2$ and 0.1 mg of purified D-HypDH. This reaction mixture was incubated overnight (16 hours) at 30 ^{o}C in the dark. The next day 0.5 mL of this reaction mixture was used as the amino donor for the Smc04388 omega amino transaminase in the transamination reaction. It was assumed that this volume contains 25 mM of P4OH2C produced by the D-HypDH. The amino transaminase reaction was prepared with 10 mM of pyruvate as amino acceptor, 0.5 mL of the reaction mixture as already described as amino donor, 0.02 mM PLP and 1mg of purified Smc04388 enzyme in 1 mL of volume. In addition, two separate controls were prepared; control 1 without adding the Smc04388 purified protein and control 2 without the amino acceptor pyruvate. After incubation for 3 hours at 30 ^{o}C the

reaction and controls mixtures were filtered and analyzed by capillarity electrophoresis-mass spectrometry (CE-MS) to detect L-alanine formation.

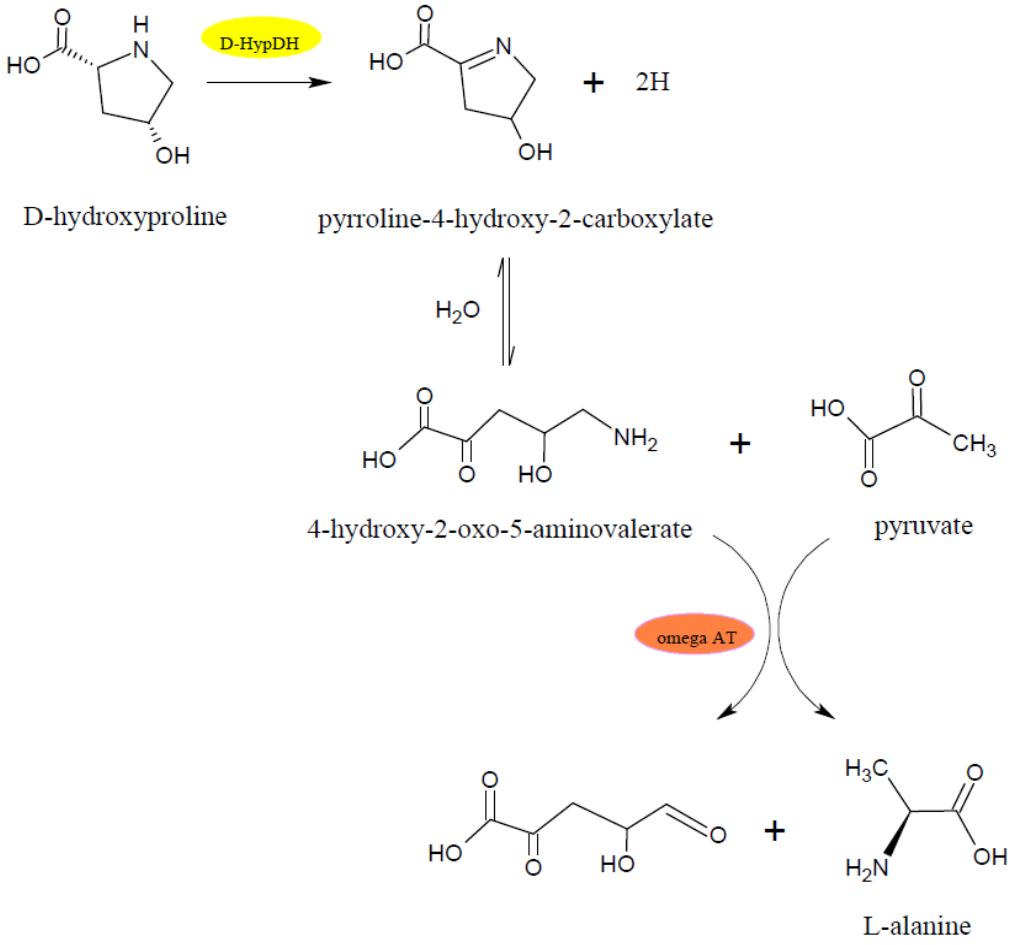

Figure 21. Diagram of the coupled enzymatic reaction with the D-HypDH from *P. putida* and the purified Smc04388 omega amino transaminase from *S. meliloti*. In the first half reaction 4-D-Hyp is converts to P4OH2C by D-Hyp-DH. This compound is hydrolyzed spontaneously to 4-hydro-2-ovo-aminovalerate, which is used as an amino donor along with pyruvate as an amino acceptor by the omega amino transaminase.

The analysis of the reaction mixture and control 1, that contains everything in the reaction mixture but the Smc04388 amino transaminase are shown in Figure 22 A, B (reaction) and C, D (control 1). The control without the amino acceptor pyruvate (control 2) produced the

same results as control 2 without the amino transaminase (Figure 35 in Appendix). Both reaction and control 1 mixtures had a peak around 22 minutes that according to the mass spectra corresponds to D-Hyp (A and C panels in Figure 22). Two other small peaks were observed at 12 and 14 minutes in both samples. The peak at 11.85 minutes was not identified to correspond to any of the reactants in the reaction mixture. Therefore is likely some product formed during the coupled reaction or probably a product from the disintegration of P4OH2C. The internal standard L-ornithine added to the samples as control can be observed at 14.3 minutes.

The peak of L-alanine appears at around the 18 minutes and was only present in the reaction mixture and not in the control mixtures (A and C panels in Figure 22). The intensity of the L-alanine peak is smaller than the D-Hyp peak, which makes it difficult to see, however in Panel B that was generated extracting the mass to charge ratio (m/z) of L-alanine the peak can be easily observed (Panel B in Figure 22).

A peak at ~23 minutes corresponding to the P4OH2C formed in the first half reaction from D-HypDH was detected in the control. This peak is very difficult to distinguish in the both reaction (A panel) and control 1 (C panel) mixtures because it nearly overlaps with the peak of D-Hyp. The signal of D-Hyp in both mixtures is very intense, and as a result the smaller peaks due to P4OH2C are obscured. The same peak of P4OH2C and with higher intensity was observed when the reaction mixture of D-HypDH was analyzed (Figure 36 in Appendix). The presence of the P4OH2C peak suggests the formation of L-alanine by the transamination reaction of the Smc04388 omega amino transaminase.

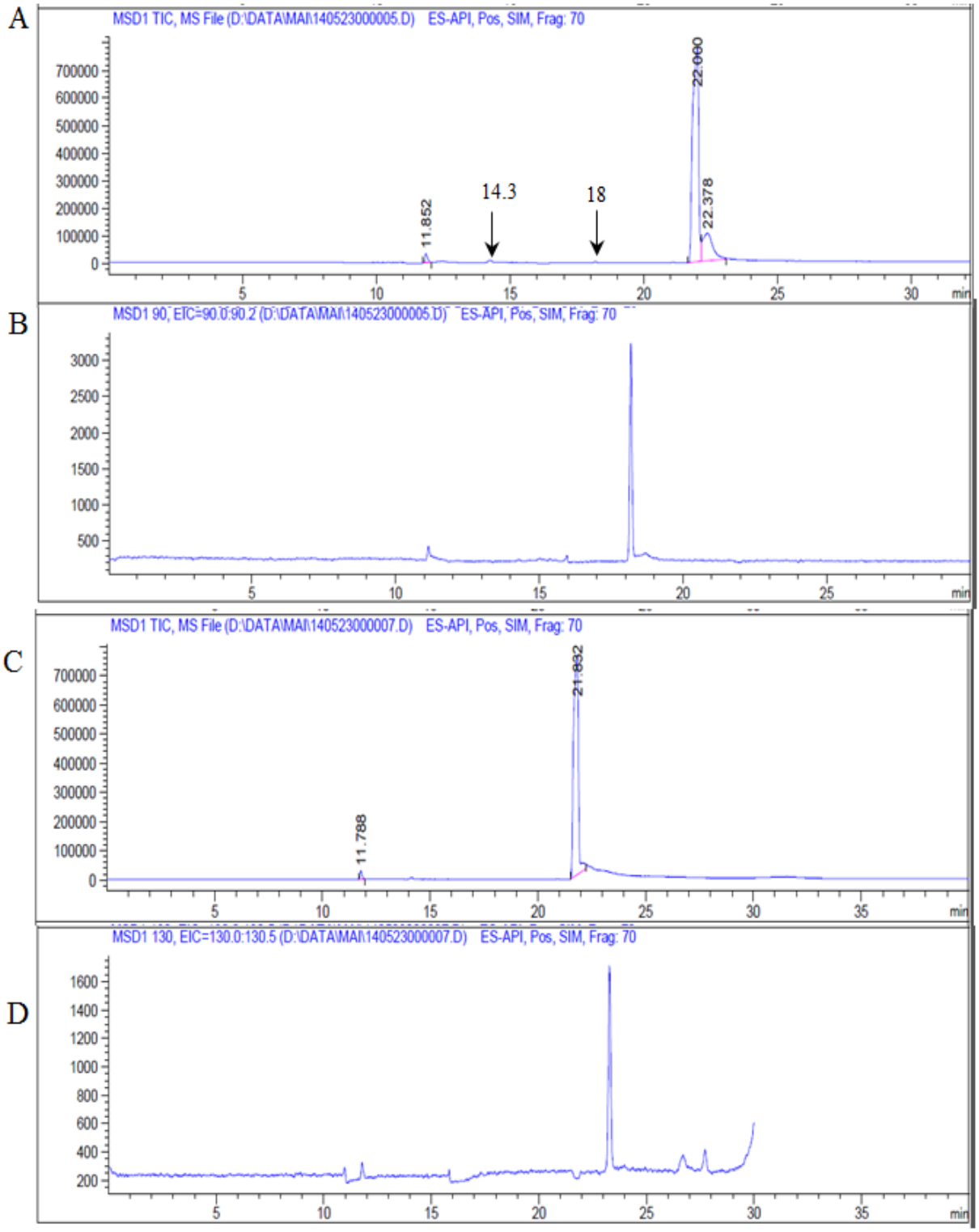
A
MSD1 TIC, MS File (D:\DATA\MAI\140523000005.D) ES-API, Pos, SIM, Frag: 70
22.060
22.378
14.3
18
11.852
B
MSD1 90, EIC=90.0:90.2 (D:\DATA\MAI\140523000005.D) ES-API, Pos, SIM, Frag: 70
C
MSD1 TIC, MS File (D:\DATA\MAI\140523000007.D) ES-API, Pos, SIM, Frag: 70
21.832
11.788
D
MSD1 130, EIC=130.0:130.5 (D:\DATA\MAI\140523000007.D) ES-API, Pos, SIM, Frag: 70
min

Figure 22: CE-MS of the coupled enzymatic reaction with the D-HypDH and the purified Smc04388 omega amino transaminase. The "y" and the "x" axis correspond to Ion count and Migration time in minutes, respectively. Panels (A) and (B) correspond to the reaction mixture. First half reaction containing 50 mM 4-D-Hyp, 2 mM $MgCl_2$, 0.05 mM PMS and 0.1 mg of purified D-HypDH was incubated in the dark at 30 ^{o}C. After incubation 500 µL of this reaction mixture was used as 25 mM P4OH2C in the second reaction along with 10 mM pyruvate, 0.02 mM PLP and 1mg of the purified Smc04388 omega amino transaminase. The second reaction was incubated for 3 hours in the dark at 30 ^{o}C. (A) The total positive ions presented in the sample are detected. (B) Same sample as A where was detected only the ions that correspond to the mass of L-alanine. Panels (C) and (D) correspond to the control mixture in which everything was added but the Smc04388 omega amino transaminase. (C) The total positive ions presented in the sample are detected. (D) Same sample as C where was detected only the ions that correspond to the mass of P4OH2C. All samples were filtered prior to their analysis to eliminate the protein present.

The concentration of L-alanine in the reaction mixture was estimated using the internal standard L-ornithine as a reference. The RPA of L-alanine was calculated using the peak area of L-ornithine (internal standard). The RPA was plotted in the L-alanine standard curve (Figure 31 in Appendix) and the concentration of L-alanine was estimated to be approximately 10 mM. The data support the occurrence of the amino transaminase reaction since P4OH2C was found in the reaction mixture and L-alanine was only detected in the reaction mixture. These results indicate that the P4OH2C compound or its open form was used as an amino donor with pyruvate as amino acceptor for the Smc04388 omega transaminase to produce L-alanine.

CHAPTER 4

DISCUSSION

Induction and phenotype of the Smc04388 omega amino transaminase in the presence of trans-4-hydroxy-L-proline

The *smc04388* gene was induced when 4-L-Hyp was used as a carbon or nitrogen source in the media. The induction of this gene by 4-L-Hyp but not in media with D or L-proline indicates the possible role of the Smc04388 omega transaminase in the metabolism of 4-hydroxy-proline. The role of the Smc04388 omega amino transaminase in a secondary pathway related to the main catabolic pathway of 4-hydroxy-proline could explain the induction observed.

To determine the role of the Smc04388 omega amino transaminase in the catabolic pathway of 4-hydroxy-proline, the growth of a single *smc04388* mutant and a double *smc04388 hypD* mutant were compared to the growth of the wild type strain in the presence of 4-L-Hyp. It was found that a mutation in the *smc04388 gene* does not have a growth defect in minimal media with 4-L-Hyp as the only carbon and nitrogen source. One of the possible causes for the lack of phenotype observed is the occurrence of a second omega transaminase. In *S. meliloti*, a second omega amino transaminase enzyme is encoded by the *smc01534* gene. According to White et al., (2012), *smc01534* was not induced in the presence of 4-L-Hyp. Although this gene was not reported to be 4-L-Hyp-inducible, it could have activity with the same substrate as the Smc04388 omega transaminase. This could be one of the reasons for the lack of a distinct phenotype for the *smc04388* mutant.

The amino transaminase activity in cell extracts of the *smc04388* mutant was evaluated. It was found that despite the lack of a growth phenotype, the single *smc04388* mutant (RmP3081)

had a slight reduction of transaminase activity in cell extracts. The residual activity found in extracts could be due to the second omega transaminase (Smc01534) present in *S. meliloti*.

A second possible explanation for the lack of a mutant growth phenotype with 4-L-Hyp may be due to the fact that the Smc04388 omega transaminase is involved in secondary reactions related to the main catabolic pathway of this amino acid in bacteria, if the substrate for this enzyme is the open form of the P4OH2C. According to Adams (1973), the second reaction of the catabolic pathway of 4-hydroxy-proline involves the oxidation of 4-D-Hyp to P4OH2C. This compound is spontaneously hydrolyzed to its open form, 4-hydroxy-2-oxo-5-aminovalerate (Adams & Frank, 1980; Wanatabe et al., 2012). In this scenario, the hypothetical transamination of the 4-hydroxy-2-oxo-5-aminovalerate and an amino acceptor (possible pyruvate), catalyzed by the Smc04388 omega transaminase could be a secondary pathway to metabolize 4-hydroxy-proline as nitrogen source.

P4OH2C is the substrate for the Δ^1-pyrroline-4-hydroxy-2-carboxylate deaminase (P4OH2C deaminase) (Singh & Frank, 1980); and this results in the formation of α-ketoglutarate semialdehyde. The P4OH2C deaminase it is required for the growth of *S. meliloti* in the presence of 4-L-Hyp as the sole carbon and nitrogen source. Therefore, a mutation in the Δ^1-pyrroline-4-hydroxy-2-carboxylate deaminase, encoded by the *hypD* gene, results in no growth in minimal media with 4-L-Hyp as carbon and nitrogen source (White and Finan, unpublished and Figure 12). The growth defect of the *hypD* mutant (RmP2510) in the presence of 4-L-Hyp as carbon and nitrogen source was also observed in the double *smc04388 hypD* mutant (RmP3272). Like its parental strain (RmP2510), this strain (RmP3272) was unable to grow in the presence of 4-L-Hyp, since both strains lack the Δ^1-pyrroline-4-hydroxy-2-carboxylate deaminase to oxidize P4OH2C to α-ketoglutarate semialdehyde.

Both strains that lacked the Δ^1-pyrroline-4-hydroxy-2-carboxylate deaminase (RmP2510 and RmP3272), grew at a very low rate in minimal media supplemented with 4-L-Hyp as the sole nitrogen source. The utilization of this amino acid as a nitrogen source may be possible by a minor or secondary pathway in the cell. It was not possible to calculate the doubling times since the cultures did not reach an absorbance of 0.3 within 48 hours; however it was observed that the double *smc04388 hypD* mutant reached an absorbance of 0.1 faster than the *hypD* mutant, indicating that in some way this mutant can better utilizes 4-L-Hyp as a nitrogen source.

The cell extracts from the *hypD* mutant strain (RmP2510) had higher omega transaminase activity than a double *smc04388 hypD* mutant (Figure 15). The increment observed could be the result of the accumulation of the intermediate P4OH2C in the cells. In the absence of the Δ^1-pyrroline-4-hydroxy-2-carboxylate deaminase, the P4OH2C can no longer be metabolized by this enzyme and may be available for alternative reactions. One of the candidate reactions is the amino transamination reaction catalyzed by the Smc04388 omega transaminase. The accumulation of P4OH2C and presumably its open form, 4-hydro-2-oxo-5-aminovalerate in the *hypD* mutant may lead to increased synthesis of the Smc04388 omega transaminase enzyme. It would be interesting to monitor the expression of *smc04388* in a *hypD* mutant in media containing 4-L-Hyp. In contrast, the amino transaminase activity did not increase in cell extracts from the double *smc04388 hypD* mutant. It can be inferred that in the absence of the Smc04388 omega transaminase the P4OH2C is no longer involved in the transaminase reaction.

Characterization of the Smc04388 omega amino transaminase

It was found that the Smc04388 transaminase shares high amino acid sequence similarity with other known omega amino transaminases from bacteria. Among the characterized transaminases, the Smc03488 enzyme is phylogenetically related to the transaminases from *P.*

putida, *P. fluorescens*, *C. violaceum* and *A. baumannii* (50%, 49%, 53% and 46% of identity respectively). These proteins also have conserved residues that have been reported to play an important role in hydrophobic interactions and binding to PLP in the active site (Yun et al., 2004; Park et al., 2012). It is common to find a high sequence similarity among the amino transaminase enzymes (Hwang et al., 2005). Despite the similarities found between the Smc04388 and 4 others known amino transaminases; this enzyme showed less similarity with transaminases from *P. denitrificans*, *R. solanasearum* and *R. sphaeroides* (36%, 34% and 31% respectively).

The transaminase activity of the recombinant purified *Strep*II-tag protein towards pyruvate as an amino acceptor and α-MBA as an amino donor was determined in this study. It was also shown that this omega amino transaminase has increased its activity between pH 9 to pH 9.8 and decreases considerably below pH 8.6. Other known amino transaminases enzymes have similar but not identical behaviour. The optimum pH for the characterized amino transaminases from *A. denitrificans* and *R. sphaeroides* has been reported to be in the range between pH 8.5 to pH 9.2 (Yun et al., 2004). However, these enzymes, unlike the Smc04388 protein, decrease their activity at pH higher than 9.4. These results are consistent with the differences in amino acid sequences between the amino transaminase from *S. meliloti* and these other α-proteobacteria.

It was also shown that the Smc04388 omega transaminase, like the transaminases from *A. denitrificans* (Yun et al., 2004) and *V. fluvialis* (Shin et al., 2003), have no reactivity with α-ketoglutarate as amino acceptor. Indeed, results indicated the reactivity of the Smc04388 omega transaminase for pyruvate as amino acceptor. The amino transaminases enzymes of the subgroup II described so far has been reported to have reactivity toward pyruvate as the most common amino acceptor (Hwang et al., 2005; Shin et al., 2001 & Park et al., 2012).

The Smc04388 omega amino transaminase belongs to subgroup II of amino transaminases. This subgroup of transaminases is comprised of the only transaminases that are able to transfer an amino group from the non α-position (Mehta et al., 1993). For this reason the substrate specificity of the amino transaminases is broader than other subgroups of transaminases (Hwang et al., 2005). These enzymes have been reported to have activity towards a variety of amines, including those that present a distal amino group (Hwang et al., 2005; Mehta et al., 1993 & Park et al., 2010). P4OH2C spontaneously converts to 4-hydroxy 2-oxo 5-aminovalerate, this could be amino donor for an omega transaminase enzyme.

S. meliloti can growth in the presence of 4-L-Hyp as the sole carbon and nitrogen source. The catabolic pathway described by Adams (1973) showed the conversion of 4-L-Hyp to α-ketoglutarate as the final product. The α-ketoglutarate is an intermediate in the Tricarboxylic acid cycle (TCA cycle) in the cell. In this way the final product of the 4-hydroxy-proline pathway is converted to energy for the metabolism in the cell. The results presented in this study suggest that the P4OH2C can be used as the amino donor in the transaminase reaction catalyzes by the Smc04388. As a result this intermediate of the 4-hydroxy-proline pathway can potentially be involved in the amino acid synthesis in the cell.

A coupled enzymatic reaction was carried out to investigate whether the Smc04388 transaminase use P4OH2C (4-hydroxy-2-oxo-5-aminovalerate) as an amino donor. In this assay purified D-HypDH was used to produce P4OH2C from *cis*-4-hydroxy-D-proline and in the second reaction, Smc04388 omega amino transaminase was added to determine whether it catalyzed the transfer of the amino group from P4OH2C (4-hydroxy-2-oxo-5-aminovalerate) to pyruvate to synthesize L-alanine. L-alanine is formed by the transfer of the amino group from 4-hydroxy 2-oxo 5-aminovalerate (open form of the P4OH2C) to pyruvate. CE-MS analysis

revealed that L-alanine was formed in the coupled reaction, whereas L-alanine was not present in the control reaction without the Smc04388 protein. The results indicated that the 4-hydroxy-2-oxo-5-aminovalerate was used as an amino donor for the Smc04388 to produce L-alanine from pyruvate.

Based on these results it is likely that the Smc04388 omega amino transaminase is involved in a secondary pathway related to the main 4-hydroxy-proline pathway. The open form of the P4OH2C intermediate generated in the second reaction from *cis*-4-hydroxy-D-proline (Figure 2) is used as an amino donor for this omega transaminase. Adams (1973) did not report such transamination reaction in the catabolic pathway of 4-hydroxy-proline. However, in the mammal's major catabolic pathway, the third reaction has been reported as a transamination (Adams & Frank, 1980).

The second intermediate formed in the mammalian pathway (Figure 23 in Appendix) is the Δ^1-pyrroline-3-hydroxy-5-carboxylate (P3OH5C). This compound is oxidized by a dehydrogenase enzyme to 4-hydroxyglutamate. Further, the 4-hydroxyglutamate participates as an amino donor in the transaminase reaction catalyzed by the 4-hydroxyglutamate transaminase (Adams & Frank, 1980). The analogue of P3OH5C in the bacterial 4-hydroxy-proline pathway is P4OH2C. Unlike P3OH5C, P4OH2C is spontaneously hydrolyzed in water to its open form, 4-hydroxy-2-oxo-5-aminovalerate, which is then convert to α-ketoglutarate semialdehyde by Δ^1-pyrroline-4-hydroxy-2-carboxylate deaminase (Adams, 1973). It would be interesting to determine if the Smc04388 omega transaminase has activity with P3OH5C.

CHAPTER 5

CONCLUSIONS

The *smc04388* gene is induced when 4-L-Hyp is present as a carbon or nitrogen source in the media. However, *smc04388* is not required for the growth of *S. meliloti* in media containing 4-L-Hyp as the sole carbon and nitrogen source. Based on these results, it appears to be involved in a secondary pathway related to the main catabolic pathway of 4-hydroxy-proline in bacteria.

It was demonstrated that the second intermediate of the 4-hydroxy-proline catabolic pathway, Δ^1-pyrroline-4- hydroxy-2-carboxylate (P4OH2C), is involved in a transamination reaction with pyruvate. The results presented here suggest that the open form of P4OH2C, 4-hydro-2-oxo-5-aminovalerate, may be used by the Smc04388 omega transaminase as the amino donor in a transamination reaction. In addition, it was shown that a cell extract lacking the enzyme that catalyses the conversion of Δ^1-pyrroline-4- hydroxy-2-carboxylate to α-ketoglutarate semialdehyde has higher transaminase activity. This result suggests that synthesis of the Smc04388 enzyme maybe induced by the 4-hydro-2-oxo-5-aminovalerate intermediate.

BIBLIOGRAPHY

Adams, E. & Frank, L. (1980). Metabolism of proline and the hydroxyprolines. Annu Rev Biochem **49**: 1005–1061.

Adams, E. (1973). The metabolism of hydroxyproline. Mol Cell Biochem **2**:109-119.

Bais, H.P., Weir, T.L., Perry, L.G., Gilroy, S. & Vivanco, J.M. (2006). The Role of Root Exudates in Rhizosphere Interactions with Plants and Other Organisms. Annu. Rev. Plant Biol. **57**: 233-266.

Berrada, H. & Fikri-Benbrahim, K. (2014).Taxonomy of the Rhizobia: Current. Perspectives. British Microbiology Research Journal. **4**: 616-639.

Bradford, M.M. (1976). A rapid and Sensitive Method for the Quantification of the Microgram Quantities of Protein Utalizing the Principle of Protein-dye Binding. Analytical Biochemestry: 248-254.

Caetano-Anolles, G. & Gresshoff, P.M. (1991). Plant genetic control of nodulation. Annu. Rev. Microbiol. **45**: 345-382.

Canfield, D.E., Glazer, A.N. & Falkowski, P.G. (2010). The Evolution and Future of Earth's Nitrogen Cycle. Science **330**: 192-196.

Capela, D., Barloy-Hubler, F., Gouzy, J., Bothe, G., Ampe, F., Batut, J., Boistard, P., Becker, A., Boutry, M., Cadieu, E., Dreano, S., Gloux, S., Godrie, T., Goffeau, A., Kahn, D., Kiss, E., Lelaure, V., Masuy, D., Pohl, T., Portetelle, D., Puhler, A., Purnelle, B., Ramsperger, U., Renard, C., Thebault, P., Vandenbol, M., Weidner, S. & Galibert, F. (2001). Analysis of the chromosome sequence of the legume symbiont *Sinorhizobium meliloti* strain 1021. Proc. Natl. Acad. Sci. USA **98**: 9877–9882.

Capoen, W., Oldroyd, G., Goormachtig & Holsters, M. (2010). *Sesbania rostrata*: a case study of natural variation in legume nodulation. New Phytologist. **186**: 340–345.

Cowie, A., Cheng, J., Sibley, C.D., Fong, Y., Zaheer, R., Patten, C.L., Richard, M.M., Golding, B., Finan, T.M. (2006). An integrated approach to functional genomics: construction of a novel reporter gene fusion library for *Sinorhizobium meliloti*. Appl Environ Microbiol. **72**: 7156–7167.

Dixon, R. & Kahn, D. (2004). Genetic regulation of biological nitrogen fixation. Nature Reviews Microbiology. **2**: 621-631.

Driscoll, B.T. & Finan, T.M. (1993). NAD^+-dependent malic enzyme of *Rhizobium meliloti* is required for symbiotic nitrogen fixation. Molecular Microbiology. **7**: 865-873.

Finan, T.M., Hartwieg, E., Lemieux, K., Bergman, K., Walker, G.C. & Signer, E.R. (1984). General Transduction in *Rhizobium meliloti*. Journal of Bacteriology. **159**: 120-124.

Finan, T.M., Kundel, B., DeVos, G.F., & Signer, E.R. (1986). Second Symbiotic Megaplasmid in *Rhizobium meliloti* Carring Exopolysaccharide and Thiamine Synthesis Gene. Journal of Bacteriology. **167**: 66-72.

Frioni, L. (1990). (Eds) Ecología microbiana del suelo. Capítulo 10: Comunidad del Sur-Edinor. Editorial Montevideo, Montevideo, Uruguay. 519 p.

Gage, D. J. (2004). Infection and invasion of roots by symbiotic, nitrogen-fixing rhizobia during nodulation of temperatura legumes. Microbiol Mol Biol Rev. **68:** 280-300.

Galibert, F., Finan, T.M., Long, S.R., Puhler, A., Abola, P., Ampe, F., BarloyHubler, F., Barnett, M.J., Becker, A., Boistard, P., Bothe, G., Boutry, M., Bowser, L., Buhrmester, J., Cadieu, E., Capela, D., Chain, P., Cowie, A., Davis, R.W., Dreano, S., Federspiel, N.A., Fisher, R.F., Gloux, S., Godrie, T., Goffeau, A., Golding, B., Gouzy, J., Gurjal, M., Hernandez-Lucas, I.,

Hong, A., Huizar, L., Hyman, R.W., Jones, T., Kahn, D., Kahn, M.L., Kalman, S., Keating, D.H., Kiss, E., Komp, C., Lelaure, V., Masuy, D., Palm, C., Peck, M.C., Pohl, T.M., Portetelle, D., Purnelle, B., Ramsperger, U., Surzycki, R., Thebault, P., Vandenbol, M., Vorholter, F.J., Weidner, S., Wells, D.H., Wong, K., Yeh, K.C., Batut, J. (2001).The composite genome of the legume symbiont *Sinorhizobium meliloti*. Science **293**: 668-672.

Goytia, M., Chamond, N., Cosson, A., Coatnoan, N., Hermant, D., Berneman, A. & Minoprio, P. (2007). Molecular and structural discrimination of proline racemase and hydroxyproline-2-epimerase from nosocomial and bacterial pathogens. PLoS ONE. **2**: 1–8.

Graham, P. H. (1975). Symbiotic Nitrogen Fixation in Plants. Nutman, Cambridge Univ. Press. 137 p.

Hanson, R.L., Davis, B.L., Chen, Y., Goldberg, S.L., Parker, W.L., Tully, T.P., Montana., M.A., Patel, R.N. (2008). Preparation of (R)-amines from racemic amines with an (S)-amine transaminase from *Bacillus megaterium*. Adv Synth Catal. **350**:1367–1375.

Hirotsu, K., Goto, M., Okamoto, A., Miyahara, I. (2005). Dual substrate recognition of aminotransferases. Chem Rec. **5**:160–172.

Hishinuma, S., Yuki, M., Fujimura, M. & Fukumori, F. (2006). OxyR regulated the expression of the two major catalases, KatA and KatB, along with peroxiredoxin, AhpC in *Pseudomonas putida*. Environmental Microbiology. **8**: 2115-2124.

Hwang, B.Y., Cho, B.K., Yun, H., Koteshwar, K., Kim, B.G. (2005). Revisit of aminotransferase in the genomic era and its application to biocatalysis. J. Mol Catal B Enzym. **37:** 47-55.

Jayaraman, K. & Radhakrishnan, A.N. (1965). Bacterial metabolism of hydroxyproline. I. Metabolism of L-allohydroxyproline by a *Pseudomonas*. Indian J Biochem. **2**: 145-153.

Jayaraman, K. & Radhakrishnan, A. N. (1965). Bacterial metabolism of hydroxyproline. I. Metabolism of L-allohydroxyproline by a *Pseudomonas*. Ind. J. Biochem. **2**: 145-53.

Jayaraman, K. & Radhakrishnan, A. N. (1965). Bacterial metabolism of hydroxyproline. II. Metabolism of L-hydroxyproline in Achromobacter. Ind. J. Biochem. **2**:153-58.

Kaulmann, U., Smithies, K., Smith, M.E.B., Hailes, H.C., Ward, J.M. (2007). Substrate spectrum of ω-transaminase from *Chromobacterium violaceum* DSM30191 and its potential for biocatalysis. Enzyme Microb Technol. **41**: 628–637.

Koo, P.H. & Adams, E. (1974). α-ketoglutaric Semialdehyde Dehydrogenase of *Pseudomonas*. Properties of the separately induced isoenzymes. Biol Chern. **249**: 1104-16.

Koszelewski, D., Tauber, K., Faber, K., Kroutil, W. (2010). ω-Transaminases for the synthesis of non-racemic α-chiral primary amines. Trends Biotechnol. **28**: 324-332.

Lloret, L. & Martínez-Romero, E. (2005). Evolución y filogenia del *Rhizobium*. Revista Latinoamericana de Microbiología. **47**: 43-60.

Long, S.R. (1996). Rhizobium Symbiosis: Nod Factors in Perspective. The Plant Cell. **8**: 1885-1898.

Luyten, E. & Vanderleyden, J. (2000). Survey of genes identified in *Sinorhizobium meliloti* spp., necessary for the development of an efficient symbiosis. Eur. J. Soil Biol. **36**: 1-26.

MacLean, A.M., White, C.E., Fowler, J.E., Finan, T.M. (2009). Identification of a hydroxyproline transport system in the legume endosymbiont *Sinorhizobium meliloti*. Mol Plant Microbe Interact. **22**:1116-1127.

Malik, M.S., Park, E.S., Shin, J.S. (2012). Features and technical applications of ω-transaminases. Appl. Microbiol Biotechnol **94**: 1163-1171.

Mehta, P.K., Hale, T.I., Christen, P. (1993). Aminotransferases: demonstration of homology and division into evolutionary subgroups. Eur. J. Biochem. **214**: 549-561.

Osorio, N.W. (2007). A review on beneficial effects of rhizosphere bacteria on soil nutrient availability and plant nutrient uptake. Rev. Fac. Nac. Agr. Medellín**. 60**: 11-31.

Ott, T., van Dongen, J.T., Gunther, C., Krusell, L., Desbrosses, G., Vigeolas, H., Bock, V., Czechowski, T., Geigenberger, P. & Udvardi, M.K. (2005). Symbiotic leghemoglobins are crucial for nitrogen fixation in legume root nodules but not for general plant growth and evelopment. Current Biology. **15**: 531–535.

Pacios-Bras, C. (2005). The symbiosis between *Lotus japonicus* and rhizobia: function of nod factor structural variation. Lotus Newsletter. **35**: 93-98.

Park, E., Kim, M., Shin, J.S. (2010). One-pot conversion of L-threonine into L-homoalanine: biocatalytic production of an unnatural amino acid from a natural one. Adv Synth Catal. **352**: 3391–3398.

Park, E. S., & Shin, J. S. (2013). ω-Transaminase from *Ochrobactrum anthropi* is devoid of substrate and product inhibitions. Applied and environmental microbiology. **79**: 4141-4144.

Park, E. S., Kim, M., & Shin, J. S. (2012). Molecular determinants for substrate selectivity of ω-transaminases. Applied microbiology and biotechnology. **93**: 2425-2435.

Prentki, P. & Krisch, H.M. (1984). In vitro insertional mutagenesis with a selectable DNA fragment. Gene. **29**: 303-313.

Relic, B., Talmont, F., Kopcinska, J., Golinowsky, W., Promé, J. C. and Broughton, W. J. (1994). Biological activity of *Rhizobium sp*. NGR234 Nod-factors on *Macroptilium atropurpureum*. Mol. Plant Microbe Interact. **6**: 764-774.

Sambrook, J. & Russell, D.W. (2001). Protocol 2, 3 and 25. In R. D. Sambrook Joseph, Molecular cloning: a laboratory manual (Third Edition) (pp. 1.32-1.37). Cold Spring Harbor, New York: Cold Spring Harbor Laboratory Press.

Schatzle, S., Hohne, M., Redestad, E., Robins, K., Bornscheuer, U.T. (2009). Rapid and sensitive kinetic assay for characterization of ω-transaminases. Anal Chem. **81**: 8244-8248.

Schröder, E.C. (2001). Importance of Symbiotic Nitrogen Fixation in tropical forage legume production. In: Tropical forage plants: development and use. CRC Press LLC. 68 p.

Schweiser, Klassen & Hoang (1996). Improved Methods for Gene Analysis and Expression in *Pseudomonas*. In H. Schweiser, T. Klassen & T. Hoang, Molecular Biology of Pseudomonas (pp. 229-237). Washington DC: ASM Press.

Shin, J.S., Kim, B.G., Liese, A., Wandrey, C. (2001). Kinetic resolution of chiral amines with ω-transaminase using an enzyme-membrane reactor. Biotechnol Bioeng. **73**: 179-187.

Shin, J.S. & Kim, B.G. (2002). Exploring the active site of amine:pyruvate aminotransferase on the basis of the substrate structure-reactivity relationship: how the enzyme controls substrate specificity and stereoselectivity. J Org Chem. **67**: 2848–2853.

Shin, J.S., Yun, H., Jang, J.W., Park, I., Kim, B.G. (2003). Purification, characterization, and molecular cloning of a novel amine:pyruvate transaminase from *Vibrio fluvialis* JS17. Appl Microbiol Biotechnol **61**: 463-471.

Singh, R.M.M. & Adams, E. (1965). Enzymatic Deamination of Δ^1-Pyrroline-4-hydroxy-2-carboxylate to 2,5-Dioxovalerate (α-ketoglutaric Semialdehyde). J. Biol. Chem. **240**: 4344-51.

Thacker, R.P. (1969). Conversion of L-hydroxyproline to glutamate by extracts of strains of *Pseudomonas convexa* and *Pseudomonas fluorescens*. Arch Mikrobiol. **64**: 235-238.

Vitousek, P.M., Menge, D.N.L., Reed, S.C. & Cleveland, C.C. (2013). Biological nitrogen fixation: rates, patterns and ecological controls in terrestrial ecosystems. Phil. Trans. R. Soc. B. **368**: 1-9.

White, C.E., Gavina, J.M.A., Morton, R., Britz-Mckibbin, P., Finan, T.M. (2012). Control of hydroxyproline catabolism in *Sinorhizobium meliloti*. Mol Microbiol. **85**:1133-1147.

Yonaha, K., Toyama, S., Yasuda, M., Soda, K. (1976). Purification and crystallization of bacterial omega-amino acid-pyruvate aminotransferase. FEBS Lett. **72**: 21-24.

Yuan, Z.C., Zaheer, R. & Finan, T.M. (2006). Regulation and Properties of PstSCAB, a High-Affinity, High-Velocity Phosphate Transport System of *Sinorhizobium meliloti*. Journal of Bacteriology. **188**: 1089-1102.

Yun, H., Lim, S., Cho, B.K., Kim, B.G. (2004). ω-Amino acid:pyruvate transaminase from *Alcaligenes denitrificans* Y2k-2: A new catalyst for kinetic resolution of β-amino acids and amines. Appl Environ Microbiol. **70**: 2529-2534.

APPENDIX

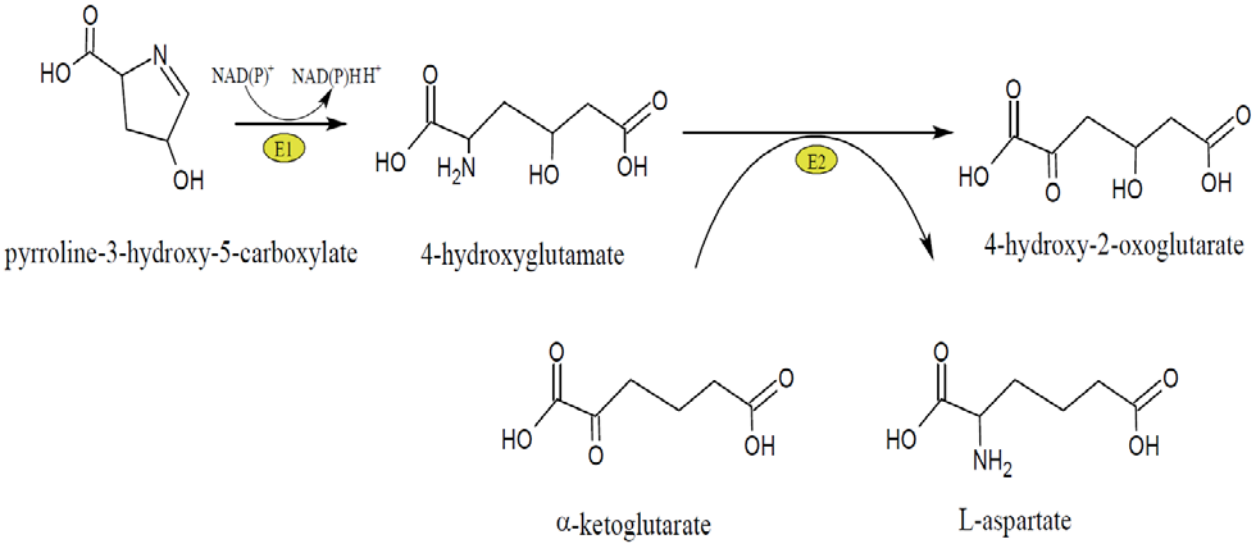

Figure 23. Second and third reactions of the hydroxyproline catabolic pathway in mammals. The conversion of pyrroline-3-hydroxy-5-carboxylate (P3OH5C) to 4-hyxydroglutamate is catalyzed by P3OH5C dehydrogenase (E1). Next, 4-hydroxyglutamate is involved in the transaminase reaction catalyzed by 4-hydroxyglutamate transaminase (E2). Chemical structures were drawn using ChemSketch program.

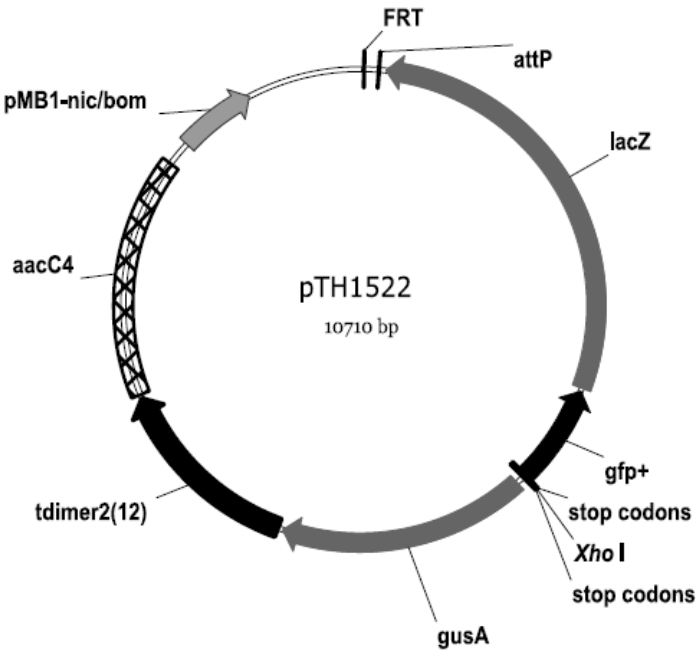

Figure 24. pTH1522 vector used to create the fusion library strains. The *gfp*/*lacZ* genes and the *gusA*/*tdimer2* are located in opposite direction from the cloning site *XhoI*. *aacC4* corresponds to the gentamicin resistance gene. Figure adapted from Cowie et al. (2006).

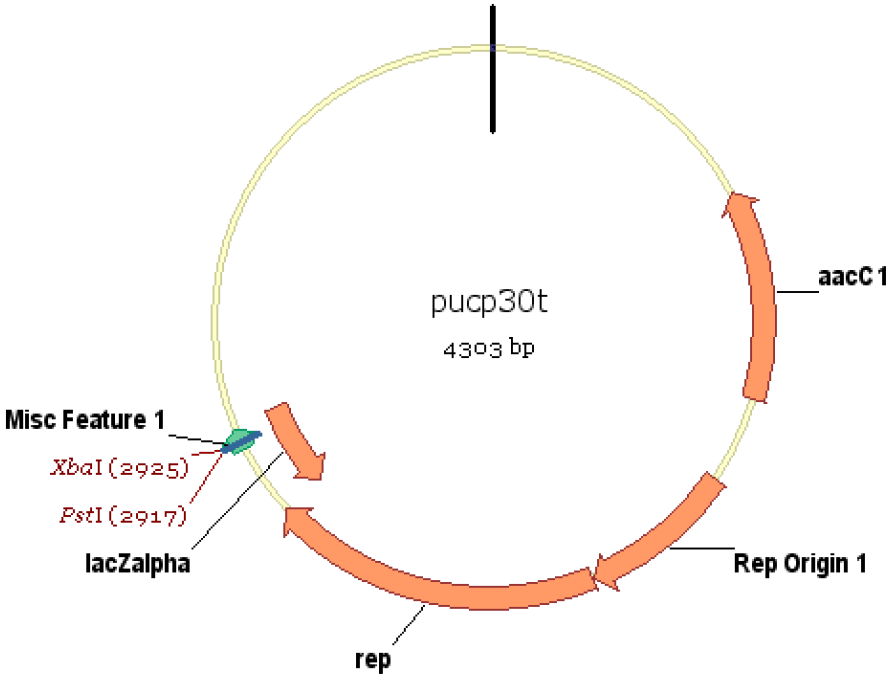

Figure 25. pUCP30T vector used for the construction of the pTH2816 recombinant plasmid. The DNA fragment of *smc04388* and 300 nucleotides around was inserted in the *Xba*I (2925) and *Pst*I (2917) sites indicated in the cloning site of the vector.

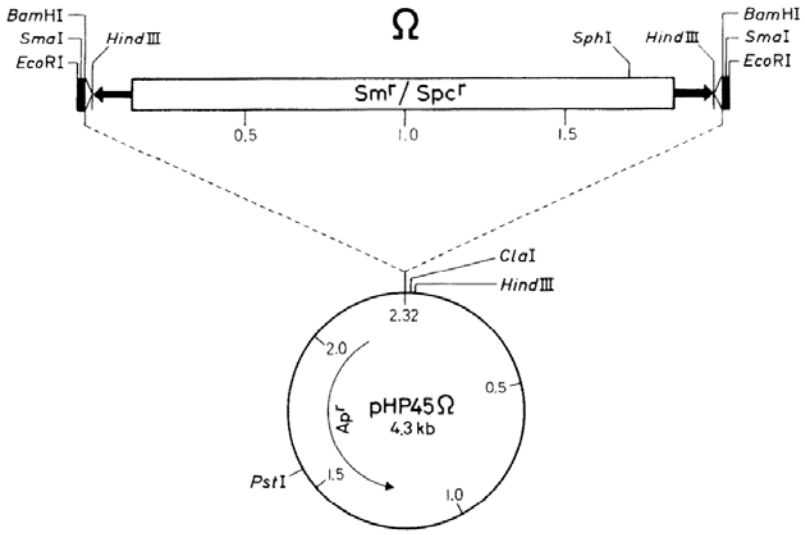

Figure 26. Vector pHP45 that carries the Sm/Sp resistant cassette. The Sm/Sp resistant cassette is located between short inverted repeats sequences. The restriction enzymes presented in both sites of the cassette allows carrying a single digestion to obtain the resistant cassette. In this work the *Sma*I site was used to isolate the Sm/Sp resistant cassette. Figure modified from Prentki & Krisch (1984).

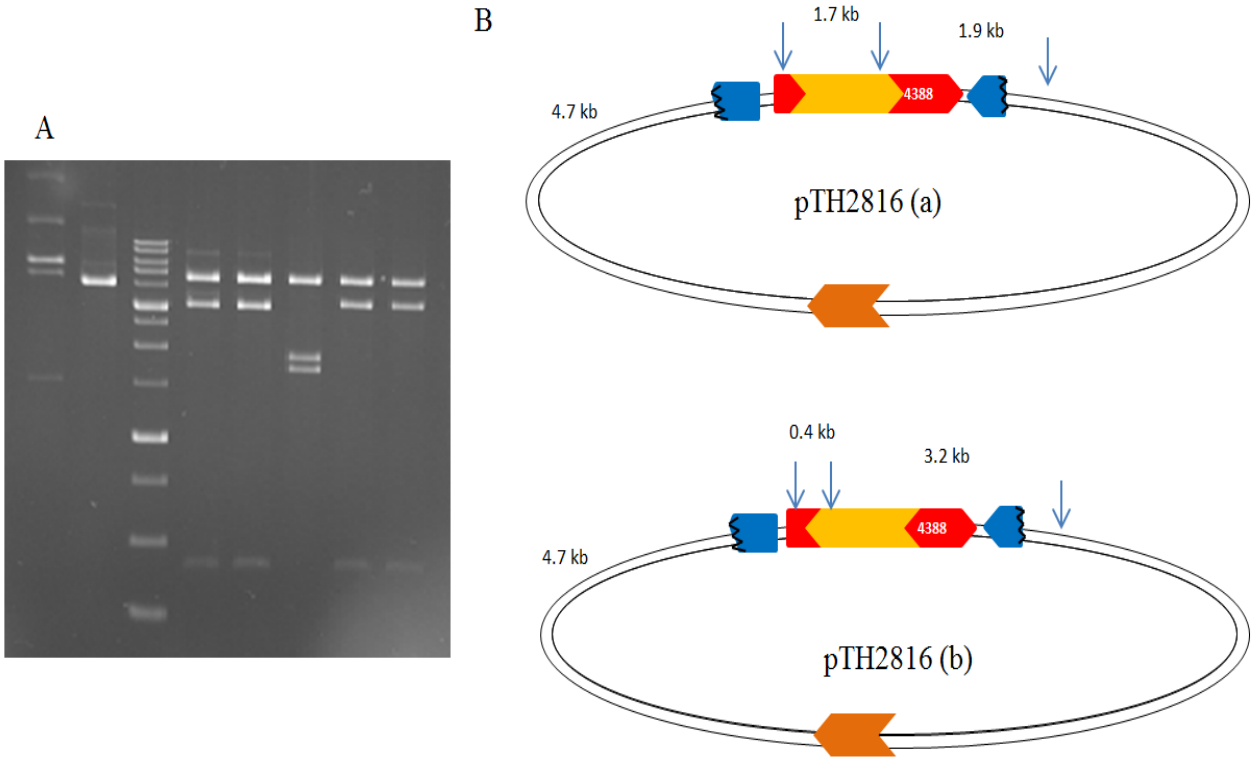

Figure 27. Restriction digest from different recombinant plasmids pTH2816 after the Sm/Sp resistant cassette was inserted. (A) Gel photo of restriction digest using *Sph*I. From the left to the right; Lane 1: pTH2816 plasmid uncut; Lane 2: pUCP30T empty plasmid uncut; Lane 3: 1 kb DNA ladder; Lane 4-8 pTH2816 plasmids digested with *Sph*I. Lanes 4, 5, 7 and 8 correspond to plasmid pTH2816 (b) and Lane 6 corresponds to pTH2816 (a). (B) Schematic representation of the two different recombinants plasmid pTH2816 depending on the direction of the Sm/Sp resistant cassette. Blue arrows indicate the cut sites for *Sph*I and numbers indicated the lengths of the restriction fragments in kb.

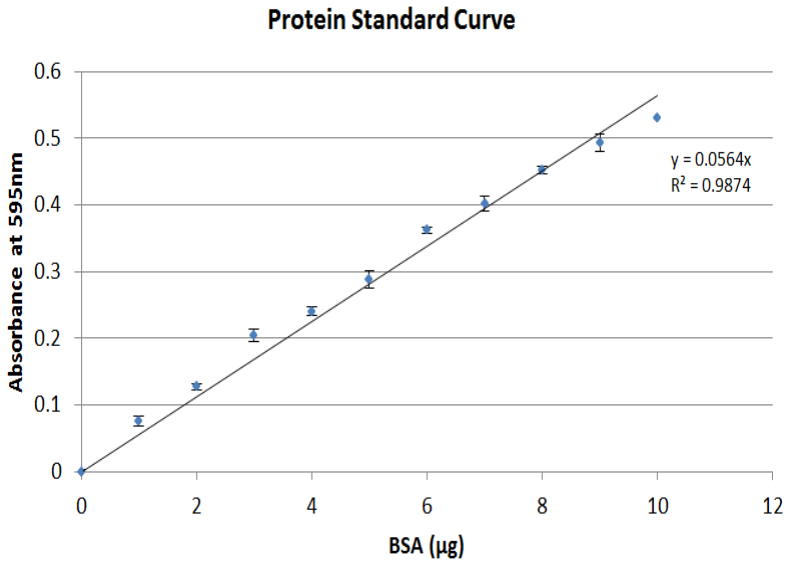

Figure 28. Protein Standard curve of BSA. The "x" represents different amount of BSA in µg and the "y" represents the absorbance at 595 nm. Each solution of BSA was prepared by triplicate. The error bars represents standard errors.

Table 7. Purification summary of *cis*-4-hydroxy-D-proline dehydrogenase (D-HypDH) from *P. putida* strain (M2116). Elution fractions were separate in two different portions depending on the amount of protein present. Portion I has high concentration of protein and portion II has less amount of protein.

		Volume (mL)	Protein conct. (µg/µL)	Total amount of protein (mg)	Specific Activity (µmole/min/mg prot)
Crude Extract		42	N/A		
Clear lysate		10	44.54	445	0.49
Flow through		10	18.01	180	N/A
Protein eluted	Portion I	3.5	1.74	6.1	2.39 ± 0.44
	Portion II	3.5	0.66	2.31	1.41 ± 0.11
Protein after dialysis	Portion I	2.6	1.88	4.89	1.72 ± 0.11
	Portion II	2.6	0.71	1.85	1.63 ± 0.13

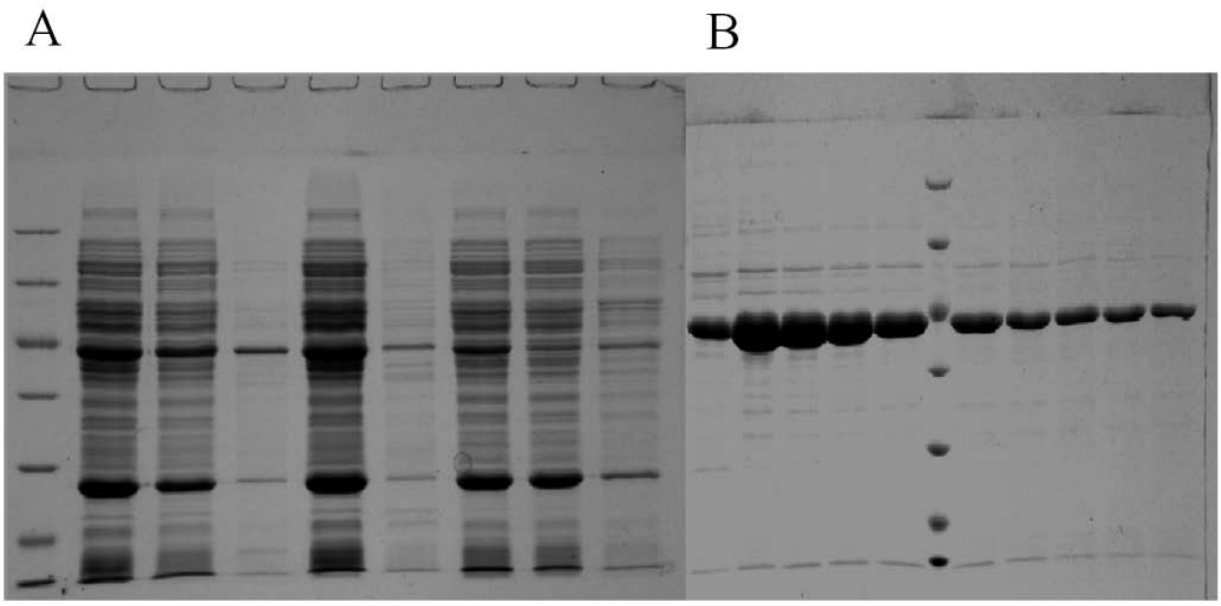

Figure 29. Purification of *cis*-4-hydroxy-D-proline dehydrogenase from *P. putida* strain. (A) SDS-PAGE gel with 10% acrylamide. From the left to the right: Lane 1: Protein molecular weight marker; Lane2: whole cells grown in LBmc plus 50 mg/mL Rif and Km; Lane 3: 1:10 dilution of French press sample; Lane 4: 1:10 dilution pellet after centrifugation at low speed; Lane 5: 1:10 dilution supernatant after low speed centrifugation; Lane 6: 1:10 dilution pellet after ultracentrifugation; Lane 7: 1:10 dilution clear lysate cells; Lane 8: 1:10 dilution flow through the column; Lane 9: wash fraction. (B) SDS-PAGE gel with 10% acrylamide. From the left to right: Lane 1-5: elution fractions (Portion I in Table 7); Lane 6: Protein molecular weight marker; Lane 7-11; elution fractions (Portion II in Table 7).

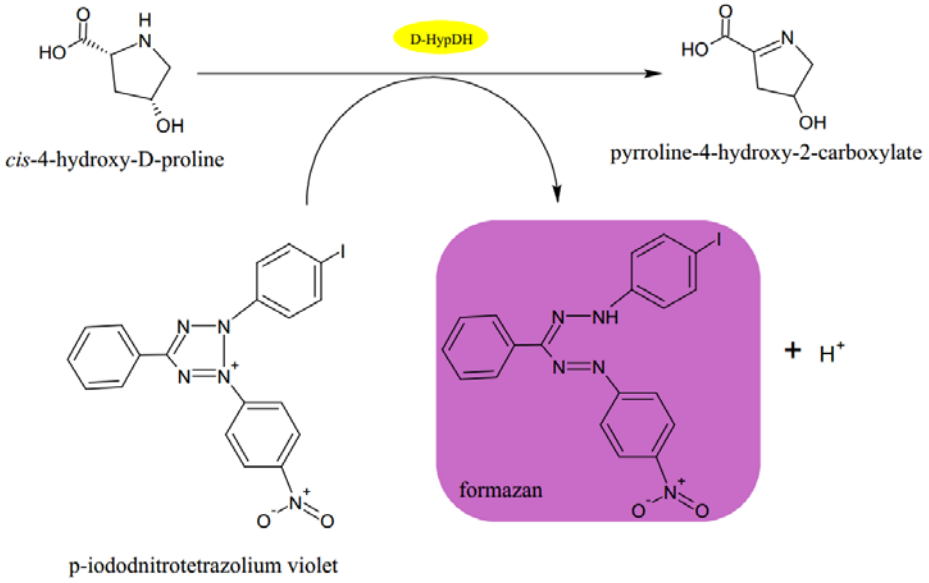

Figure 30. Principle of an enzymatic assay to detect the activity of *cis*-4-hydroxy-D-proline dehydrogenase enzyme (D-HypDH). Reduction of p-iodonitrotetrazolium produces the purple dye formazan. The intensity of the color can be detected by spectrometry since formazan has a maximum of absorbance at 490 nm. Chemical structures were drawn using ChemSketch program.

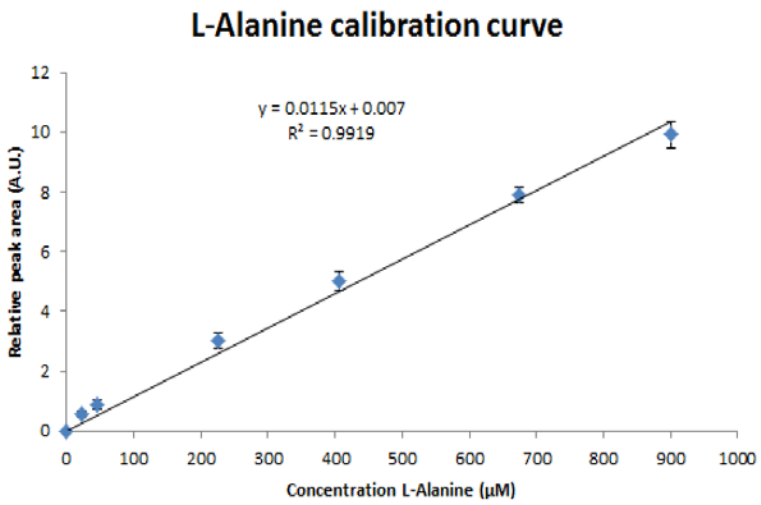

Figure 31. L-alanine standard curve. Concentration of L-alanine in µM in "x" axis was plotted against the Relative Peak Area (RPA) in the "y" axis. Graph was made by Mai Yamamoto.

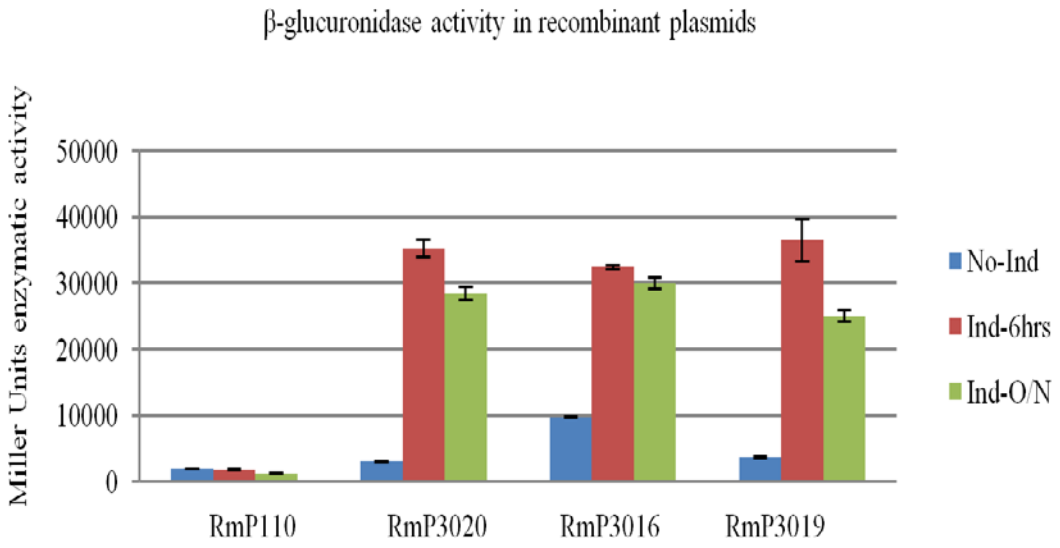

Figure 32. β-glucuronidase activity in recombinant plasmids harbouring the *smc04388* gene. Cultures were induced in LBmc at 30 ^{o}C by adding 0.4 mM of IPTG for 6 hours (Ind-6hrs) and overnight (Ind-O/N). The culture without adding IPTG (No-Ind) was used as background activity. RmP110 correspond to wild type strain without any plasmid in. RmP3020 is wild type strain (RmP110) harbouring the empty pTH1227 vector. RmP3016 and RmP3019 contain the recombinant plasmid pTH2814, which has inserted the *smc04388* gene.

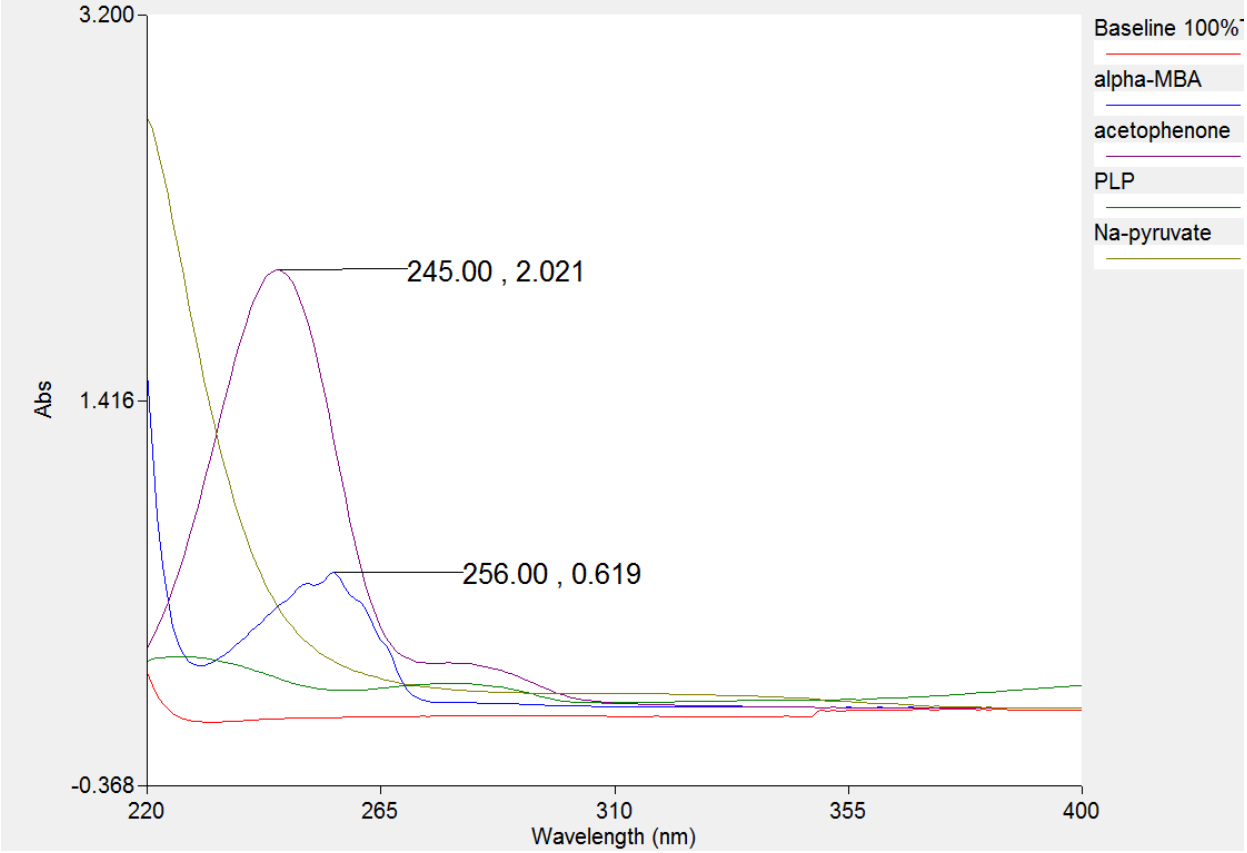

Figure 33. Spectra of each reactant of the reaction mixture and acetophenone. Absorbance readings were taking from 400 nm to 220 nm using a Cary 1E UV-visible Spectrophotometer. The concentration used for each compound was 2.5 mM α-MBA, 2.5 mM pyruvate, 0.02 mM PLP, and 0.5 mM acetophenone. Solutions were prepared in Tris-HCl buffer pH 9.

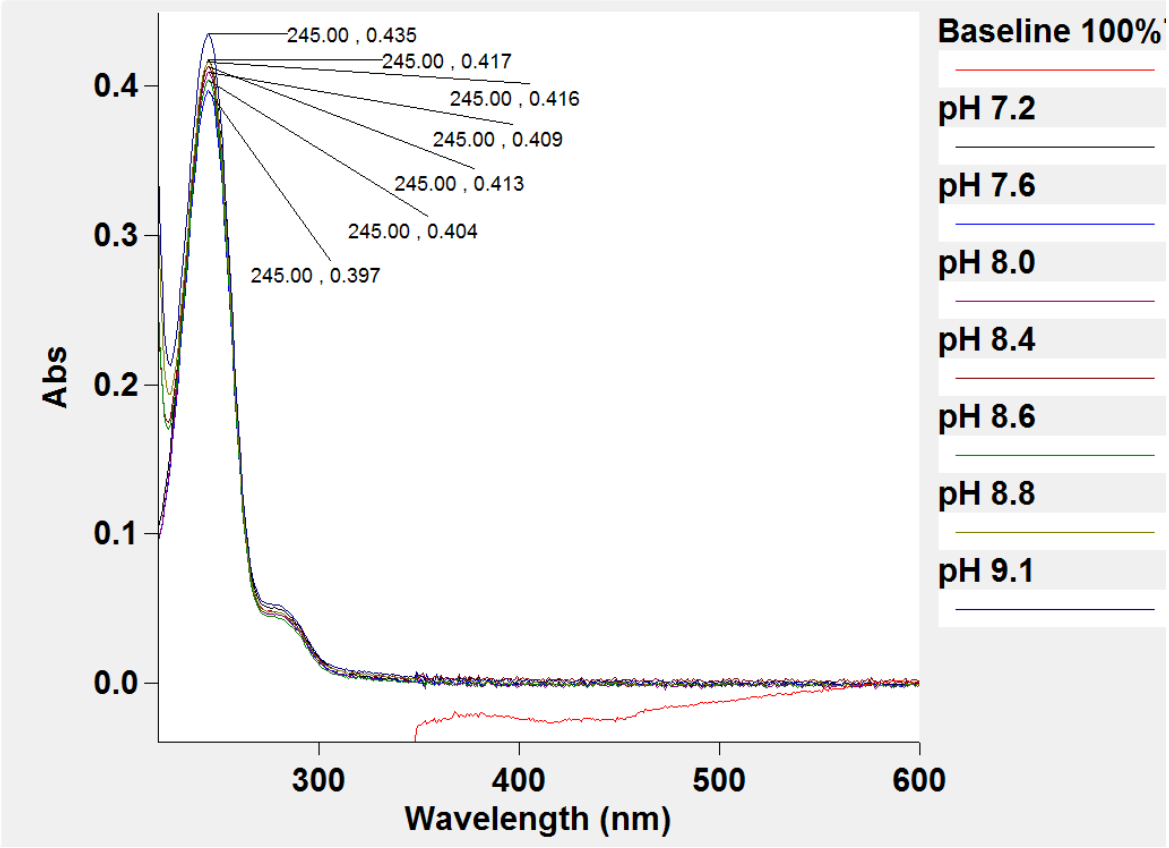

Figure 34. Spectra of 0.1 mM acetophenone at different pHs. Absorbance readings were taking from 600 nm to 200 nm using a Cary 1E UV-visible Spectrophotometer. The acetophenone has a maximum of absorbance at 245 nm. Acetophenone solutions were prepared in buffer 0.05 mM buffer phosphate for pH 7.2, pH 7.6 and pH 8.0, whereas 0.1 mM Tris-HCl buffer was used for pH 8.4, pH 8.6, pH 8.8 and pH 9.0.

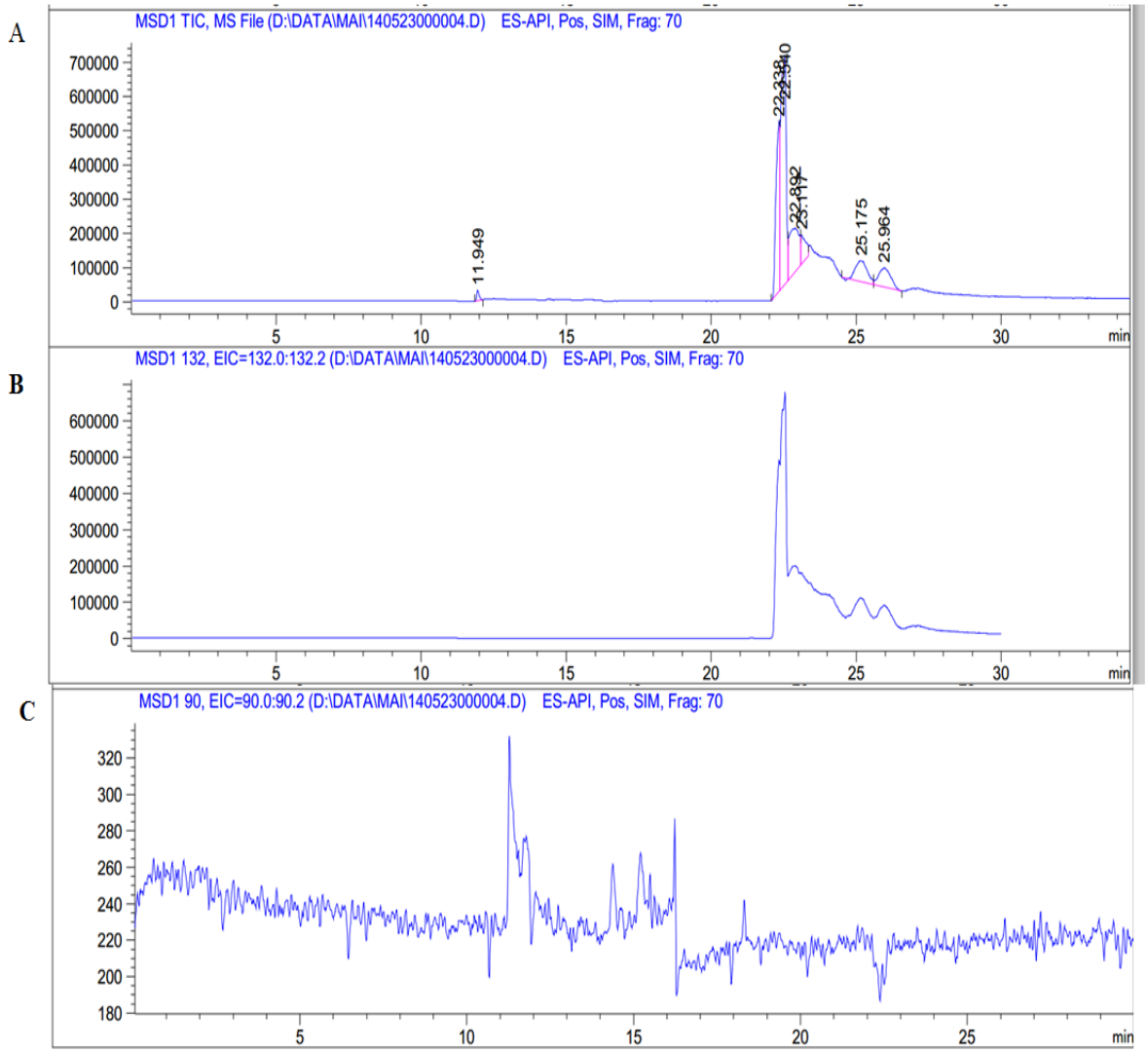

Figure 35. CE-MS of the control 2 (without pyruvate) in the coupled reaction with the D-HypDH from *P. putida* and the purified Smc04388 omega amino transaminase. The "y" and the "x" axis correspond to Ion count and Migration time in minutes, respectively. (A) First half reaction containing 50 mM 4-D-Hyp, 2 mM $MgCl_2$, 0.05 mM PMS and 0.1 mg of purified D-Hyp-DH was incubated in the dark at 30 ^{o}C. After incubation 500 µL of this reaction mixture was mixed along with 0.02 mM PLP and 1mg of the purified Smc04388 omega amino transaminase. This mixture was incubated for 3 hours in the dark at 30 ^{o}C. The total positive ions presented in the sample are detected. (B) Same sample as A where was detected only the ions that correspond to the mass of P4OH2C. (C) Same sample as A where was detected only the ions that correspond to the mass of L-alanine. All samples were filtered prior to their analysis to eliminate the protein present.

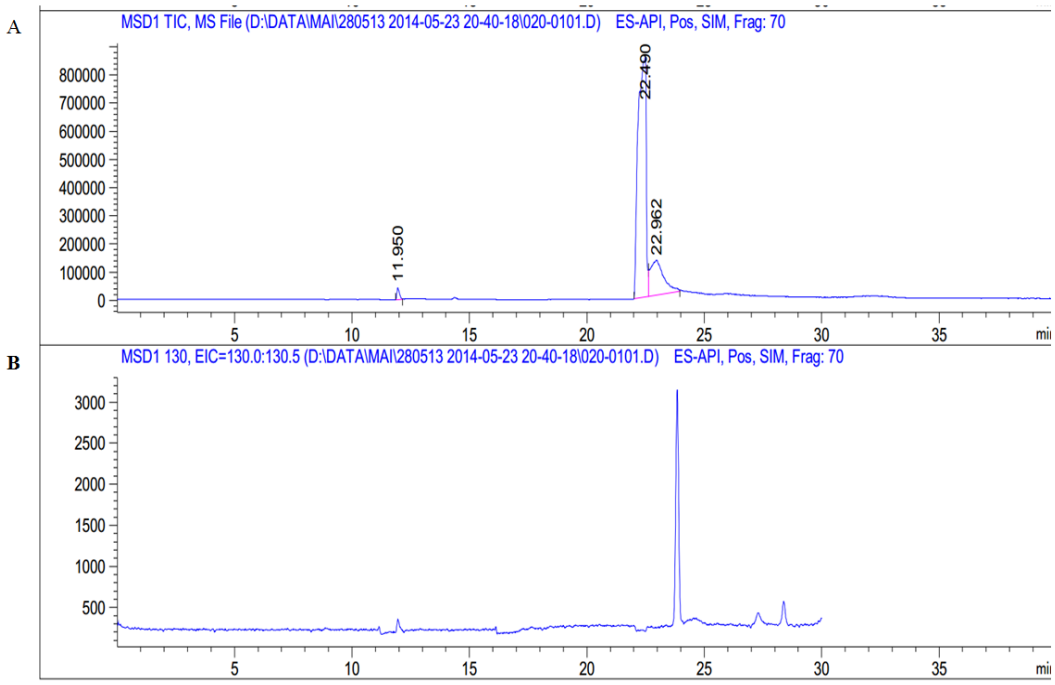

Figure 36. CE-MS of the enzymatic reaction with the D-HypDH from *P. putida*. The "y" and the "x" axis correspond to Ion count and Migration time in minutes, respectively. (A) Reaction mixture contains 50 mM 4-D-Hyp, 2 mM $MgCl_2$, 0.05 mM PMS and 0.1 mg of purified D-HypDH incubated in the dark at 30 ^{o}C. The total positive ions presented in the sample are detected. (B) Same sample as A where was detected only the ions that correspond to the mass of P4OH2C. All samples were filtered prior to their analysis to eliminate the protein present.